# Molecular Studies on the Action of APOBEC3G against HIV-1 and Development of an APOBEC-Based Anti-HIV Approach

by

Xiaoxia Wang

A Thesis submitted to the Faculty of Graduate Studies of

The University of Manitoba

in partial fulfilment of the requirements of the degree of

DOCTOR OF PHILOSOPHY

Department of Medical Microbiology

University of Manitoba

Winnipeg

# ABSTRACT

Currently, the HIV pandemic remains a major global health challenge. In order to effectively control and cure HIV-1 infection, it is necessary to perform greater research on host-HIV interactions and develop novel preventive and therapeutic approaches. The human cytidine deaminase APOBEC3G (A3G) is the first identified host restriction factor, which can serve as an initial line of defense against HIV-1 by inducing lethal mutations on proviral DNA and disrupting viral reverse transcription and integration.

In order to better understand the action of A3G on HIV-1 replication, my study was focused on characterizing the interplay between A3G and HIV-1 reverse transcriptase (RT). The results indicated that A3G directly bound to RT, which contributed to A3G-mediated inhibition of viral reverse transcription. Overexpression of the RT-binding polypeptide $A3G_{65-132}$ was able to disrupt wild-type A3G and RT interaction, consequently attenuating the anti-HIV effect of A3G on HIV replication.

While the potent antiviral activities of A3G make it an attractive candidate for gene therapy, the actions of A3G can be counteracted by HIV-1 Vif during wild-type HIV infection. In order to overcome Vif-mediated blockage and maximize the antiviral activity of A3G, this protein was fused with a virus-targeting polypeptide (R88) derived from HIV-1 Vpr, and various mutations were then introduced into R88-A3G fusion protein. Results showed that Vif binding mutants R88-$A3G_{D128K}$ and R88-$A3G_{P129A}$ exhibited very potent antiviral activity, and blocked HIV-1 replication in a $CD4^+$ T lymphocyte cell line as well as human primary cells. In an attempt to further determine their potential against drug resistant viruses and viruses produced from latently infected cells,

R88-A3G$_{D128K}$ was chosen and delivered by an inducible lentiviral vector system. Expression of R88-A3G$_{D128K}$ in actively and latently HIV-1 infected cells was shown to be able to inhibit the replication of both drug sensitive and resistant strains of HIV-1.

In conclusion, this thesis has demonstrated one of the mechanisms that how A3G can disrupt HIV-1 reverse transcription. Meanwhile, an A3G-based anti-HIV-1 strategy has been developed, which provides a proof-of-principle for a new gene therapy approach against this deadly virus.

# ACKNOWLEDGEMENTS

First and foremost, I would like to express my deepest thanks to my supervisor Dr. Xiaojian Yao. Thank you for your guidance and inspiration. I am grateful to have this opportunity to work with you, and I will never forget what I have learned over these past few years.

Secondly, I would like to express overwhelming thanks to my committee members, Dr. Blake T. Ball, Dr. Yan Li, Dr. Sam Kung for their valuable advice and constant support throughout my Ph.D. study. Additionally, I sincerely thank my external examiner Dr. Chen Liang (McGill University) for the willingness to review this thesis.

Next, I am extremely thankful to past and current members of Dr. Yao's lab. It has been a pleasure working with each of them. Especially, I would like to thank Dr. Zhujun Ao for providing me technical and moral help, and keeping the lab running smoothly. My thanks are extended to Dr. Yingfeng Zheng, Kallesh Danappa Jayappa, Jinyu Peng, Bihe Chen, Binchen Wang, Kamal Parvez, Ke Jiang, Drs. Liyu Chen, Ranzun Zhao, and Rong Zhu for their technical assistance and stimulating discussions.

I would also especially like to thank the faculty, staff and students of Department of Medical Microbiology at the University of Manitoba. Particularly, members from Dr. Gary P. Kobinger's lab for their kind assistance in AAV vector preparation. The special thanks go to Angela Nelson, Sharon Tardi, Sue Ramdahin, Jude Zeiske for their kindness guidance and technical support.

I am indebted to the China Scholarship Council for providing studentship, and the Canadian Institutes of Health Research and Canadian Foundation of Innovation for

providing research funding.

Last but not least, I would like to thank my family members for being so supportive and believing in me. I could not have come as far as I have without them. Also, I'd also like to thank my friends both at University of Manitoba and outside, who have supported and encouraged me throughout my graduate studies.

# TABLE OF CONTENTS

# LIST OF TABLES

# LIST OF FIGURES

# LIST OF ABBREVIATIONS

| | |
|---|---|
| AAV | adeno-associated virus |
| AGM | africa green monkey |
| AID | activation-induced deaminase |
| AIDS | acquired immunodeficiency syndrome |
| APOBEC3G /A3G | apolipoprotein B mRNA-editing enzyme catalytic polypeptide-like 3G |
| BST-2 | bone marrow stromal cell antigen 2 |
| CA | capsid |
| CDD | cytidine deaminase domain |
| CMV | cytomegalovirus |
| Co-IP | co-immunoprecipitation |
| CRF | circulating recombinant form |
| CTD | C-terminal domain |
| CTL | cytotoxic T lymphocyte |
| Cul5 | cullin5 |
| CypA | cyclophilin A motif |
| DAPI | 4'-6-Diamidino-2-phenylindole |
| DIS | dimer initiation site |
| DMEM | Dulbecco's Modified Eagle's Medium |
| dNTP | deoxynucleoside triphosphate |
| Dox | doxycycline |
| ELAV | equine infectious anemia virus |
| Elo | elongin |
| Env | envelope glycoprotein |
| ER | endoplasmic reticulum |
| ESCRT | endosomal sorting complex required for transport |
| FACS | fluorescence-activated cell sorter |
| FCS | fetal calf serum |
| FITC | fluorescein isothiocyanate |
| FV | foamy virus |
| GFP | green fluorescent protein |
| GPI | glycophosphatidylinositol |
| HAART | highly active antiretroviral therapy |
| HBV | hepatitis B virus |
| HPC | hematopoietic progenitor cell |
| HTLV-1 | Human T cell leukemia virus type-1 |
| IFN | interferon |
| IN | integrase |
| IP | immunoprecipitation |
| IRES | internal ribosome entry sites |
| ITR | inverted terminal repeat |

| | |
|---|---|
| LRT | late reverse transcription |
| LTR | Long terminal repeat |
| MA | matrix |
| M-CSF | macrophage colony-stimulating factor |
| MHC-I | major histocompatibility complex class I |
| MLV | murine leukemia virus |
| M-MLV | moloney murine leukemia virus |
| MPMV | Mason-Pfizer monkey virus |
| NC | nucleocapsid |
| Nef | negative factor |
| NK | natural killer |
| NTD | N-terminal domain |
| ORF | open reading frames |
| PBMC | peripheral blood mononuclear cell |
| PBS | primer binding site/phosphate buffered saline |
| PHA | phytohemaglutinin |
| PI | propidium iodide |
| PIC | pre-integration complex |
| pis | packaging signal |
| PKA | protein kinase A |
| PL | ProLabel |
| PMA | phorbol-12-myristate-13-acetate |
| PPT | polypurine tract |
| PR | protease |
| pTZ | pTRIPZ |
| puro | puromycin |
| PuroR | puromycin selectable marker |
| P-TEFb | positive transcription elongation factor |
| Rev | regulator of expression of virion protein |
| RING | really interesting new gene |
| RNAPII | RNA polymerase II |
| RNase H | ribonuclease H |
| RNP | ribonucleoprotein |
| RPMI | Roswell Park Memorial Institute |
| RT | reverse transcriptase |
| RTC | transcription complexe |
| rtTA3 | reverse tetracycline transactivator 3 |
| SAMHD1 | sterile alpha motif and histidine-aspartic domain 1 |
| SIV | simian immunodeficiency virus |
| TAR | Tat-actiong region |
| Tat | transactivator |
| TM | transmembrane |
| TNF | tumor necrosis factor |
| TRE | tetracycline response element |

| | |
|---|---|
| TRIM | tripartite motif |
| UBA2 | ubiquitin-associated domain 2 |
| UBC | ubiquitin C promoter |
| Vif | virion infectivity factor |
| VLP | viral like particle |
| Vpr | virion protein R |
| Vpu | virion protein U |
| WB | Western Blot |
| WST-1 | 4-[3-(4-iodophenyl)-2-(4-nitrophenyl)-2H-5-tetrazolio]-1,3-benzenedisulfonate |
| ZFN | zinc finger nuclease |
| Ψ | packaging signal |

# CHAPTER 1

## Introduction

### 1.1 Overview

Human immunodeficiency virus (HIV) is the cause of acquired immunodeficiency syndrome (AIDS) (24, 267). Within years of its initial recognition, HIV/AIDS has expanded rapidly throughout the world and become a major global health challenge. According to estimates by the Joint United Nations Program on HIV/AIDS (UNAIDS), 34 million people were living with HIV by the end of 2011. In 2011 alone, 2.5 million people became newly infected and 1.7 million people died from AIDS. The HIV epidemic varies substantially between countries and regions, where Sub-Saharan Africa continues to be the most severely affected region with an average adult HIV-1 prevalence of 4.9%, followed by Caribbean, Eastern Europe and Central Asia with an adult prevalence rate of 1.0% (http://www.unaids.org/).

Globally, HIV is predominantly transmitted via sexual contact (129). However, HIV can be transmitted by other identified routes, including mother-to-child, drug injection and exposure to blood products (59). Regardless of how the virus was acquired, after initial infection, HIV disseminates into draining lymph nodes within days, and then systemically spreads throughout the body (59, 207). HIV preferentially targets activated $CD4^+$ T lymphocytes and induces their massive depletion during acute infection (77, 78). In the prolonged chronic infection stage, intense interplay between HIV and the immune system leads to progressive loss of $CD4^+$ T cell

responses and accelerated disease progression (77, 218). Eventually, HIV-induced immune dysfunction results in the development of AIDS with its associated opportunistic infections and cancers (78, 254).

In the last three decades, promising progress has been made in controlling HIV/AIDS around the world. Effective antiviral therapies, especially the introduction of highly active antiretroviral therapy (HAART), have dramatically prolonged life expectancy of people with HIV and reduced AIDS-related deaths (256). However, there are still limitations associated with antiviral therapies. While considerable research has been conducted in designing and developing vaccines to prevent HIV infection, the progress has been slower than expected. Most vaccine candidates were tested to be ineffective, and only a small portion of candidates showed even modest effects (307, 334).

Thus, continued efforts are needed to eliminate HIV/AIDS. Knowledge of the host restriction factors would greatly contribute to our understanding of the mechanisms by which host defense against HIV infection and provide the basis for subsequently design of new therapeutic approaches. The aim of this thesis is to define the action of A3G in HIV replication, and develop an A3G based antiviral approach.

## 1.2 HIV-1 virology

### 1.2.1 Classification of HIV

HIV is a member of the genus *Lentivirus* in the family *Retroviridae*. Retroviruses are defined by their RNA genome, which is transcribed into DNA within the cell using

the viral enzyme reverse transcriptase (RT). Lentiviruses are one of the seven genera of retroviruses, they are so-called because of their long incubation period before the onset of overt disease (39). There are three subtypes of primate lentivirus: HIV-1, HIV-2 and simian immunodeficiency virus (SIV). The first two are the causative agents of AIDS (82). SIV targets various species of African nonhuman primates (345). Unlike HIV, SIV infection does not cause AIDS-like illness in natural host, despite their high viral loads levels (117, 255). SIVcpz from chimpanzees is believed to be the zoonotic origin of HIV-1. It is phylogenetically and geographically closely related to HIV-1 (101).

Based on full-length viral genome sequencing, HIV-1 strains are classified into four highly divergent groups, named M (main), O (outlier), N (non M or O) and P (putative) (265, 303). Group M is the predominant group in the world and is responsible for more than 95% of HIV-1 infections (295). Prevalence of the other groups is extremely low and remains restricted to West Central Africa (257, 328, 329). Group M can be further divided into phylogenetic subtypes or clades. Currently, nine clades, A, B, C, D, F, G, H, J, and K have been recognized and are distributed relatively evenly worldwide. For example, clade B is the dominant form in Americas and Europe, but is barely found in Africa (104). Furthermore, different clades within multiple infected individuals can genetically recombine to create circulating recombinant forms (CRFs) (274, 323). Currently, the most prevalent HIV-1 subtype is clade C, accounting for the highest number of infections (50%), followed by clade A (12%), clade B (10%), CRF02-AG (5%) and CRF01-AE (4.8%) (125, 323).

HIV-2 is also highly divergent and can be classified into eight distinct groups (A to H). In contrast to the global prevalent of HIV-1, HIV-2 is geographically more restricted, and has been found in West Africa and most recently in Europe and India (38, 69). Although HIV-2 shares similar genetic properties with HIV-1, it is different from HIV-1 by 50-60% in nucleotide sequence (114), and more closely related to the SIVsmm from the West African sooty mangabey (69). In terms of the level of disease, HIV-2 infected patients develop AIDS slower and survive longer (205, 268) than HIV-1 infected patients. Additionally, the vertical and horizontal transmissibility of HIV-2 is significantly lower than that of HIV-1 (152, 247). Hereafter, we will mainly discuss HIV-1 in this thesis.

### 1.2.2 HIV-1 structure and genome

HIV-1 is about 100 to 120 nm in diameter with spherical shape as shown in Fig. 1.1. The virion is coated with a lipid envelop, which contains cell-derived lipid bilayers and viral envelope glycoproteins (Envs) (347). On the surface of the mature virion, Envs are displayed in knobbed spike structure, formed from surface protein gp120 and transmembrane protein gp41. These two glycoproteins noncovalently bind to each other and form the heterodimers (124). The central core of the virion is constituted of the Gag structural proteins: p17, p24, and p7. The matrix (MA) protein p17 forms the inner surface of the viral envelope; the capsid (CA) protein p24 forms the cone-shaped core; and the nucleocapsid (NC) protein p7 is located within the core,

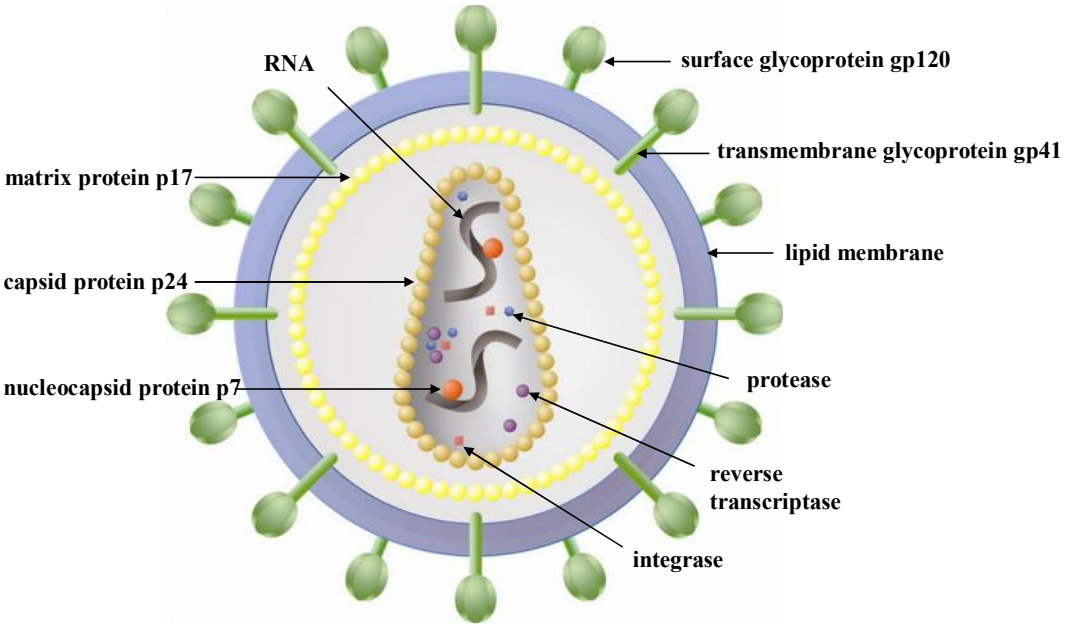


**Fig. 1.1 Morphologic structure of HIV-1.** HIV-1 virus is enveloped by a lipoprotein membrane. Env glycoprotein complexes composed of gp120 and gp41 are integrated into this lipid membrane. MA is anchored to the inner surface of viral envelop. CA forms the cone-shaped core. NC is associated with two copies of HIV-1 genome RNA within the core. The viral particle also contains viral enzymes RT, IN, PR, and non-structural proteins.

as a binding partner of viral RNA (180). Inside the core, there are two identical copies of single-stranded RNA genome, which is associated with viral enzymes and accessory proteins (356). Besides that, cellular molecules such as tRNAs, annexins, actin A3G and moloney leukemia virus 10 from the infected cells are incorporated into virions as bystanders or through interacting with viral proteins (51, 163, 251, 279, 296, 337).

The HIV-1 genome is a 9.2 kb positive-stranded RNA molecule. It contains nine open reading frames (ORFs) and several structural landmarks (Fig. 1.2). Three of ORFs encode Gag, Pol and Env polyprotein precursors, which are proteolytically processed into individual proteins. Gag precursor p55 is cleaved by protease (PR) to generate structural proteins p17, p24, p7, and p6. Gag-pol precursor is proteolytically processed into three enzymes PR, RT and integrase (IN). Env precursor gp160 is cleaved by endoprotease furin into gp120 and gp41 (118). HIV-1 also encodes six non-structural proteins which have particular regulatory or accessory functions, including transactivator (Tat), regulator of expression of virion protein (Rev), negative factor (Nef), virion infectivity factor (Vif), viral proteins R and U (Vpr and Vpu, respectively) (183). In addition, the HIV-1 RNA genome forms several secondary structures, including the internal ribosome entry site (IRES), packaging signals (pis), psudoknots, transfer RNA mimics, ribosomal frameshift motifs, *cis*-regulatory elements, Tat-acting region (TAR), primer binding site (PBS), dimer initiation site (DIS) and polypurine tract (PPT)(340, 344). These RNA structures regulate viral

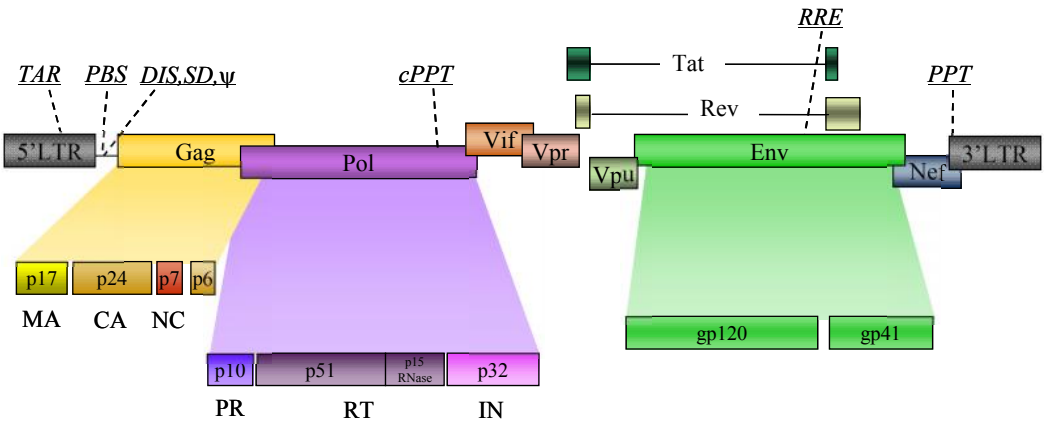


**Fig. 1.2 Genomic organization of HIV-1.** HIV-1 genome flanked by the long terminal repeats (LTRs) contains 9 ORFs (shown as rectangles) and several structural landmarks (shown in underlined italic characters). Gag and Gag-pol polyproteins are processed by viral protease into matrix (MA), capsid (CA), nucleocapsid (NC), p6, protease (PR), reverse transcriptase (RT), integrase (IN). Envelop (Env) is cleaved by cellular proteases into gp120 and gp41. Landmarks include Tat-acting region (TAR), primer binding site (PBS), dimer initiation site (DIS), splice donor (SD) and central polypurine tract (cPPT), rev response element (RRE) and PPT.

replication, from reverse transcription initiation and reading frames manipulation to RNA nuclear export and viral RNA packaging.

### 1.2.3 Overview of HIV-1 proteins

#### 1.2.3.1 HIV-1 structural proteins

Viral structural proteins are shared by all retroviruses, their functions are reviewed as below.

**Gag** encodes a 55 kDa precursor Pr55-Gag that is cleaved to produce the mature proteins: MA, CA, p2, NC, p1 and $p6^{Gag}$. These proteins play critical roles at several steps of viral replication.

**MA** is a 17 kDa structural protein that is post-translationally myristoylated at N-terminus (25). During viral assembly, being the N-terminal domain of Gag, MA regulates the Gag intracellular location, and directs Gag to the plasma membrane (25). It also interacts with the gp41 cytoplasmic tail and promotes incorporation of Env into the virion (27, 102). Additionally, it contributes to nuclear migration, nuclear import and integration as a part of the reverse transcription complexe (RTC) and pre-integration complex (PIC) (37, 262, 333).

**CA** is a 24 kDa protein responsible for the formation of viral core. During viral assembly, the interactions between CA domains promote Gag multimerization and formation of the immature virion (3). After entry into the target cell, CA is thought to modulate the core uncoating through controlling capsid stability and disassembly (2,

140). Interaction between CA and host protein cyclophilin A enhances early stages of viral replication (186).

**NC** is a 7 kDa nucleic acid binding protein. During viral assembly, by binding to genomic RNA, NC drives selection, dimerization and encapsidation of genomic RNA into virions (68, 226). NC also facilitates nucleic acid structural reorganization which is required for efficient reverse transcription, viral DNA maintenance and integration (36, 181).

**P6** $^{Gag}$ is located at the C terminus of Gag and regulates the final step of virus budding. It promotes separation of assembled virion from the plasma membrane through interacting with components of cellular budding machinery such as endosomal sorting complex required for transport (ESCRT) (327). It is also required for the incorporation of Vpr into virions (166, 358).

**Env** encodes the polyprotein precursor gp160 that is cleaved by the cellular protease furin into two subunits gp120 and gp41. These two subunits non-covalently bind to each other and form the gp120/gp41 complex. HIV-1 Env mediates viral entry into target cells, in which the gp120 subunit is responsible for cell receptor (CD4) and coreceptor (CCR5 or CXCR4) binding, and gp41 facilities the fusion between viral and cellular membranes (63, 347).

#### 1.2.3.2 HIV-1 enzymatic proteins

**Pol** ORF partially overlaps with Gag, and is expressed as 160 kDa Gag-Pol polyprotein Pr160-Gag-Pol through -1 ribosomal frameshifting (144). During viral

maturation, viral PR auto-activates and cleaves Gag-Pol into MA, CA, p2, NC, the transframe protein, and vial enzymes PR (p10), RT (p66/p51), IN (p32).

**PR** is an aspartic protease that functions as a homodimer. Besides cleaving viral precursors, PR also targets host cellular proteins, such as cytoskeletal proteins, Bcl-2, and contributes to viral induced cytotoxicity (301, 311).

**RT** is an asymmetric heterodimer that consists of a 66 kDa (p66) and 51 kDa (p51) subunit. The p51 subunit is produced by proteolytic cleavage of p66 C-terminal ribonuclease H (RNase H) domain (127). The p66 subunit exhibits all catalytic activities, whereas p51 is catalytically inactive and plays primarily structural role (269). RT is responsible for several distinct activities, including DNA- and RNA-dependent DNA polymerase, RNase H, strand transfer and strand displacement synthesis (105, 283).

**IN** exists as tetramers and catalyzes integration of viral DNA into host chromosome. It facilities site-specific endonucleolytic cleavage of the 3′-ends of the viral DNA (3′ processing), and integration of processed viral DNA ends into host chromosomal DNA (strand transfer) (53). In addition to integration, IN also contributes to other steps of viral replication, including reverse transcription, nuclear import and post-integration steps (polyprotein processing, assembly, and maturation) (85).

#### 1.2.3.3 HIV-1 regulatory proteins

**Tat** is a 9-11 kDa (size varies in different viral strains) protein that is essential for

HIV-1 transcription from the viral LTR promoter. Rather than other transcriptional activators, Tat functions at the stage of transcription elongation through interacting with TAR. Their interaction promotes recruitment of positive transcription elongation factor (P-TEFb) to increase hyperphosphorylation and functional capacity of RNA polymerase II (RNAPII) (200). In addition to its primary role as endogenous trans-activator, Tat is secreted by infected cells and acts as an extra-cellular toxin (98). Exogenous Tat can induce various biological effects, including production of certain cytokines, apoptosis of uninfected bystander $CD4^+$ T cells and neurotoxicity in the central nervous system (183, 281).

**Rev** is a 19 kDa phosphoprotein located predominantly in the nucleus (58). During the late stages of viral replication, it binds to single spliced or unspliced viral mRNAs via the RRE, and mediates their nuclear export through interacting with the cellular nuclear export receptor CRM1 (95). Rev also affects stability, translation and encapsidation of Rev-bound viral transcripts (110). In addition to an essential role in late stage of viral replication, Rev has been shown to regulate HIV-1 integration frequency by binding to integrase and LEDGF/p75, as well as preventing superinfection at a post-entry step (109).

#### 1.2.3.4 HIV-1 accessory proteins

Although several viral nonstructural proteins are found to be dispensable for viral replication in certain *in vitro* cell culture systems, these proteins are important in determining the course and severity of viral infection *in vivo*. They often play critical

roles in HIV-1 pathogenesis and host defence evasion. Here, their functions are discussed in detail.

**Vif** is a 23 kDa protein that is highly expressed in the cytoplasm of infected cells. It is essential for *in vivo* infectivity and pathogenesis. During viral assembly, it binds to genomic RNA and the NC domain of Pr55-Gag, and acts as a temporal regulator of viral assembly (126). More importantly, Vif counteracts the antiviral activity of A3G, and a detailed Vif-A3G interaction will be discussed in the section 1.4.

**Vpr** is a 14 kDa nuclear protein that plays multifunctional roles *in vivo*. The ORF encoding Vpr is found in most HIV-1 primary isolates (197). During viral replication, virion-associated Vpr participates in the nuclear entry of the PIC, and promotes PIC binding to nuclear pore proteins (72). In the nucleus, it acts as coactivator to induce translational activation of HIV LTR and host genes (165). Vpr is shown to induce $G_2$ cell cycle arrest in infected proliferating cells, and thereby optimize the cellular environment for efficient HIV-1 transcription (106). It also modulates T-cell apoptosis by inducing apoptosis through mitochondria-dependent pathway (20, 64, 146).

**Vpu** is a 9 kDa integral membrane protein that has two primary functions in HIV-1 replication. First, it hijacks βTrCP/SCF ubiquitin ligases to degrade newly synthesized CD4, which further prevents CD4-Env binding in the endoplasmic reticulum and at cell surface (179, 202, 322); second, Vpu enhances the release of virion through promoting the virion detachment from the cell surface (235). More recently, studies found that Vpu counteracts host factor BST-2 mediated inhibition of viral release through β-TrCP and endo-lysosomal trafficking (79, 216).

**Nef** is a 27 kDa myristoylated protein that is abundantly expressed at the early stage of viral replication (305). It promotes viral replication and survival through multiple ways, and its pathogenic role is highlighted in long-term nonprogressors whose HIV-1s are Nef-deleted (84). Long-term nonprogressors is a group of HIV-1 seropositive, therapy-native individuals who remain asymptomatic for prolonged length of time(214). Nef mediates down-regulation of cell surface CD4, CXCR4, CCR5 coreceptors, and thereby restricts superinfection (213, 331). It also down-regulates cell surface expression of major histocompatibility complex class I (MHC-I) and facilitates evasion of infected cells from cytotoxic T lymphocytes mediated lysis (353). Additionally, Nef promotes viral replication through modulating cytoskelatal remodeling, vesicular transport and cellular signal transduction pathways (183).

### 1.2.4 HIV-1 life cycle

HIV-1 replication is a complex procedure regulated by both viral and cellular proteins. At the cellular level, HIV-1 life cycle can be divided into two phases: the early stage from viral entry to viral DNA integration; and the late stage from transcription of integrated DNA to virus budding and maturation (Fig. 1.3).

#### 1.2.4.1 Early phages

**HIV-1 binding and entry** HIV-1 initiates infection through entry of target cells. First, HIV-1 attaches to the host cell by binding to cellular receptor CD4 via gp120

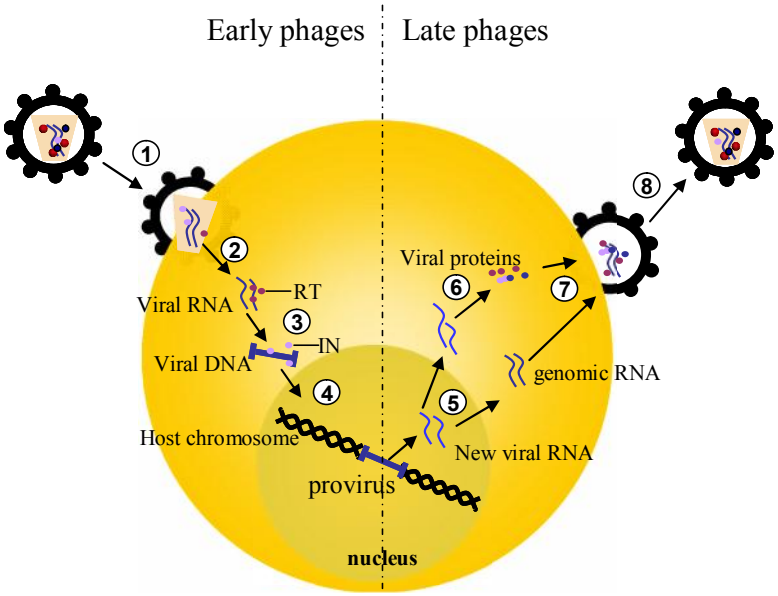


**Fig. 1.3 HIV-1 life cycle.** After binding and fusing to host cell membrane (step 1), the viral core enters the cytoplasm and undergoes uncoating (step 2). The viral RNA is reverse transcribed into double-strand DNA (step 3), and transported into nucleus, where viral DNA is integrated into host chromosome (step 4). After integration, the provirus is transcribed into viral RNA genome and mRNAs, which are transported into cytoplasm (step 5). Viral mRNAs are translated into viral proteins (step 6), together with viral genome are incorporated into viral particles (step 7). New virions bud from cell membrane, followed by PR-mediated maturation (step 8).

protein. CD4 binding triggers a conformational change in gp120, resulting in exposure of coreceptor (CCR5 or CXCR4) binding sites. Together, CD4 and coreceptor binding induces gp41 rearrangement and exposure of the hydrophobic gp41 fusion peptide, which further promotes virus-cell membrane fusion by inserting into the cell membrane (221, 343).

**HIV-1 uncoating** Following the entry of HIV-1 core into target cell, CA shell undergoes a disassembly process that allows the release of genomic RNA. Although the precise location and timing of uncoating are poorly defined, this process is believed to be regulated by viral and host cellular factors through modulating capsid stability (2, 16).

**HIV-1 reverse transcription** Reverse transcription is a complex process that occurs in the RTC and is catalyzed by the virus-encoded RT. By using cellular $tRNA^{lys3}$ as primer, this enzyme first converts the plus-strand viral RNA template to minus-strand DNA. Meanwhile, it performs RNase H activity to degrade the reverse transcribed viral RNA except PPT regions. PPTs function as the primer and initiate plus-strand DNA synthesis. Then the minus- and plus strand DNAs are elongated, leading to the synthesis of the complete, double stranded linear viral DNA (137, 181).

**Nuclear import and integration** Once synthesized, viral DNA is transported into nucleus as part of the PIC. PICs cross the nuclear envelop with the help of cellular active transport machineries (319). Following entry nucleus, virus-encoded IN protein catalyzes integration of the viral DNA into chromosomal DNA. During 3′ processing, IN recognizes and removes a pGT dinucleotide from each 3′ end of LTR. This step,

termed strand transfer, generates 3′-hydroxyl group viral DNA ends, which are covalently ligated to the 5′-phosphates of staggered cut in chromosomal DNA. Subsequently, unpaired viral 5′ ends and DNA gaps created between viral and chromosomal DNA are repaired by cellular DNA repair enzymes (66, 330). Thus, viral DNA is completely integrated into host genome as provirus, serving as the template for new virion synthesis (148).

#### 1.2.4.2 Late phages

**HIV-1 transcription and nuclear export** Following integration, HIV-1 provirus acts as a template for mRNA synthesis. This step is catalyzed by cellular RNA polymerase II (252). Initially, completely spliced short mRNAs encoding Tat, Rev and Nef are synthesized and exported to the cytoplasm through an endogenous cellular pathway. As the transcriptional activator-Tat protein accumulates, transcription is actively up-regulated, and incompletely spliced mRNAs encoding Env, Vpu, Vif and Vpr are synthesized. It is followed by the production of full-length unspliced transcripts, which are served as virion genomic RNA and mRNA for Gag-Pol polyprotein (157, 326). Unspliced and incompletely spliced mRNAs are transported through the nuclear pore to cytoplasm *via* Rev dependent export pathways (157).

**HIV-1 translation** Prior to translation initiation, HIV-1 mRNA undergoes 3′ processing and polyadenylation, which are directed by HIV-1 regulatory elements within the 3′ LTR region (157). Once in the cytoplasm, HIV-1 recruits the cellular translation machinery to synthesis viral proteins (157). Gp160 is synthesized in the

endoplasmic reticulum (ER), and transported to the cell membrane for virus assembly via vesicular transport. Gag and Gag-Pol precursor are synthesized on free polyribosomes from unspliced genomic RNA, and Gag-Pol is generated by a programmed -1 ribosomal frameshift (103, 326).

**Assembly** In most cell types, HIV-1 assembles on the plasma membrane, which is initiated by Gag multimerization. Gag acts as "assembly machine" that drives a number of essential events in virion assembly (100, 151). It specifically recruits viral genomic RNA and protein components, targets viral membrane and assembles into spherical particles. Meanwhile, upon post-translational modification, Env glycoproteins traffic independently to the assembly site, and incorporate into immature virions (225).

**Budding and maturation** In order to begin the budding process from host cells, HIV-1 recruits the ESCRT pathway through a late-assembly domain in $p6^{Gag}$. The ESCRT complex promotes membrane fission and facilitiates virion release from the plasma membrane (327). During or shortly after budding, immature virion undergoes maturation. Gag and Gag-Pol polyproteins are cleaved by viral PR and rearranged to create fully mature and infectious virions.

### 1.3 Host restriction factors and their roles in HIV-1 infection

It is apparent that HIV-1 replication largely relies on multiple cellular factors. Further studies have revealed that host cells also harbor intrinsic defense proteins that function in blocking intracellular replication of HIV-1. These proteins are termed host

restriction factors.

Since the discovery of A3G in 2002 (296), several unrelated host restriction factors were uncovered. These factors target viral replication through different mechanisms and are important in determining viral host range and cross-species transmission. Nevertheless, HIV-1 encodes viral accessory proteins to antagonize them. The interaction between host restriction factors and viral proteins further reflects host-pathogen coevolution (81).

### 1.3.1 General properties of restriction factors

So far, four HIV-1 restriction factors have been identified: A3G, tripartite motif (TRIM) 5α, bone marrow stromal cell antigen 2 (BST-2) (also known as tetherin) and sterile alpha motif and histidine-aspartic domain 1 (SAMHD1). These factors share several universal properties, which are summarized in Table 1.1.

First, restriction factors must have very potent antiviral effect and impair viral infectivity by at least 10-fold. Rather than innate immune response which is meditated by immune cells via complex pathways, restriction factors act in a cell-autonomous manner and mediate 'cell-intrinsic' immune response. Their antiviral activity can be demonstrated experimentally by single-cycle viral replication assay, where restriction factors are either overexpressed in permissive cells or knocked out in non-permissive cells (30, 81).

Second, restriction factors are germline-encoded and expressed constitutively in some relevant cell types. They respond to interferon (IFN) stimulation, which

**Table 1.1 Characteristics of host restriction factors**

| Restriction factor | Regulation | Targeted viruses | Targeted step | Viral antagonist | Antagonistic mechanism |
|---|---|---|---|---|---|
| A3G | IFN | retroviruses, retrotransponsons, hepadnaviruses | reverse transcription and integration | Vif | polyubiquitination and degradation |
| TRIM5α | IFN | retroviruses | uncoating | high variability | variation in retroviral capsid |
| BST-2 | IFN | retroviruses, flaviviruses, herpesviruses, rhabdoviruses, paramyxoviruses, arenaviruses | viral release | HIV-1 Vpu; HIV-2 SIVmac Env, SIV Nef | internalization and sequestration from sites of viral assembly |
| SAMHD1 | IFN, IFN-stimulatory DNA | Retroviruses, herpes simplex virus type 1, vaccinia virus | reverse transcription | HIV-2, SIVmac Vpx; SIVdeb, SIVagm Vpr | proteasomal degradation |

up-regulates their protein expression, thereby enhancing their antiviral activity (234). However, IFN induction is not necessary for achieving considerable antiviral effect (30).

Third, restriction factors are antagonized by viral proteins with the exception of TRIM5α. Although viral antagonists overcome antiviral effect through diverse mechanisms, antagonism is exclusively triggered by direct protein-protein interactions between viral antagonist and corresponding restriction factors, and often recruits cellular degradation or transport pathways (121). As the consequence of positive selection, their interactions may further drive the evolutionary change in both hosts and viruses (30, 81).

### 1.3.2 APOBEC3G

A3G is a 46 kDa cytoplasmic protein that localizes in the mRNA processing (P) bodies and stress granules, which are the ribonucleoprotein-rich cytoplasmic microdomains (99). A3G is a single-stranded DNA cytidine deaminase that blocks HIV-1 infection in the absence of Vif. It induces the G-to-A hypermutations in viral cDNA, and inhibits HIV-1 reverse transcription and integration. However, HIV-1 Vif counteracts the action of A3G through multiple mechanisms (4), which will be discussed in detail in section 1.4.

### 1.3.3 TRIM5α

TRIM5α is the second discovered restriction factor identified by screening of a rhesus macaque cDNA library (315). It is a 57 kDa cytoplasmic protein (30). Immediately following viral entry, TRIM5α targets incoming viral CA for disassembly and/or degradation, thereby disturbing viral uncoating and promoting

downstream innate immune response (259).

As a member of the TRIM family proteins, TRIM5α contains a typical TRIM composed of N-terminal Really Interesting New Gene (RING), B-box and coiled-coil domains (30). RING is a zinc-binding domain that confers E3 ubiquitin ligase activity. B box and coiled-coil domains mediate formation of TRIM5α multimers, which is required for antiviral activity. C-terminal domain (CTD) of TRIM5α, called B30.2 or SPRY domain, recognizes the lattice of viral CA in a species-specific manner, and determines specificity of restriction (30, 196).

Generally, TRIM5α is ineffective against retroviruses that naturally infect same host species, but actively blocks replication of retroviruses that are found in other species. For example, human TRIM5α (hTRIM5α) only exhibits relatively weak anti-HIV activity, but potently inhibits equine infectious anemia virus (ELAV) and N-tropic murine leukemia virus (MLV) infection. In contrast, rhesus TRIM5α actively restricts HIV-1 infection (315). Interestingly, the point mutation at residue 332 (R332P) in CTD of hTRIM5α confers its restriction potential against HIV-1 (359).

### 1.3.4 BST-2

BST-2 is a 19.7 kDa IFN-induced protein that acts as an inhibitor against the release of HIV-1 and other enveloped viruses. It blocks viral release by trapping nascent virions on the surface of the infected cells, from where they may be endocytosed (236). BST-2 is an unusual type II single-pass transmembrane protein. It is composed of a short N-terminal cytoplasmic tail (CT) followed by an α-helical transmembrane (TM) anchor, a extracellular coiled-coil domain and a C-terminal glycophosphatidylinositol (GPI) lipid anchor. It also contains three extracellular cysteines that promote BST-2 dimerization (258).

BST-2 is concentrated at sites of viral assembly and directly cross-links virions to the plasma membrane (92). A study from Perez-Caballero et al. clarified that BST-2 configuration, but not its primary sequence, is critical for its antiviral activity (258). They further proposed the model of the action of BST-2. One pair of anchors, either TM anchor or GPI anchor, is incorporated into virion envelope, whereas the other pair of anchors remains in the plasma membrane, thereby physically tethering virions to cells. Alternatively, both anchors are incorporated into virions and link virions to each other, or trap the virions on the cell surface through multimerization of BST-2 distributed between virion envelope and plasma membrane (258).

However, in order to replicate efficiently, viruses have adapted diverse strategies to antagonize BST-2. More than one antagonist has been employed by primate lentiviruses, including Vpu, Nef, and Env. HIV-1 Vpu directly interacts with BST-2 via their transmembrane domains and transports BST-2 to the trans-Golgi network/ early endosomes where BST-2 undergoes proteasomal and/or lysosomal degradation (162). Instead of Vpu, some SIVs use Nef to antagonize BST-2. Nef recruits Adaptor Protein-2 clathrin adaptor complex to target BST-2 and induces its endocytosis (364). Additionally, Env gp41 cytoplasmic tail of HIV-2 and $SIV_{MAC}$ physically interacts with BST-2 and promotes the internalization and sequestration of BST-2 from sites of viral assembly on the cell surface (121, 177).

### 1.3.5 SAMHD1

Most recently, SAMHD1 was defined as a restriction factor. It is highly expressed in myeloid cells and resting $CD4^+$ T cells, and indirectly inhibits viral reverse transcription by reducing intracellular deoxynucleoside triphosphate (dNTP) levels (22, 136, 173). SAMHD1 is 72 kDa protein that is responsive to IFN-γ and tumor

necrosis factor (TNF)-α (188). It is composed of an N-terminal nuclear localization domain, SAM domain, HD domain and C-terminal variable domain (370). The SAM domain mediates protein-protein interaction. The HD domain contains conserved histidine and aspartate residues, and is involved in nucleic acid metabolism and RNA binding (15, 342).

SAMHD1 depletes the intracellular dNTP pool through dNTPase activity. After activation by dGTP, SAMHD1 hydrolyzes dNTPs substatrates to deoxynucleosides and inorganic triphosphate (107, 174). SAMHD1 mediated restriction can be relieved by addition of exogenous dNTPs to the level required for the synthesis of viral cDNA.

However, HIV-2 and certain SIVs express Vpx to antagonize the effect of SAMHD1. Vpx recognizes the C-terminal residues of SAMHD1 and binds to it through the N-terminal unstructured region. Meanwhile, Vpx binds to the DDB1-Cul4A-associated-factor-1 protein and recruits a Cullin4A-based unbiquitin ligase complex for polyubiquitination and degradation of SAMHD1 (370). In contrast, HIV-1 does not encode Vpx or alternative proteins capable of counteracting SAMHD1. This deficiency provides explanation for the fact that HIV-1 replicates poorly in macrophages, dendritic cells and resting $CD4^+$ T cells (172). Restricted HIV-1 replication limits immune detection in these cells, thereby ensuring initial viral infection and transmission.

## 1.4 APOBEC3G protein

### 1.4.1 General properties of A3G

A3G, originally called CEM15, belongs to the APOBEC enzyme family (296). APOBEC family consists of a panel of polynucleotide (deoxy) cytidine deaminases that share a conserved zinc-coordinating motif His-X-Glu-$X_{23–28}$-Pro-Cys-$X_{2–4}$-Cys(X

stands for any residue) (147). These enzymes catalyze the hydrolytic deamination at the C4 position of the cytosine, thereby converting cytidine to uridine (122).

The APOBEC family in humans includes activation-induced deaminase (AID), APOBEC1, APOBEC2, seven paralogs of APOBEC3 (A-H) and APOBEC4 (55, 275). The functions of the first two deaminases have been well-studied. APOBEC1 is involved in lipid metabolism by introducing a premature stop codon in apolipoprotein B mRNA (210). AID is required for the antibody diversification via promoting somatic hypermutation and class switch recombination (224). Besides A3G, other APOBEC3 family members also have the antiviral potency against various viruses including HIV-1 (54).

Human A3G is encoded on q13.1 of chromosome 22. It contains two homologous zinc binding domains, of which only the C-terminal domain (residue 195-384) has catalytic activity (Fig. 1.4 A). The N-terminal domain (NTD, residue 1-194) is responsible for the virion packaging and Vif interaction (48, 196). Structural studies indicate that the CTD of A3G consists of five α-helices and five β-strands. α1-β3-α2 further forms zinc-coordinating motif (50). In this motif, the catalytic zinc is coordinated by a histidine (H257) and two cysteines (C288, C291) (294). Guided by structure of APOBEC2, Zhang et al. modeled the structure of A3G NTD (366). Together with other studies, it was shown that residues 124 to 127 are critical for A3G packaging into HIV-1 virions, and adjacent residues 128 to 130 are crucial for Vif binding (141). In correspondence with active catalytic glutamate E259 in CTD, NTD contains a pseudo-catalytic residue E67 (115).

The level of A3G varies in different tissues. It is highly expressed in spleen followed by lymph node and lung, but poorly expressed in skeletal muscle and brain (167, 270). Also, A3G expression in hepatocytes and lymphoid cells are induced upon

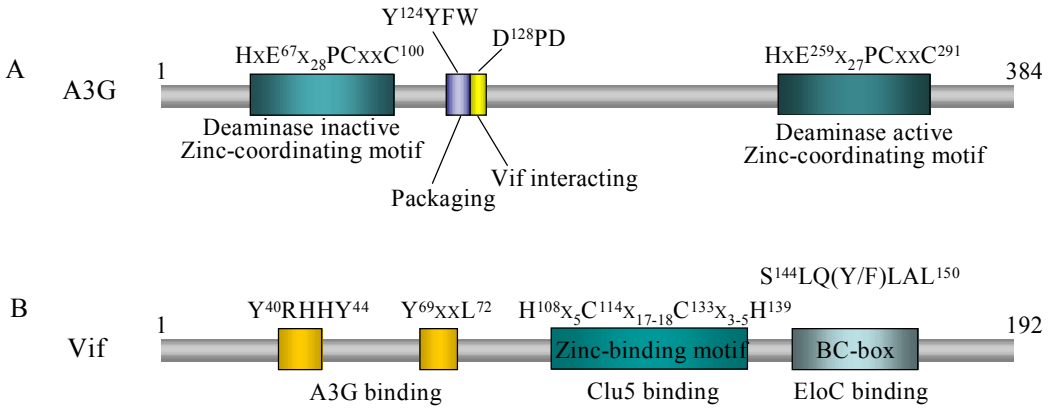


**Fig. 1.4 Domain structure of A3G and Vif.** (A) Human A3G contains two zinc finger domains with the conserved zinc-coordinating motifs (HECC), only the C-terminal motif is enzymatically active. Virion packaging motif (YYFW) and Vif-interacting motif (DPD) are located at N-terminal domain as indicated. (B) HIV-1 Vif is a 194 amino acid protein with indicated functional domains. Vif interacts with Cul5 and ElonC via the C-terminal Zinc-binding motif and BC-box. N-terminal domains (YRHHY and YXXL) bind to A3G. Numbers indicate amino acid positions.

T-cell activation or certain cytokine and mitogen treatment (33, 222, 284). One cellular function of A3G is to protect host cell genome from invasion by exogenous retroviruses and endogenous retrotransposons, such as musD, and Alu elements (56, 139).

### 1.4.2 A3G and HIV-1 replication

The action of A3G in HIV-1 replication was discovered during the investigation of the function of Vif (4, 296). According to Vif's requirement for productive infection, human cell lines are grouped as "Vif-dependent/nonpermissive" for cells that do not support the replication of Vif⁻ HIV (eg. H9, CEM, HUT78), or "Vif-independent/permissive" (eg. CEM-SS, SupT1, 293T, C8166). Once permissive and non-permissive cells were fused, virions produced from heterokaryons were non-infectious, suggesting that nonpermissive cells contain a restriction factor that Vif overcomes (193). Later on, by using a suppression subtractive hybridization technique, Sheehy et al. identified this restriction factor-A3G. They have demonstrated that A3G is expressed preferentially in nonpermissive cells, and expression of A3G renders permissive cells nonpermissive for the replication of Vif⁻ virus (296). Since then, a number of studies have been conducted to explore the antiviral mechanisms of A3G (Fig. 1.5A).

#### 1.4.2.1 Deaminase-dependent antiviral activity

In the absence of Vif, endogenous or overexpressed A3G from viral producing cells is packaged into budding HIV-1 virion and carries-out its function in the subsequent round of infection. In the target cells, during viral reverse transcription, A3G specifically targets minus-strand DNA and deaminases cytidine to uracil. Next,

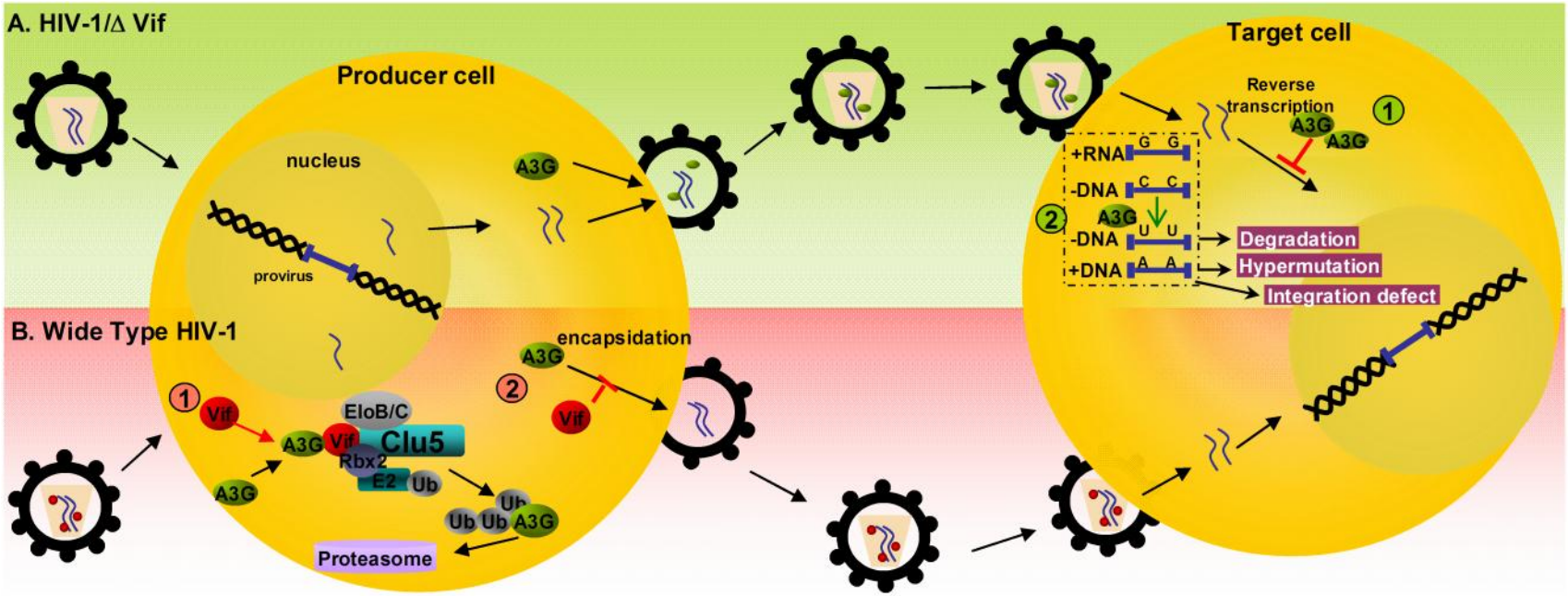


**Fig. 1.5 Effect of A3G on HIV-1 replication.** (A) Effect of A3G on Vif⁻ HIV-1. In the absence of Vif, A3G is efficiently incorporated into newly formed virions. After A3G-containing virions enter the target cell, A3G impedes HIV-1 reverse transcription through a deaminase-independent antiviral action (1). Once reverse transcription starts, A3G induces the dC to dU mutations on minus-strand DNA (2). (B) Effect of A3G on wild type HIV-1. In viral producing cells, Vif binds to A3G and recruits the E3 ubiquitin ligase complex for A3G polyubiquitination and proteasomal degradation (1). Also, Vif physically inhibits A3G encapsidation (2). Thus the produced virions remain infectious and are able to complete the replication cycle.

during plus-strand DNA synthesis, adenine is incorporated as the complementary base to uracil, resulting in Guanine to Adenine (G-to-A) hypermutation in viral plus-strand (195, 198). Consequently, the proviral DNA harboring such hypermutation would encode viral proteins with premature stop codons or mutated proteins (360). Alternatively, uracil in minus-strand DNA could be recognized and excised by cellular DNA repair enzymes (eg. uracil DNA glycosylases-2, single-strand selective monofunctional uracil DNA glycosylase-1). The resulting abasic sites may further trigger apurinic/apyrimidinic endonuclease mediated degradation of viral DNA (120). Detailed features of A3G-mediated mutagenesis have been demonstrated through analyzing hypermutated HIV-1 genomes. First, A3G preferentially causes mutations within 5′ GG dinucleotide motifs on the plus-strand, especially 5′ TGGG site (target cytidine underlined) (360). This preference by converting tryptophan codon (TGG) to a stop codon (TAG) offers explanation for the fact that hypermutation commonly induces formation of truncated viral proteins. Second, A3G induces two highly polarized gradients of hypermutation, where mutation rates increase in a 5′ to 3′ direction from cPPT and 3′ PPT (46, 318). Given that plus-strand synthesis is initiated at these two PPT sites, the gradients are consistent with the time that minus strand DNA substrates remain single stranded (318). Additionally, biochemical studies indicated that A3G binds ssDNA randomly and scans for the processive substrates through either sliding within a localized region or jumping among multiple regions (47, 293).

#### 1.4.2.2 Deaminase-independent antiviral activity

The catalytic activity of A3G is not the only determinant of its antiviral activity (299). A number of studies indicated that A3G is capable of inhibiting HIV-1

replication through deaminase-independent effects. Replacement of critical residues (H257R, E259Q, C291S) in CTD abolishes the enzymatic activity of A3G, but fails to significantly impair their antiviral activity (237).

Results from *in vitro* systems where nucleases are absent suggest that A3G affects viral DNA content by impeding DNA synthesis (195). Indeed, it is shown that A3G interferes with several steps of HIV-1 reverse transcription, including the inhibition of $tRNA^{lys3}$ primer annealing through interaction with NCp7 (111, 112), the blocking of strand transfers which consequently reduces late viral DNA synthesis (185, 206) and the suppression of $tRNA^{lys3}$ cleavage and removal which produces aberrant viral 3′-LTR ends (206). Using purified A3G protein, Iwatani et al. showed that A3G significantly inhibits all RT-catalyzed DNA elongation reactions (143). Additionally, endogenous reverse transcription assays in cell-free HIV-1 particles demonstrated that A3G reduces HIV-1 viral DNA levels by inhibiting the elongation of reverse transcripts rather than enhancing degradation (10).

Still, the effect of deaminase-defective A3G on the accumulation of viral DNA is debatable. Since most studies proved its antiviral effect in the context of overexpression systems (eg. transfection of expression plasmids for cell culture experiments and artificially high amount of purified protein for *in vitro* experiments) (195), it is therefore desirable to clarify the relative contributions of deamination-dependent versus -independent effects of A3G in physiologic relevant concentrations and *in vivo* infections.

#### 1.4.2.3 Effect of A3G *in vivo*

Several *in vivo* studies carried out in rhesus macaques indicated that following immunization, the level of A3G in lymphatic tissues and immune cells is significantly

increased. A3G expression is further shown to correlate with vaccine and adjuvant-induced protection against subsequent SIV challenge (316, 338, 339). Meanwhile, increasing evidence has linked upregulated A3G expression with improved clinical status. Albin et al. summarized data from 11 cohort studies and concluded that, A3G mRNA levels and hypermutation rate positively correlate with $CD4^+$ T cell counts and negatively correlate with viremia (4). Moreover, higher level of A3G expression has been found in HIV-exposed seronegative individuals and HIV-1-infected long-term nonprogressors.

Despite some researchers proposed that A3G induced hypermutation may contribute to HIV-1 evolution, leading to the occurrence of drug resistant and immune escape mutations. This theoretical possibility is supported only by limited *in vivo* data (4). Also, results obtained from *in silico* model suggest that the effect of A3G on the HIV-1 evolution is very low (149). Therefore, A3G can still be considered a suitable target for the development of new anti-HIV-1 strategies.

### 1.4.3 The role of A3G against other viruses

In addition to HIV, other retroviruses including SIV, ELAV, MLV and foamy viruses (FVs) are also the target of A3G (198). A3G triggers G-to-A hypermutation in their viral genome through editing activity (71).

A3G has shown a more general antiviral activity against T cell leukemia virus type-1 (HTLV-1) and hepatitis B virus (HBV), mainly in a manner that does not require deamination. Both wild type and catalytically inactive A3G are able to be incorporated into HTLV-1 virions and regulate viral infectivity. But hypermutations are not abundant in HTLV-1 viral DNA (285). As to HBV infection, G-to-A mutations are found rarely in infected individuals (243, 273). Instead, studies using

human hepatoblastoma cell lines indicated that A3G targets the DNA-RNA hybrid, and reduces virus synthesis at early steps of viral reverse transcription and elongation through deamination-independent activity (238, 242).

In addition, A3G acts as an ancestral defense against endogenous retroelements (86, 87). Retroelements are mobile genetic elements, which make up 8-10% of host genome (194). Both human A3G and murine homologue A3G are shown to be able to inhibit retrotransposition of murine intracisternal A-particles and MusD, and induce G-to-A hypermutations in their transposed sequences. Thus, partially due to its catalytic activity, A3G is capable of inhibiting replication of multiple viruses and endogenous retroelements.

### 1.4.4 Interactions between A3G and viral components

In order to be incorporated into virions and perform antiviral effects, A3G interacts with several viral components. Meanwhile, HIV-1 regulates the action of A3G by Vif protein, mainly through proteasomal degradation pathway.

#### 1.4.4.1 Interaction with HIV-1 Vif

Lentiviruses, such as HIV-1, encode a viral accessory protein Vif to counteract the antiviral effect of A3G. In the viral producing cells, Vif neutralizes A3G's activity through at least three different actions. First, Vif binds to A3G and promotes its degradation through the 26S proteasome; second, Vif directly inhibits A3G encapsidation; and third, Vif impairs the translation of A3G mRNA (Fig. 1.5B) (4, 126).

In order to promote A3G's degradation, Vif recruits an E3 ubiquitin ligase complex comprising the proteins Cullin5 (Cul5), Rbx2, Elongins B (EloB) and C

(EloC). Vif binds to this complex via two motifs (Fig. 1.4B). In particular, the C-terminal conserved $S^{144}LQ(Y/F)LAL^{150}$ motif forms the BC-box and binds to EloC. The highly conserved zinc-binding motif $H^{108}$-$X_5$-C-$X_{17-18}$-C-$X_{3-5}$-$H^{139}$ (HCCH) binds to Cul5. Substitution of the BC-box domain (SLQ portion) or the HCCH motif in Vif is sufficient to prevent A3G polyubiquitylation and degradation (54).

At the same time, Vif interacts with A3G through motifs mainly located in the N-terminal region (Fig. 1.4B). Both *in vitro* and cell-based binding assays have demonstrated that residues 40 to 71 contain a nonlinear A3G binding site, in which histidine residues at positions 42/43 are of crucial importance (209). Double-alanine-scanning further indicates that the hydrophobic motif $Y^{40}RHHY^{44}$ is essential for A3G binding, and replacement of YRHHY with alanines almost abolishes Vif-A3G binding (280). Another conserved motif $Y^{69}XXL^{72}$ has been reported to mediate A3G interaction (260). In particular, Tyr69 and Leu72 are shown to be important for degradation of A3G. Additionally, rather that affecting EloC and Cul5 binding, mutations in C-terminal motif $P^{161}PLP^{164}$ impair Vif mediated degradation by reducing interacting with A3G (75).

The motif in A3G responsible for interaction with Vif was discovered based on the observation that a single-amino-acid difference between the A3G proteins of human and Africa Green Monkey (AGM) at position 128 modulates the species-specific recognition of HIV/$SIV_{AGM}$ Vif (32, 199). Replacement of aspartic acid residue at this position in human A3G with lysine found at the corresponding position in AGM A3G renders $hA3G_{D128K}$ resistant to HIV-1 Vif but sensitive to $SIV_{AGM}$ Vif-induced degradation. Detailed studies revealed that the $D^{128}PD^{130}$ motif in hA3G is critical for recognition by Vif. Pro129 and Asp130 contribute to an overall negative charge that is necessary for Vif binding. This motif specially interacts with

$D^{14}RMR^{17}$ of HIV-1 Vif (141, 291). Replacement of DRMR in HIV-1 Vif with corresponding residues SEMQ in $SIV_{AGM}$ Vif allows HIV-1 Vif to counteract AGM A3G and $hA3G_{D128K}$ mediated restriction (332). Moreover, phosphorylation is involved in the regulation of A3G-Vif functional interaction. Phosphorylation of residue Thr32 in hA3G by protein kinase A (PKA) reduces its binding and degradation by HIV-1 Vif, thereby promoting its antiviral activity (300).

In addition to the amino acids in A3G that are critical for Vif interaction, lysine residues at position 297, 301, 303, 334 in the C-terminal domain were identified to be responsible for A3G ubiquitination (142). Substitution of these four lysine residues blocks Vif-mediated degradation. Once four lysine residues were all mutated to arginine, A3G became completely resistant to Vif induced degradation, and capable of suppressing the replication of $Vif^+$ virus (142).

Meanwhile, there is evidence suggesting that Vif directly impedes A3G encapsidation, and this action is separable from Vif-induced degradation. First, substitution of the conserved phosphorylation sites in Vif impairs the infectivity of progeny virus without affecting Vif-mediated A3G degradation (208). Furthermore, Vif was able to inhibit the encapsidation and antiviral activity of an A3G mutant C97A, which is resistant to degradation (249). In Kao et al.'s study, the intracellular level of A3G was adjusted by transfecting various amounts of A3G-expressing vector. Then the amount of A3G incorporated into wild type virions was compared to Vif$^-$ virions, and it was found that less A3G was packaged into wild type virions (153, 154). This suggests that Vif can directly inhibit A3G packaging through degradation-independent pathway. Indeed, it is proposed that Vif may interfere with A3G packaging by competitively binding to components that are critical for A3G encapsidation, such as viral genomic RNA or NC proteins (54, 126).

Vif has also been shown to inhibit A3G translation (211, 310). By using biochemical and biophysical methods, it was demonstrated that Vif binds to sites in 5′ and 3′ UTRs of A3G mRNA with high affinity, and blocks both 5′ UTR-dependent and -independent translation of A3G (211).

Moreover, virion-associated Vif could serve as the last defense against A3G by directly disrupting the catalytic activity of A3G (34). In bacterial models where proteasomal degradation pathway is absent, the presence of Vif leads to the reduction of A3G-induced hypermutation (282). Also, recombinant Vif protein or Vif-derived peptide $Vif_{25-39}$ inhibits A3G-mediated deamination *in vitro* (34). Recently, a biochemical study demonstrated the mechanism by which Vif inhibits A3G enzymatic activity. It indicated that through physically interacting with A3G, Vif could inhibit either jumping or sliding movement of A3G on single-stranded DNA (90).

In summary, Vif interacts with both A3G mRNA and protein. Their interaction may directly neutralize the action of A3G, or promote A3G degradation by recruiting proteasomal degradation pathway. Also Vif attempts to inhibit A3G virion encapsidation, which is independent of Vif-A3G interaction. Thus, the tumultuous relationship between Vif and A3G demonstrates that Vif-A3G axis could be an attractive target for developing new therapeutics for HIV-1 infection.

#### 1.4.4.2 Interaction with other viral proteins

HIV-1 Gag facilitates the virion incorporation of A3G (96). Studies found that NC domain of Gag mediates direct interaction with A3G. Mutations/deletions in the NC domain reduced the packaging of A3G into virions (5, 76). In A3G, NTD is responsible for NC interaction, especially the $Y^{124}YFW^{127}$ motif that is critical for A3G encapsidation (191, 195).

By using bimolecular fluorescence complementation assay, Friew et al. analyzed the interaction between Gag and A3G in living cells. They found that both Gag and A3G form multimers in RNA dependent manner, and multimerization is required for their interaction and A3G incorporation (96). In contrast, the function of betaretrovirus Mason-Pfizer monkey virus (MPMV) Gag is opposite. MPMV Gag poorly binds to simian A3G, thus limits the amount of simian A3G incorporated into virion and avoids restriction by host A3G (73).

Besides viral structural protein, A3G binds to two viral enzymes that are critical for early stage of viral replication. Luo et al. reported that both wild type A3G and catalytic defective mutant $A3G_{C291S}$ bind to HIV-1 IN, and interfere with proviral DNA formation (192). Our group identified the interaction between A3G and HIV-1 RT. Peptide competition experiment further confirmed that their interaction contributes to A3G-mediated inhibition on HIV-1 reverse transcription (336). Additionally, Nguyen et al. revealed that A3G binds to the RT of HBV, which is required for the incorporation of A3G into HBV virions (239).

#### 1.4.4.3 Interaction with RNAs

A3G is an RNA binding protein that interacts with nonautonomous retroelement Y RNAs, Alu RNAs, and mRNAs encoding A3G, ubiquitin, and protein phosphatase 2A (57, 168, 276). Among them, interaction between A3G and 7SL RNA was well studied. Host noncoding RNA 7SL RNA is involved in the signal peptide recognition, which is selectively packaged by HIV through interaction between Gag and *cis*-acting sequences of 7SL RNA (159). As a component of viral ribonucleoprotein (RNP) complex, 7SL RNA interacts and promotes A3G associating with RNP, which may contribute to A3G association with RTC (368). Additionally, 7SL RNA has been

identified as the cofactors of A3G virion packaging (248, 335).

Studies also suggested that viral genomic RNA is required for A3G packaging. A3G was found to bind to viral genomic RNA and form A3G complex (168, 308). In the virion, their association inhibits enzymatic activity of A3G. However in the following round of infection, this inhibitory effect is eliminated by RNase H treatment during reverse transcription (308).

Although which type of RNA is involved in A3G encapsidation remains controversial, increasing evidences indicate that association of A3G with cellular and viral RNAs promotes A3G packaging, oligomerization and antiviral function (314, 320).

### 1.5 HIV-1 therapeutics based on host restriction factors

Identification and characterization of restriction factors has inspired the development of novel therapeutics against HIV. Indeed, detailed understanding of interactions between viral antagonist and restriction factors provides a rational to design small molecules of interaction inhibitors and/or artificially engineer restriction factors to which HIV-1 is sensitive.

#### 1.5.1 Pharmacological inhibitors

By blocking the interaction of restriction factors with viral antagonists or host machinery required for antagonism, pharmacological inhibitors should be able to inhibit the antagonistic effect of viral proteins, and thereby mobilize the activity of restriction factors. Due to the limitations on the detailed information as to their interacting domains and three-dimensional structures which are required to effectively target their interaction, so far, only a few small molecules that disrupt A3G/Vif

interactions have been identified.

RN-18 is the first reported small molecule antagonist of HIV-1 Vif (230). It blocks the function of Vif by downregulating its protein levels, and thereby increases A3G expression and incorporation. Later, Cen et al. discovered two compounds that protect A3G from Vif-induced degradation (44). Rather than inducing global inhibitory effect on the ubiquitin-proteasome pathway, compounds IMB-26 and IMB-35 specifically bind to A3G and disrupt A3G/Vif interaction, resulting in reduced polyubiquitination of A3G by Vif. Thus, treatment by these compounds restores A3G protein expression and virion encapsidation in the presence of Vif. IMB-26 and IMB-35, together with RN-18 have shown antiviral activity against $Vif^+$ HIV-1 replication in A3G expressing cells, which provide proof of principle that A3G/Vif can be targeted by small molecules.

Additionally, the compound PF74 is found to be able to mimic the action of TRIM5α, and destabilize HIV-1 CA. This compound binds specifically to and induces rapid dissolution of HIV-1 CA, resulting in premature HIV-1 uncoating in target cells (298). Moreover, in order to identify inhibitors targeting Vpu/BST-2, Zhang et al. developed a high-throughput cell-based ELISA, which can be used to measure the amount of BST-2 on the cell surface (367).

### 1.5.2 Gene therapy approaches

Gene therapy, as a promising alternative anti-HIV approach is attracting increasing attention (312). By targeting one or more steps of viral life cycle, gene therapy is able to suppress viral replication, or even block the initial infection and keep the modified cells virus-free. Additionally, though gene modification, gene therapy may provide life-long protection particularly if hematopoietic progenitor cells

are targeted. Until now, both viral components and cellular genes critical for viral replication have been exploited in HIV-1 gene therapy, and host restriction factors are not exceptions (135).

Several groups, including ours, have targeted A3G for gene therapy (4). Despite difference in targets, all strategies attempt to achieve a unique goal: to increase A3G encapsidation. Once substantial amounts of A3G are incorporated into virions, the virions become non-infectious regardless the presence of HIV-1 Vif.

To indirectly increase A3G encapsidation by preventing its degradation, in a pilot study ubiquitin-associated domain 2 (UBA2) was fused at the C-terminal end of A3G (184). UBA2 is a stabilization signal that protects proteins from proteasome-mediated proteolysis. UBA2 fusion made A3G protein more resistant to Vif-inducted degradation, and modestly improved the inhibitory effect of A3G against $Vif^+$ HIV-1.

Alternatively, strategies directly increasing A3G encapsidation by actively directing it into virion have been proposed. In our previous study, A3G was fused with virus-targeting polypeptide R88 (14). R88 is a fragment of HIV-1 Vpr that is incorporated into virion through interaction with Gag p6 (356). R88-A3G was able to overcome the HIV-1 Vif barrier and efficiently packaged into the $Vif^+$ virus. Similarly, A3G can be delivered via Nef7 fusion (108). Nef7 mutant is derived from HIV-1 Nef, whose pathogenicity is abolished after two point mutations (V153L, E177G). Both delivery vehicles have natural HIV-1 core access, and their fusion was sufficient for A3G to be packaged into virion and exhibit antiviral activity.

Together, strategies discussed above provide proof-of-concept that simple modification on A3G is able to override Vif-targeted inhibition and restore its anti-HIV activity. Additionally, in order to determine how effective A3G-based gene therapy could be, Krisko et al. used humanized mice to evaluate the action of A3G *in*

*vivo* (170). In their study, A3G efficiently blocked the replication of CCR5-tropic Vif⁻ viruses, as indicated by the extensive G to A mutation in proviral DNA, which further confirmed *in vivo* antiviral potential of A3G.

Meanwhile, studies on human and rhesus TRIM5α promote the development of gene therapy strategies based on TRIM5α. Anderson et al. generated a chimeric human-rhesus TRIM5α, which contained the critical region from rhesus macaque involved in HIV-1 capsid recognition (6). This chimeric TRIM5α was shown to inhibit HIV-1 infection in a hematopoietic stem cell gene therapy setting. Moreover, a human TRIM5α derived protein hTRIMCyp acquired the ability to target HIV-1 by fusing with human cyclophilin A motif (CypA) (233). hTRIMCyp was shown to exhibit more potent anti-HIV activity than rhTRIM5α, and be effective against HIV in humanized mouse model.

In conclusion, these encouraging results, especially data from humanized mouse models, support the promise of restriction factors based therapeutic approaches. Furthermore, the development of the most effective and safest approach, where restriction factors specifically inhibit viral replication without disturbing host functions, will be benefited from studies aimed at better understanding of host factors and HIV-1 restriction.

### 1.6 Scope of thesis

The interaction between A3G and HIV-1 viral components as a representative example reflects host-pathogen interactions. For one thing, the host suppresses HIV-1 replication and pathogenesis by encoding restriction inhibitors such as A3G; for another, HIV-1 evades this inhibitory action by encoding viral antagonist, e.g. Vif. In order to counteract A3G, Vif binds to A3G and targets it for proteasomal degradation,

or physically blocks its encapsidation. However, in the absence of Vif, A3G exhibits its antiviral effect by binding to several viral components. For example, A3G incorporates into viral particles through interaction with Gag NC domain and/or viral RNA. A3G also binds to IN, which promotes deaminase-independent inhibition on viral DNA formation.

In order to further uncover A3G-mediated restriction and identify its potential viral partners, in Chapter 3, co-immunoprecipitation (Co-IP) experiments were carried out to examine the interplay between A3G and HIV-1 RT. Peptide competition assay was used to elucidate the role of their physical interaction in HIV-1 replication, especially in HIV-1 reverse transcription.

Moreover, protein-protein interactions between A3G and viral components provide tempting targets for HIV-1 therapeutics. In order to help A3G to evade HIV-1 Vif, either A3G or Vif can be targeted. However, given the high mutational rates of HIV-1, Vif appears to be a less attractive target than A3G, and the relatively immutable host protein A3G can be a better candidate for therapies against HIV-1.

In our lab, the project aimed at developing an A3G-based anti-HIV strategy was initiated by fusing A3G with viral targeting peptide R88. R88 helps A3G to overcome Vif's physical blockage and incorporate into virions. However, R88-A3G remains sensitive to Vif induced proteasomal degradation. Thus, in order to prevent A3G degradation, in Chapter 4, mutagenesis analysis was conducted to characterize the critical residues in A3G and select Vif-resistant mutants. In Chapter 5, knowledge on Vif-resistant A3G mutants was extended, and optimized A3G: R-A3G$_{D128K}$ was delivered into susceptible cells by inducible lentiviral vector. The antiviral effect of R-A3G$_{D128K}$ against active and latent HIV-1 infection was characterized.

In summary, my research aims to provide greater understanding on A3G-mediated

restriction, and to develop and verify A3G based anti-HIV gene therapy strategy. The central hypothesis is that A3G restricts viral replication through interaction with viral partners. Through optimization, A3G is able to exert advanced antiviral activity and used as a gene therapy candidate to restrict HIV-1 replication and dissemination. To test this hypothesis, the following objectives were undertaken:

1. Study the physical and functional interaction between A3G and viral partner-RT.
2. Characterize the critical residues in A3G involved in viral interaction, including viral incorporation and Vif-induced degradation.
3. Screen potential A3G mutants as candidate for anti-HIV gene therapy.
4. Generate and characterize the inducible lentiviral vectors for R88-A3G$_{D128K}$ delivery.
5. Evaluate antiviral activity mediated by the pTZ-R88-A3G$_{D128K}$ in susceptible cell populations.

# CHAPTER 2

## Materials and Methods

### 2.1 General reagents

#### 2.1.1 Antibodies

Antibodies for cellular proteins: mouse anti-α-tubulin antibody (Sigma) and rabbit anti-hA3G antibody (catalog no. 10201) obtained through the NIH AIDS Research and Reference Reagent Program, were used for Western Blot (WB) analysis. Mouse anti-CD4 monoclonal antibody (OKT4) used for fluorescence-activated cell sorter (FACS) was described previously (10, 11, 355).

Epitope tag antibodies: rabbit anti-HA antibody (Sigma) and mouse anti-T7 tag antibody (Novagen) were used for immunoprecipitation (IP) and WB. HRP-conjugated anti-T7 antibody was purchased from Novagen.

Antibodies for viral proteins: rabbit anti-RT (catalog no. 6195) and mouse anti-Vif (catalog no. 2221) antibodies were obtained through the NIH AIDS Research and Reference Reagent Program. Mouse anti-HIV-1 p24, rabbit anti-Vpr and rabbit anti-IN monoclonal antibodies were described previously (10, 11, 355, 356, 358).

Secondary antibodies: HRP-conjugated donkey anti-rabbit IgG and sheep anti-mouse IgG were purchased from Amersham Biosciences. Fluorescein isothiocyanate (FITC)-conjugated anti-rabbit antibody (Kirkegaard & Perry Laboratories) was used in the fluorescence assay.

#### 2.1.2 Chemicals

Protease Inhibitor Cocktail Set III, puromycin (puro) and NP-40 were purchased from Calbiochem. 4'-6-Diamidino-2-phenylindole (DAPI) and TRIZOL reagent was

purchased from Invitrogen. Doxycycline (Dox) and Propidium Iodide (PI) were obtained from Sigma. ProLabel™ Detection Kit II was purchased from Clontech. WB-detection ECL kit was purchased from PerkinElmer Life Sciences. 4-[3-(4-iodophenyl)-2-(4-nitrophenyl)-2H-5-tetrazolio]-1,3-benzenedisulfonate (WST-1) was purchased from Roche.

### 2.1.3 Constructed plasmids

#### 2.1.3.1 Plasmids for A3G

The plasmid pAS1B-HA-A3G was constructed previously (14). A3G amplified from Homo sapiens cDNA clone IMAGE: 1284557 was kindly provided by Dr. S.K. Petersen-Mahrt (61, 261). The pAS1B-HA-A3G truncation mutants (65-132, 102-257, and 195-384) were constructed by the PCR-based mutagenesis method with the following primers:

$A3G_{65}$-Kpn I-5′:

5-CGGGGTACCTATCCTTATGACGTGCCTGACTATGCCAGCCACCCAGAG-3;

$A3G_{132}$-BamH I-3′: 5-CGGGATCCCTGGTAATCTGGG-3;

$A3G_{102}$-Xba I-5′: 5-CTAGTCTAGAAGGGATATGGCCACGTTC-3;

$A3G_{257}$-Pst I-3′: 5-AACTGCAGTCAATGCGGCCTTCAAGGAA-3;

$A3G_{195}$-Xba I-5′: 5-GGAGATTTCTAGACACTCGATG-3;

$A3G_{384}$-Bgl II-3′: 5-ATAGATCTATCGATTCAGTTTTCCTGATT-3.

ProLabel-HA-A3G was constructed by subcloning HA-A3G into a ProLabel-C vector (Clontech). ProLabel-$A3G_{D128K}$ was generated by a two-step mutagenic PCR-based method. The presence of D128K in A3G was confirmed by sequencing. Primers used were as follows:

HA-Kpn I-5′: 5-CGGGGTACCGCTTCTAGCTAT-3;

A3G-SmaI I-3′: 5-TCCCCCGGGTCAGTTTTCCTG-3;

$A3G_{D128K}$-5′: 5-ACTTCTGGAAACCAGATTAC-3;

$A3G_{D128K}$-3′: 5-GTAATCTGGTTTCCAGAAGTA-3.

CMVin-R14-88-pcs-A3Gwt (R88-A3Gwt), HA-A3Gwt and pYEF1-R88-A3Gwt were constructed previously (14). The CMVin-R88-A3G mutants were generated by a PCR-based mutagenesis method (11). The presence of the corresponding mutations in A3G was confirmed by sequencing. The primers used for generating different A3G mutants were:

A3G-Xba I-5′: 5-TCATCTAGAAAGCCTCACTTCAG-3;

A3G-Bgl II-3′:5-TAAGAGCTCATGCCTGCAGCC-3;

$A3G_{Y124A}$-5′: 5-GCACGCCTAGCATACTTCTGG-3;

$A3G_{Y124A}$-3′: 5-CCAGAAGTATGCTAGGCGTGC-3;

$A3G_{P129A}$-5′: 5-TTCTGGGACGCAGATTACCA-3;

$A3G_{P129A}$-3′: 5-TGGTAATCTGCGTCCCAGAA-3;

$A3G_{E259Q}$-5′: 5-CGCCATGCACAACTATGCTTCCT-3;

$A3G_{E259Q}$-3′: 5-AGGAAGCATAGTTGTGCATGGCG-3.

The AAV2-*lacZ* vector was described previously, which expresses the *lacZ* reporter gene from a cytomegalovirus (CMV) promoter and flanked by AAV2 inverted terminal repeats (ITRs) (18, 26). The AAV2-R88-$A3G_{P129A}$ was constructed by replacing the *lacZ* gene with R88-$A3G_{P129A}$ amplified from plasmid CMVin-R88-$A3G_{P129A}$ using the following primers:

R88-Not I-5′: 5-ATAGCGGCCGCCATGCCACACAATGAA-3;

A3G-BamH I-3′: 5-GCTCGGATCCTCAGTTTTCCTGATT-3.

To construct plasmid pTZ-R88-$A3G_{D128K}$, R88-$A3G_{D128K}$ was amplified from CMVin-R88-$A3G_{D128K}$. The PCR fragment was digested with Age I and Cla I, and

cloned into pTRIPZ-empty vector (pTZ-control, Open Biosystems) by replacing the original RFP expressing region between Age I (nt 2992) and Cla I (nt 3702). The following primers were used:

R88-Age I-5′: 5-ATCGCACCGGTCGCCACCATGCCACACAATGAAT-3;

A3G-Cla I-3′: 5-ATAGATCTATCGATTCAGTTTTCCTGATT-3.

**2.1.3.2 Plasmids for viral proteins**

To generate the RT expression plasmid, HIV-1 RT was amplified from HIV-1 HxBru using mutagenesis primers to create a BamH I site in the 5′ end with the start codon removed and a Not I site preceded by the stop codon. The PCR fragment was digested with BamH I and Not I, and cloned into the SVCMVin-T7 vector that was digested with the same restriction enzymes to generate the plasmid SVCMVin-T7-RT (11). The T7-RT truncation mutants (1-243, 1-323 and 1-439) were obtained using the same strategy. The following primers were used:

RT-BamH I-5′: 5-CGCGGATCCCCCATTAGTCCT-3;

RT-Not I-3′: 5-ATTTGCGGCCGCCTATAGTACTTTCCT-3;

$RT_{243}$-Cla I-3′: 5-CCATCGATCTAAGGCTGTACTGTCCATTTA-3;

$RT_{323}$-Cla I-3′: 5-CCATCGATCTATTTTGATGGGTCATAATAC-3;

$RT_{439}$-Cla I-3′: 5-CCATCGATCTACGTTTCTGCTCCTACTATG-3.

pcDNA-hVif was obtained from the NIH AIDS Research and Reference Reagent Program (240). pcDNA-$Vif_{SEMQ}$ was generated by PCR-based mutagenesis method with the following primers:

$Vif_{SEMQ}$-5′: 5-TGTGGCAGGTGAGCGAGATGCAGATTAACACCTG-3;

$Vif_{SEMQ}$-3′: 5-CAGGTGTTAATCTGCATCTCGCTCACCTGCCACA-3.

**Table 2.1 List of constructed plasmids**

| | |
|---|---|
| Plasmid for A3G | pAS1B-HA-A3G$_{65\text{-}132}$ |
| | pAS1B-HA-A3G$_{102\text{-}257}$ |
| | pAS1B-HA-A3G$_{195\text{-}384}$ |
| | ProLabel-HA-A3G |
| | ProLabel-HA-A3G$_{D128K}$ |
| | CMVin-R88-A3G$_{Y124A}$ |
| | CMVin-R88-A3GY$_{D128K}$ |
| | CMVin-R88-A3GY$_{P129A}$ |
| | CMVin-R88-A3G$_{E259Q}$ |
| | AAV2-R88-A3G$_{P129A}$ |
| | pTZ-R88-A3G$_{D128K}$ |
| Plasmid for viral proteins | SVCMVin-T7-RT |
| | SVCMVin-T7-RT$_{1\text{-}243}$ |
| | SVCMVin-T7-RT$_{1\text{-}323}$ |
| | SVCMVin-T7-RT$_{1\text{-}439}$ |
| | pcDNA-Vif$_{SEMQ}$ |
| Plasmid for provirus | HxBruΔRI-Vif$^{-}$ |

## 2.2 Cells and viruses

### 2.2.1 Cells and transfection

Human embryonic kidney 293T cells, 293 cells and HeLa cells were maintained in Dulbecco's Modified Eagle's Medium (DMEM) supplemented with 10% fetal calf serum (FCS), 100units/ml penicillin and 100μg/ml streptomycin. ACH-2 cells are obtained through the NIH AIDS Research and Reference Reagent Program (94). ACH-2 cells and $CD4^+$ C8166 T cells were maintained in Roswell Park Memorial Institute (RPMI)-1640 medium containing 10% FCS, 100units/ml penicillin and 100μg/ml streptomycin. Peripheral blood mononuclear cells (PBMCs) were isolated from the blood of healthy adult volunteers by sedimentation on a Ficoll (Lymphoprep; Axis-Shield) gradient. $CD4^+$ T lymphocytes were isolated from PBMCs by negative selection with EasySep™ Human $CD4^+CD25^+$ T Cell Isolation Kit (STEMCELL Technologies). Isolated PBMCs and $CD4^+$ T lymphocytes were stimulated with 3μg/ml phytohemaglutinin (PHA) for 3 days and maintained in RPMI-1640 supplemented with 10 U IL-2. PBMC-derived macrophages were generated by dispensing fresh PBMCs into 12-well plates at the desired density at 37 ºC for 2 hours. After gentle washing with DMEM, the adherent cells were cultured in DMEM containing 10% FCS and 10ng/ml macrophage colony-stimulating factor (M-CSF; R&D Systems) for 7 days. DNA transfection of 293T or HeLa cells was performed using the standard calcium phosphate DNA precipitation method (358).

### 2.2.2 Viruses production and infection

The HIV-1 proviral clones pNL4.3-$Nef^+$/GFP, pNL4.3-Bal, HxBru-$Vif^+$, HxBru-$Vif^-$ and HxBruΔRI were previously constructed (9, 11, 14). In HxBru $Vif^-$, the amino acids at positions 21 and 22 of Vif were changed to a stop codon (14). In

HxBruΔRI, RT and IN gene sequences were deleted, while a 194-bp sequence harboring cPPT/CTS cis-acting elements was maintained, as previously described (11). HxBruΔRI-Vif$^-$ provirus was constructed by two-step PCR. First, cDNA that encompassed a region between the Apa I and Sal I sites of the provirus was amplified, in which the amino acids at positions 21 and 22 of Vif were changed to a stop codon. Then, the amplified PCR fragment was digested with Apa I and Sal I restriction enzymes and used to replace the corresponding region in HxBruΔRI. The mutagenic primers were:

Vif Stop-5′: 5-GAGGATTAGAACATGATGACGTGTAGTAAAACACC-3

Vif Stop-3′: 5-GGTGTTTTACTACACGTCATCATGTTCTAATCCTC-3.

AZT resistant HIV-1, HIV-$1_{LAI\text{-}M184V}$ (3TC-resistant), Nevirapine resistant HIV-1, Protease inhibitors resistant HIV-1 (L10R/M46I/L63P/V82T/I84V), Raltegavir resistant HIV-1(1556/W1235426-1) were obtained through the NIH AIDS Reagent Program.

To produce HIV-1 viruses that incorporated different HA-A3G or R88-A3G fusions, 293T cells were co-transfected with the corresponding HIV-1 proviral DNA and HA-A3G or R88-A3Gwt/mut plasmids. Virus-containing supernatants were collected at 48 hours post-transfection and subjected to ultra-centrifugation (35,000 rpm for 1.5 hours at 4 ºC) to pellet the virus. The quantification of virus stocks was determined by Gag-p24 measurements using an HIV-1 p24 ELISA Kit (purchased from the AIDS Vaccine Program of the Frederick Cancer Research and Development Center) (357).

To infect CD4$^+$ C8166 T cells, equal amounts of viruses were incubated with susceptible cells at 37 ºC for 2 hours. Then, the cells were washed and incubated with fresh medium. At different time points as indicated in the result sections, HIV

replication levels in each infected culture were monitored by measurement of HIV-1 Gag-p24 antigen by HIV-1 p24 ELISA. The infection level mediated by the pNL4.3-GFP HIV-1 virus was monitored by FACS (Becton Dickenson FACSCalibur) or observed under fluorescence microscopy after the infected cells were fixed with PBS-4% paraformaldehyde. For the WB analysis, viruses were pelleted by ultra-centrifugation through a 20% sucrose cushion. Then, the lysed virus samples were resolved by 10% SDS-PAGE followed by WB.

As to primary cell infection, Nevirapine-resistant HIV-1 was used to infect PBMCs and $CD4^+$ T cells. pNL4.3-Bal virus was used to infect macrophages. Unstimulated $CD4^+$ T cells were infected with Nevirapine-resistant virus by previously described method (175, 253). Briefly, cells were suspended at a concentration of $1\times10^7$cells/ml, and spinoculated with virus at 1200×g for 2 hours at room temperature. Then cells were washed twice and incubated in fresh medium. HIV-1 replication was monitored by HIV-1 Gag-p24 ELISA.

## 2.3 General methods

### 2.3.1 Real-time PCR analysis

#### 2.3.1.1 Quantitative detection of synthesized viral DNA

To examine the effects of A3G and IN on HIV-1 reverse transcription, C8166 T cells were infected with equal amounts of $Vif^-$ viruses (containing A3G and/or IN or not) produced from 293T cells. A heat-inactivated virus (pretreated at 80°C for 30 min) was used as a negative control for infection. Prior to infection, viruses were treated with 340 U/ml DNase (Roche) for 60 min in 37°C to remove residual plasmid DNA. After 2 hours of infection, the cells were washed with PBS and cultured in RPMI medium. At 12 hours post-infection, the infected cells were collected, and

DNA was extracted using a QIAamp DNA Blood Mini Kit (Qiagen) following the manufacturer's instructions. The DNA samples were processed for detecting late reverse transcription (LRT) products using the following primers:

TD-Gag-Fr: 5-ATCAAGCAGCCATGCAAATG-3;

TD-Gag-Rv: 5-CTGAAGGGTACTAGTAGTTCC-3.

Real-time PCR was performed on a Mx3000P detection system (Stratagene, CA) with following optimized thermal conditions: initial hot start (95 °C for 15 min) followed by 35 to 40 cycles of denaturation (94 °C for 30 s), primer annealing (60 °C for 30 s) and extension (72 °C for 1 min). To evaluate the DNA content of the extracted chromosomal DNA preparations, a detection of the human β-globin gene was performed by real-time PCR with following primers as described previously (304):

β-glob1 (forward): 5-CAACTTCATCACGTTCACC-3;

β-glob2 (reverse): 5-GAAGAGCCAAGGACAGGTAC-3.

**2.3.1.2 Quantitative detection of lentiviral vector DNA**

To determine the transduction efficiency of lentiviral vectors with or without A3G, C8166 T cells were transduced with equal amounts of vectors produced from 293 T cells. To avoid carryover plasmid DNA contamination, vectors were pretreated with 340U/ml DNase (Roche) for 60 min in 37°C. 2 hours after transduction, cells were washed and cultured in complete RPMI medium for another 6 hours. Then, cells were collected and DNA was isolated using a QIAamp blood DNA minikit. The total levels of vector DNA were quantified with Mx3000P real-time PCR system as described earlier with the following primers (9):

R-Fr: 5-GGCTAACTAGGGAACCCACTGC- 3;

U5-Rv: 5-CTGCTAGAGATTTTCCACACTGAC-3.

DNA template was normalized by β-globin gene amplification as described above.

#### 2.3.1.3 Quantitative detection of A3G/R88-A3G mRNA and DNA

Human PBMCs and macrophages were transduced with AAV2/5-*LacZ* or AAV2/5-R88-A3G$_{P129A}$ vectors. 72 hours after transduction, total RNA from 1x10$^6$ cells was extracted using the TRIZOL reagent following the manufacturer's instructions. RNA was subjected to reverse transcription with Moloney murine leukemia virus reverse transcriptase (M-MLV RT, Promega). The cDNA was then PCR-amplified with Taq DNA polymerase (Fermentas) using 5′ and 3′ primers targeting Vpr and A3G, respectively:

R88-Not I-5′: 5-ATAAGCGGCCGCCATGCCACACAATGAA-3;

A3G$_{P129A}$-3′: 5-TGGTAATCTGTCCCAGAA-3.

The mRNA content was normalized by amplifying the human β-globin gene as described previously (304). All PCR products were electrophoresed through 1.2% agarose gels.

To quantitatively determine the levels of R88-A3G$_{P129A}$ mRNA and the total cellular A3G mRNA (including endogenous A3G mRNA) in PBMCs and macrophages, the extracted RNA was first subjected to reverse transcription with M-MLV RT. Then, the reverse transcripted DNA from each sample was quantified by real time-PCR analysis using two sets of primers:

One set for R88-A3G$_{P129A}$:

Vpr-5′: 5-GATACTTGGGCAGGAGTGG-3;

A3G-3′:5-CACCTGGCCTCGAAAGAT-3.

Another set for A3G:

A3G-5′: 5-CTTCAGAAACACAGTGGAGC-3;

A3G-3′: 5-CACCTGGCCTCGAAAGAT-3.

The reaction was carried out in 20 μL final volume, consisting 1X FastStart DNA Master SYBR Green I (Roche) and 0.2 μM of each sense and antisense primers.

Similarly, to quantitatively determine the levels of R88-A3G$_{D128K}$ DNA in transducted CD4$^{+}$ T cells and macrophages, DNA from transduced cells was isolated at 3 days after transduction. Real-time PCR analysis was performed with primers targeting Vpr and A3G as described above.

### 2.3.2 Co-IP assay in 293T cells and produced HIV-1 virions

To detect the interaction of A3G/RT and identify their binding regions, a cell-based Co-IP assay was performed. Briefly, the T7 or T7-RTwt/mutant plasmid was co-transfected with HA-A3Gwt/mutant into 293T cells for 48 hours. Then, 90% of the transfected cells were lysed in 0.5% NP-40 prepared in 199 medium containing a cocktail of protease inhibitors (Roche) for 30 min and clarified by centrifugation at 14,000 rpm for 30 min at 4 ºC. After centrifugation, the clarified supernatant was subjected to immunoprecipitation using a mouse anti-T7 antibody. The immunoprecipitates were then resolved by 10% SDS-PAGE. The RT-bound proteins were detected by WB using anti-HA or anti-A3G antibodies. In addition, the presence of T7-RTwt/mutant in the immunoprecipitates was detected by an anti-T7 antibody. To detect the expression of HA-A3Gwt/mutant and T7-RTwt/mutant, 10% of the transfected cells were lysed in 0.5% NP-40 199 medium, and the lysates were analyzed by WB with corresponding antibodies. For the ProLabel assay, the ProLabel activity of ProLabel-HA-A3G and the ProLabel-T antigen from the Co-IP samples and cell lysates were measured by the ProLabel™ Detection Kit II.

To detect the interaction between HA-A3G and RT in the virions, Vif$^-$ virions were lysed with 0.5% NP-40 in 199 and immunoprecipitated with a mouse anti-HA antibody, followed by WB with an anti-RT antibody to detect A3G-bound RT. In the RNase treatment assay, the viral lysates in 199 medium (containing 0.5% NP-40) were pretreated with 100 μg/ml RNase A (Invitrogen) for 1 hour before immunoprecipitation.

### 2.3.3 Isolation and detection of HIV-1 IN mRNA

To detect the presence of HIV-1 IN mRNA, HIV Vif$^-$ viruses were either treated or untreated with RNase and lysed. RNA was extracted from the viral lysates using the TRIZOL reagent. Isolated RNA was subjected to reverse transcription with M-MLV RT. Then, the reverse transcribed DNA was amplified with Taq DNA polymerase using following primers:

IN-5′: 5-GAAAGTAGGAGCTCTAGATGGAATA-3;

IN-stop-3′: 5-CTAAACGGATCCATGTTCTAA-3.

The PCR products were electrophoresed through 1% agarose gel.

### 2.3.4 Radiolabeling and detection of R88-A3Gwt/mutant

To perform pulse-chase radiolabeling experiments, 293T cells were co-transfected with wild type R88-A3G or mutants and a pcDNA-hVif plasmids. After 48 hours, cells were incubated for 30 min with starvation medium (DMEM without methionine, plus 10% dialyzed FBS) followed by pulse-labeling for 30 min with 250 μCi of [$^{35}$S]-methionine (Perkin Elmer). After labeling, the radiolabeled medium was replaced with medium containing an excess of unlabeled methionine, and the cells were

incubated at 37ºC. Labeled cells were collected at 0, 3.5 or 5 hours and subjected to immunoprecipitation using an anti-Vpr antibody. Immunoprecipitates were resolved by SDS-PAGE in a 12% gel followed by autoradiography.

### 2.3.5 Immunofluorescence

HeLa cells were grown on glass coverslips (12 $mm^2$) in 24-well plates and transfected with CMVin-HA-A3Gwt or different R88-A3Gwt/mutant plasmids. After 48 hours, the cells were washed with PBS and fixed and permeabilized with methanol/acetone (1:1 ratio) for 30 min at room temperature. The coverslips were incubated with a rabbit anti-A3G antibody (1:500) for 2 hours at 37ºC followed by incubation with a 1:500 dilution of FITC-conjugated anti-rabbit antibody for 1 hour. Nuclei were stained with DAPI. The coverslips were mounted with Mowiol 4-88, and the cells were visualized under a Carl Zeiss microscope (Axiovert 200) with a 20x objective.

### 2.3.6 Western blot analysis

For detection of protein expression in cells or viral particles, cell lysates or lysed viral samples were directly loaded onto a 10% or 12% SDS-PAGE gel, and electroblotted to nitrocellulose transfer membrane (Bio-Rad). The presence of individual proteins was analyzed by corresponding antibodies, and visualized with a WB-detection ECL kit.

### 2.3.7 Transduction and establishment of R88-A3Gwt/mutant-expressing cell lines

Pseudotyped lentiviral particles harboring pYEF-R88-$A3G_{wt/P129A}$, pTZ-R88-$A3G_{D128K}$ and corresponding control vectors were produced from 293 T cells

by triple transfection. Briefly, 293T cells were transfected with pYEF or pTZ plasmid, packaging plasmid Δ8.2 and VSV-G expressing plasmid (164). Virus-containing supernatants were collected at 48 hours after transfection and subjected to ultra-centrifugation (35,000 rpm for 1.5 hour at 4°C) to pellet the viral like particles (VLPs). Quantification of VLP stocks was determined by Gag-p24 measurement using HIV-1 p24 ELISA Kit.

To establish R88-A3Gwt/mutant-expressing cell lines, target cells were spinoculated with VLPs for 2 hours at room temperature and incubated overnight. 48 hours after transduction, the transduced cells and non-transduced cells were placed under puromycin (0.5μg/ml) selection for at least 10 days, and resistant clones were maintained in medium supplemented with puromycin (0.5μg/ml). As control, non-transduced cells were likewise submitted to selection and did not survive beyond day 4 under the same concentration of puro.

### 2.3.8 Flow cytometry analysis

To examine the cell-cycle profiles of transduced C8166 T cells, cells were collected, washed with cold PBS and fixed with pre-chilled 70% ethanol for 30 min on ice. After an additional wash, cells were resuspended in PBS, treated with RNaseA (180U/ml), and stained with 30μg/ml PI for 30 min. The DNA content was determined with a FACS flow cytometer (BD Biosciences).

The CD4 receptor expression on the surfaces of transduced C8166 T cells was evaluated by anti-CD4 staining and analyzed by FACS. Briefly, cells were incubated with mouse anti-CD4 antibody at 4°C for 2 hours, then washed and stained with anti-mouse IgG-FITC antibody in the dark for 30 min at 4°C. After three washes with PBS, cells were fixed with 4% paraformaldehyde and analyzed by FACS.

The viability of puro-selected C8166 T cells was evaluated by PI staining and analyzed by FACS. Briefly, harvested C8166 T cells were washed once and resuspended in 0.5% BSA/PBS with a concentration of $10^6$ cell per ml. PI was added to the final concentration of 5µg/ml, and incubated for 5 min at room temperature in the dark. Cell viability was analyzed using a FACS flow cytometer with excitation at 488 nm. Data was analyzed with FCS Express software (Denovo software).

### 2.3.9 Cell proliferation assay

The WST-1 assay was used to measure the proliferation of pYEF1-MCS and pYEF1-R88-A3$G_{wt/P129A}$ transduced C8166 cells. Briefly, transduced cells were cultured at a density of $1.5\times10^4$ cells/well in 96-well plates and incubated at 37°C. On different culture days, WST (10µl/well) was added in the culture and the cells were incubated for 4 hours at 37°C. After shaking thoroughly for 1 min, the absorbance was measured at 490 nm using POLARstar OPTIMA microplate reader.

### 2.3.10 AAV production and transduction

AAV2/5 production: The AAV2/5 vectors were produced by triple transfection of HEK 293 cells with AAV2/5-*lac*Z or AAV2/5-R88-A3$G_{P129A}$, the pACK2/5 packaging plasmid that comprises *rep* from AAV2 and *cap* from AAV5 (26), and the pAd.DELTA F6 helper plasmid containing adenoviral genes necessary to drive AAV replication (E2a, E4, VARNA). Transfections were performed with calcium phosphate co-precipitation (26). Recombinant AAV2/5 vectors were all purified by the standard cesium chloride sedimentation method (348). The titers of AAV2/5 vector preparations were determined by TaqMan PCR with primers for the bGH polyA (26).

AAV2/5 transduction: Target cells were transduced with recombinant

AAV2/5-LacZ or AAV2/5-R88-A3G$_{P129A}$ at 1x10$^{6}$ vector particles/cell in serum-free medium and incubated for 2 hours at 37 ºC with gentle agitation every 15 min followed by the addition of fresh media with 10% FBS and overnight incubation.

# CHAPTER 3

## A3G Interacts with HIV-1 Reverse Transcriptase and Inhibits its Function during Viral Replication

### 3.1 Introduction

Several cellular proteins have been defined as intrinsic restriction factors because of their ability to inhibit HIV replication and/or dissemination (7, 173, 236, 296). Among them, A3G is one that restricts HIV-1 replication through more than one mechanism (86, 178, 195, 198, 206). In the absence of the HIV-1 Vif, A3G is incorporated into progeny viruses through interaction with the NC domain of Gag protein and/or viral RNA (5, 76, 320, 363). Once these progeny viruses initiate new infection, the incorporated A3G will deaminate the cytidine to uridine in the viral minus-strand DNA during reverse transcription, resulting in hypermutation in the viral DNA (89, 120).

However, cytidine deamination may not be the only antiviral function of A3G. In the case of HBV and HTLV-1, A3G was shown to block their replication without causing cytidine deamination of viral DNA (238, 313). Also, A3G mutants that lack deaminase activity still exert substantial inhibitory effect against HIV-1 and HBV (143, 237, 325). These data indicated that A3G has a deamination- independent inhibitory effect. Indeed, increasing studies showed that A3G directly targets steps in HIV-1 reverse transcription (1, 192, 195, 206), leading to reduced viral DNA accumulation, which is separated from enhanced degradation of hypermutated viral DNA.

The step HIV-1 reverse transcription is catalyzed by HIV-1 RT, therefore it is desired to study the potential interaction between A3G and RT (127). It is hypothesized that A3G inhibits HIV-1 reverse transcription through interaction with RT. The following objectives were undertaken to test this hypothesis:

1. Characterize interaction between A3G and HIV-1 RT.

2. Explore the mechanisms by which A3G inhibits RT's function.

## 3.2 Results

### 3.2.1 The inhibitory effect of A3G on reverse transcription

In this study, we first tested the effect of A3G on HIV-1 reverse transcription using real-time PCR (9) to quantitatively measure the accumulation of proviral DNA at 12 hours post-infection. First, the HIV-1 Vif$^-$ virus and the HIV-1 Vif$^-$ virus encapsidated with HA-A3G (HIV-1-Vif$^-$+A3G) were produced from 293T cells by co-transfection of the HxBru-Vif$^-$ provirus (14) with an HA-tag plasmid or an HA-A3G expression plasmid. After the virus stocks were collected by ultracentrifugation, the presence of different virus-associated proteins, including HIV-1 RT and Gag-p24, and encapsidated HA-A3G in each virus stock sample were detected by WB analysis using corresponding antibodies (Fig. 3.1A, left panel). Then, equal amounts of HIV-1 Vif$^-$ and HIV-1 Vif$^-$+A3G viruses were used to infect CD4$^+$ C8166 T cells. At 12 hours post-infection, the amount of late reverse transcription (LRT) products were measured as described in the Materials and Methods. The level of LRT in HIV-1 Vif$^-$ virus-infected cells was arbitrarily set as 100%. The results showed that the LRT level after infection with the HIV-1 Vif$^-$+A3G virus was reduced to less than 20%, compared to that of HIV-1 Vif$^-$-infected cells (Fig. 3.1A, right panel). Since the reverse primer TD-Gag-Rv (5′-CTGAAGGGTACTAGTAGTTCC-3′) used for the measurement of LRT products (Fig. 3.1A) contained a CC pair at the 3′ end which may be a potential target for A3G deaminase, we also quantified the LRT

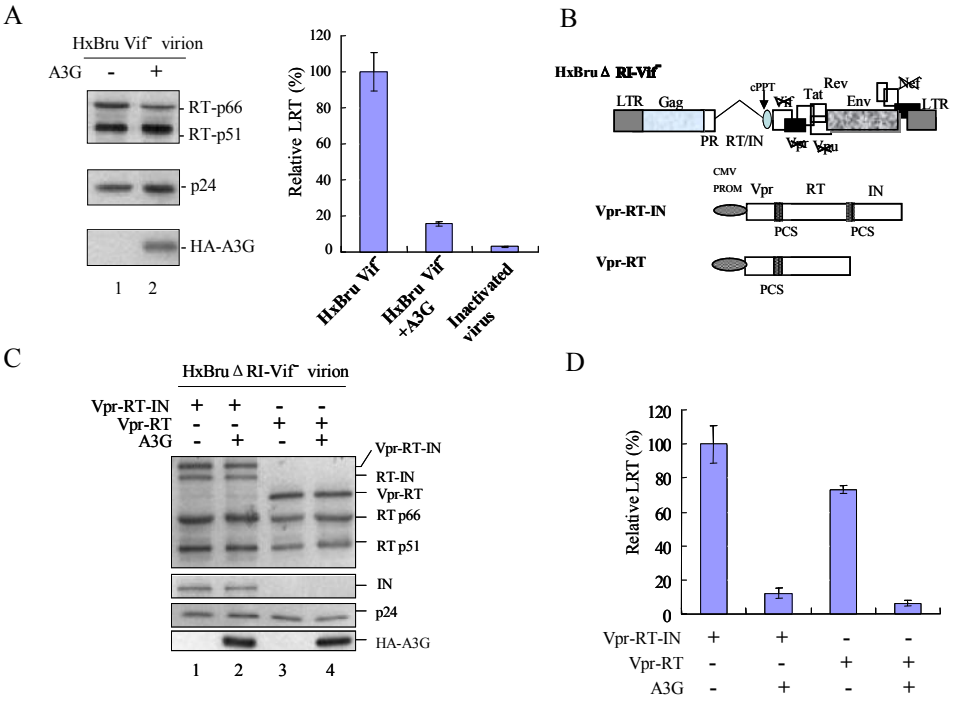


**Fig. 3.1 Inhibitory effect of A3G on HIV-1 RT. (**A) Vif- HIV-1 virions were produced from 293T cells in the presence or absence of A3G. Virus-associated proteins, including HIV-1 RT, Gag p24 and incorporated HA-A3G were analyzed by WB with the corresponding antibodies (left panels). Also, equal amounts of viruses (normalized by amounts of HIV-1 Gag p24) were used to infect $CD4^+$ C8166 T cells. Twelve hours post-infection, total DNA was extracted from the infected cells. HIV-1 late reverse transcription (LRT) products were analyzed by real-time PCR (right panels). The level of LRT in HIV-1 Vif- virus-infected cells was set to 100%, with errors bars representing the standard deviation from three independent experiments. (B) A schematic structure of the RT/IN-deleted HIV-1 provirus HxBruΔRI-Vif- and the Vpr-RT-IN and Vpr-RT expression plasmids, which have been previously described (10, 13, 369). PCS stands for protease cleavage site. (C) WB analysis of the RT/IN trans-complemented HxBruΔRI-Vif- viruses, which were produced from co-transfected 293T cells with HxBruΔRI-Vif- and Vpr-RT-IN or Vpr-RT in the presence or absence of A3G. Briefly, viruses were collected, lysed and loaded into SDS-PAGE. Then, the presence of viral proteins and HA-A3G were analyzed by WB with corresponding antibodies. (D) Real-time PCR analysis of the level of LRT in C8166 T cells infected with equal amounts of the trans-complemented HxBruΔRI viruses in the presence or absence of A3G. The level of LRT was measured at 12 hours post-infection by real-time PCR as (A). The values presented are the means and standard deviation from three independent experiments. A and D show representative WB image from three independent experiments.

products by using another reverse primer TD-Gag-Rv2 which has no CC pair near the 3′ end. Results showed that both TD-Gag-Rv and TD-Gag-Rv2 primers detected similar levels of HIV-1 proviral DNA from $A3G^+$ and $A3G^-$ HIV-1 infected cells (data not shown), suggesting that the decrease of LRT level in $A3G^+$ HIV-1 infected cells was due to A3G-mediated inhibition of HIV reverse transcription, but not through an impact on real-time PCR efficiency. All together, in agreement with previous reports (28, 131, 192, 206), our result indicates that the presence of A3G disrupted HIV-1 reverse transcription in the absence of the Vif protein.

HIV-1 reverse transcription was previously shown to be facilitated by the viral protein IN (346), which is known to be able to interact with RT and A3G (192). Therefore, the A3G-induced reverse transcription inhibition may have been caused by the interaction between A3G and HIV-1 IN, which may interfere with the effect of IN on reverse transcription. To test this possibility, we modified a previously described HIV-1 single-cycle replication system (13) by constructing a $Vif^-$ RT-IN-deleted HIV-1 provirus (HxBruΔRI-$Vif^-$) and a Vpr-RT expression plasmid (Fig. 3.1B). The viruses produced by the co-expression of the HxBruΔRI-$Vif^-$ provirus with the Vpr-RT-IN or Vpr-RT plasmids were able to enter cells and process reverse transcription. The different viruses were produced from co-transfected 293T cells in the presence or absence of HA-A3G. The viral protein compositions and the incorporated HA-A3G were detected by WB using specific antibodies as indicated in Figure 3.1C. The results showed that HIV-1 IN was only detected in viruses produced from 293T cells co-transfected with the HxBruΔRI-$Vif^-$ provirus with the Vpr-RT-IN plasmid (Fig. 3.1C, middle panel, compare lanes 1-2 to 3-4). Moreover, the data

indicated that the RTp66, RTp51 and Gagp24 levels in the virions were not affected by the presence of IN or HA-A3G (Fig. 3.1C, upper and middle panels). Equal amounts of viruses (adjusted by p24) were used to infect $CD4^+$ C8166 T cells. After 12 hours of infection, the level of HIV-1 LRT was quantified by real-time PCR. When the level of LRT in the HIV-1 virus trans-complemented with Vpr-RT-IN-infected cells was arbitrarily set as 100%, the amount of LRT was reduced to 70% when the infecting viruses lacked IN (Fig. 3.1D, compare bar 3 to 1), confirming that the presence of IN increased reverse transcription. Interestingly, our data also showed that regardless of the presence or absence of HIV-1 IN, A3G was able to efficiently inhibit viral DNA synthesis to more than 80% (Fig. 3.1D), indicating that the inhibitory effect of A3G on reverse transcription does not require the presence of IN.

### 3.2.2 Interaction between A3G and RT in the virions

For a better understanding of the mechanism by which A3G affects HIV reverse transcription, we performed a Co-IP assay to detect the possible interaction between RT and A3G in the virus. Briefly, equal amounts of HIV-1 $Vif^-$ and HIV-1 $Vif^-$+A3G viruses, produced from 293T cells by co-transfected with the HxBru-$Vif^-$ provirus with HA-tag or HA-A3G, were lysed and immunoprecipitated with an anti-HA antibody to pull down the HA-A3G protein. Then, the co-immunoprecipitated RT protein was detected by WB using an anti-RT antibody. Interestingly, the results showed that both RTp66 and RTp51 were co-immunoprecipitated with A3G (Fig. 3.2A, lane 2), suggesting that A3G is able to interact with RT. To rule out the possibility that the co-immunoprecipitated RT was due to the variable amounts of viral protein in each viral sample, we also detected the RT level in the lysed virions. The results showed no differences in the RT p66 and p51 levels between the different

viral samples (Fig. 3.2A, compare lane 3 to 4).

In the HIV-1 virion, RT forms a heterodimer with two subunits, p66 and p51 (324). p51 is derived from p66 by proteolytic processing during viral maturation. Although the p66 subunit contains activity sites for both of the catalytic activities of RT, the p51 subunit has been shown to be essential for maintaining the structural stability of the RT heterodimer (145, 269, 283). RT dimerization is believed to be required for RT enzymatic activity (271, 272). Because A3G interacts with both the p66 and p55 subunits of RT in the virus, we wanted to test whether the proteolytic processing of RT was affected in the presence of A3G. The HxBru-Vif$^-$ provirus was co-transfected with various amounts of the A3G plasmid into 293T cells. After 48 hours, virions were collected, and the amounts of RT p66, p51, p24 and incorporated A3G were determined by WB with the corresponding antibodies (Fig. 3.2B). The results showed that A3G was packaged into the Vif$^-$ virus in a dose-dependent manner (lower panel). Additionally, a comparable amount of RT p66 and RT p51 was present in each viral sample (upper panel). We set the virus-associated p66:p51 ratio in the absence of A3G as 1.00 and calculated the relative p66:p51 ratio in all of the other samples. As shown at the bottom of the RT panel, the levels of p66/p51 were similar for all of the samples. In addition, we further analyzed the RT proteolytic processing of viruses released from the HIV-1-infected control CD4$^+$ T cells and from the infected CD4$^+$ T cells that stably expressed a low level of HA-A3G (14). A similar p66:p51 ratio was obtained from HA-A3G and the control cell lines (Fig. 3.2C). All of these results provide evidence that the A3G/RT interaction has no effect on RT proteolytic processing.

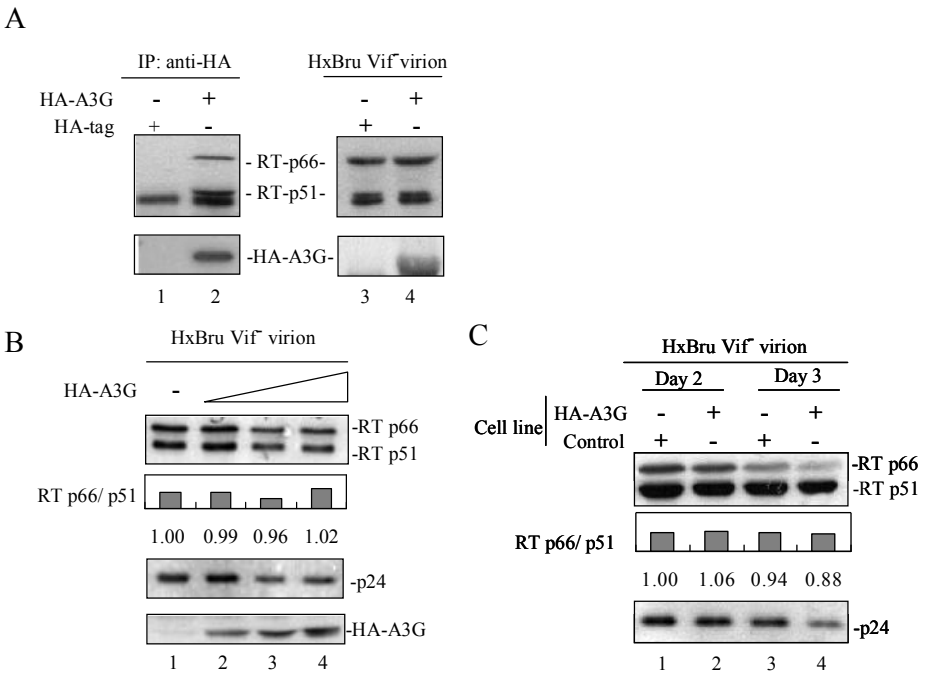


**Fig. 3.2 A3G interacts with HIV-1 reverse transcriptase in the virus.** (A) To test the A3G/RT interaction in the virus. The HIV-1 Vif⁻ provirus was co-transfected with the pAS1B-HA or pAS1B-HA-A3G expression plasmids in 293T cells. Seventy-two hours post-transfection, viruses were purified from the culture supernatants. The viral lysates were immunoprecipitated with an anti-HA antibody followed by WB with anti-RT or anti-HA antibodies (lanes 1 and 2). The expression of virus-associated RT and HA-A3G were also detected by directly loading viral lysates into SDS-PAGE followed by WB with the corresponding antibodies (lanes 3 and 4). A non-specific band below RT p51 was found in each testing sample. (B) To test the effect of A3G on HIV-1 RT processing, the Vif⁻ viruses produced in 293T cells in the various expression level of HA-A3G were collected, lysed and loaded into SDS-PAGE. Then, the RT, Gag p24 and HA-A3G expression levels were analyzed by WB using anti-RT (top panel), anti-p24 (middle panel) and anti-HA (lower panel) antibodies. The total amounts of RT p66 and p51 from two independent experiments were measured by imaging analysis. The p66:p51 ratios in the viral lysates are shown at the bottom of the RT panel. (C) The Vif⁻ viruses produced in A3G⁻ C8166 cells (lanes 1 and 3) or A3G-expressing C8166 T cells (lanes 2 and 4) after 2 to 3 days of infection were collected, lysed and loaded into SDS-PAGE. Then, the levels of RT and Gag p24 were detected by anti-RT antibody (top panel), anti-p24 antibody (lower panel). The p66:p51 ratios in each lysates of two independent experiments are shown at the bottom of the RT panel. A and B show representative WB results from three independent experiments.

### 3.2.3 Role of other viral components in A3G/RT interaction

As a member of the APOBEC family, A3G shares the property of RNA binding (147, 250), which inhances A3G packaging efficiency into virions (160, 288, 320) and enhances the stability of the A3G association with the reverse transcription complex (RTC) (160). Given that both RT and A3G are RNA-binding proteins, we evaluated the possible role of RNA on the A3G and RT interaction. The viral lysates were initially treated or untreated with RNase and then divided into two parts. One part was subjected to a Co-IP assay to detect the RT/A3G and IN/A3G interaction (Fig. 3.3A, lanes 1-3). The other part was used to test the efficiency of the RNase treatment (Fig. 3.3A, lanes 4-6). Upon RNase treatment, the HIV-1 gene sequence was unable to be amplified, confirming that viral RNA was efficiently digested (Fig. 3.3A, compare lane 4 to 5). Meanwhile, the IN/A3G interaction was reduced upon RNase treatment (Fig. 3.3A, second panel, compare lane 2 to 3), which further confirmed the efficiency of RNase treatment, as IN/A3G interaction was RNA dependent (192). However, the binding of A3G and HIV-1 RT was not significantly affected by the RNase treatment (Fig. 3.3A, first panel, compare lane 2 to 3), suggesting that their interaction does not require the presence of viral RNA.

Having demonstrated that the A3G interacts with RT in the viral particles and that the interaction does not require the presence of viral RNA, we further examined their association in 293T cells where no other viral proteins were expressed. The plasmid T7-RT was co-transfected with HA-A3G or a ProLabel-A3G (PL-A3G) expression vector into 293T cells (Fig. 3.3B). PL-T (an SV40 large T antigen fused at the C-terminus of the PL tag) was co-transfected with T7-RT as a control. Forty-eight hours after transfection, cells were lysed and immunoprecipitated with an anti-T7 antibody. Bound HA-A3G and PL-A3G were determined by WB using an anti-HA

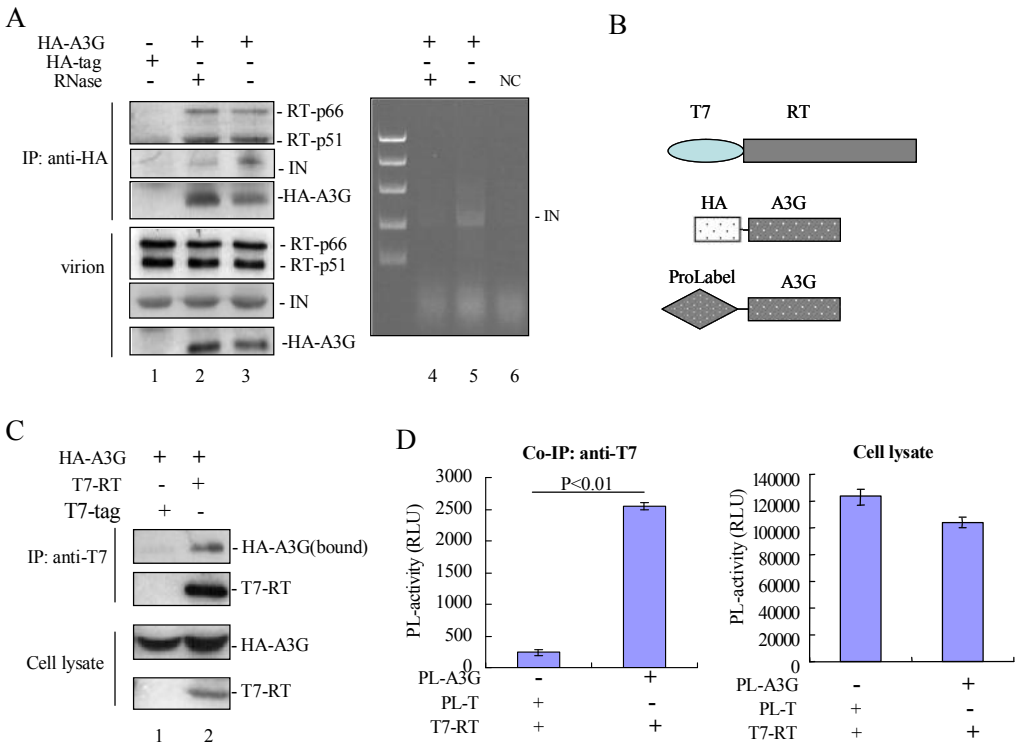


**Fig. 3.3 A3G/RT interaction in the absence of other viral components.** (A) The A3G/RT interaction was not mediated by the RNA bridge. HIV-1 Vif⁻ viruses produced from 293T cells in the presence or absence of HA-A3G were either untreated (lanes 1 and 3) or treated with RNase (lane 2) and then lysed. After lysis, 50% of viral samples were subjected to immunoprecipitation with anti-HA antibody. Then, the precipitated samples (left upper panels) and other 25% of viral samples (left lower panels) were loaded into SDS-PAGE followed by WB with anti-RT, anti-IN and anti-HA antibodies respectively. Meanwhile, the remaining 25% of viral lysates were subjected to viral RNA isolation followed by reverse transcription. Then, the reverse transcribed DNA was detected by PCR and analyzed by agarose gel electrophoresis (right panel). NC stands for negative control. (B) A schematic structure of the T7-tagged RT, HA-tagged and Prolabel-tagged A3G expression plasmids. ProLabel is a fragment of the split β-Galatosidase, which has no enzymatic activity. However, the ProLabel-tagged fusion protein can recombine with a Ω fragment of β-Galatosidase to reconstitute an active enzyme which is able to cleave chemiluminescence substrate. (C) To test RT/A3G interaction in the absence of other viral proteins, the pAS1B-HA-A3G was co-transfected with SVCMVin-T7 or SVCMVin-T7-RT expression plasmid into 293T cells. After 48 hrs, cells were lysed, and 10% of them (input) were analyzed by WB using anti-HA or anti-T7 antibodies to detect HA-A3G and T7-RT (lower two panels). Meanwhile, the remaining cell lysates were immunoprecipitated by the anti-T7 antibody to pull down T7-RT protein, and the co-precipitated HA-A3G were detected by WB with anti-HA antibody (upper panel). (D) The A3G/RT interaction was also detected by a chemiluminescence-based enzyme complementation (ProLabel) assay. Briefly, T7-RT and ProLabel-A3G (PL-A3G) were co-expressed in 293T cells. After 48 hrs, cells were lysed and immunoprecipitated by an anti-T7 antibody. The Co-IP samples (left panel) and cell lysates (right panel) were analyzed by the ProLabel activity assay. Value are an average from three independent experiments, error bars indicate standard deviations from the mean. Statistical significance was calculated using the student's *t*-test, P values are shown above the bars.

antibody and by measuring PL activity, respectively (Fig. 3.3C and D). The results showed that the immunoprecipitation of T7-RT was able to specifically pull down HA-A3G (Fig. 3.3C). Additionally, significant PL activity was only detected from the precipitated T7-RT sample in the 293T cells co-expressing T7-RT and PL-A3G but not in the 293T cells co-expressing T7-RT and PL-T (Fig. 3.3D, left panel), even though similar levels of PL-A3G and PL-T were detected in 293T cells (Fig. 3.3D, right panel). All of these experiments demonstrated a specific interaction between RT and A3G in the absence of other viral proteins.

### 3.2.4 Critical regions in RT and A3G required for their interaction

To define the region in HIV-1 RT that is required for binding to A3G, we constructed a series of T7-tagged RT deletion mutants, including T7-$RT_{1-243}$, T7-$RT_{1-323}$, and T7-$RT_{1-439}$ (Fig. 3.4A). 293T cells were co-transfected with HA-A3G and wild-type RT (T7-$RT_{wt}$) or each truncated mutant. In parallel, 293T cells co-transfected with HA-A3G and T7-tag plasmids were used as a negative control. As shown in Figure 3.4B, anti-T7 immunoprecipitation was able to pull down a similar level of individual T7-RTwt/mutant, and comparable amounts of A3G were co-pulled down with T7-$RT_{wt}$ or all of the truncated T7-RT proteins, including a RT-truncated mutant with 318 amino acids removed from its C-terminus ($RT_{1-243}$) (Fig. 3.4B, upper panel, lanes 2-5). In contrast, no bound A3G could be detected in the HA-A3G/T7-tag co-expressing sample (Fig. 3.4B, upper panel, lane 1). To rule out the possibility that this difference was due to various levels of HA-A3G in each sample, we directly measured the amount of HA-A3G in the cell lysates by WB, and the data showed that similar levels of HA-A3G were detected in each sample (Fig. 3.4B, lower panel). These data suggest that the N-terminal fingers-palm domain of RT ($RT_{1-243}$) is

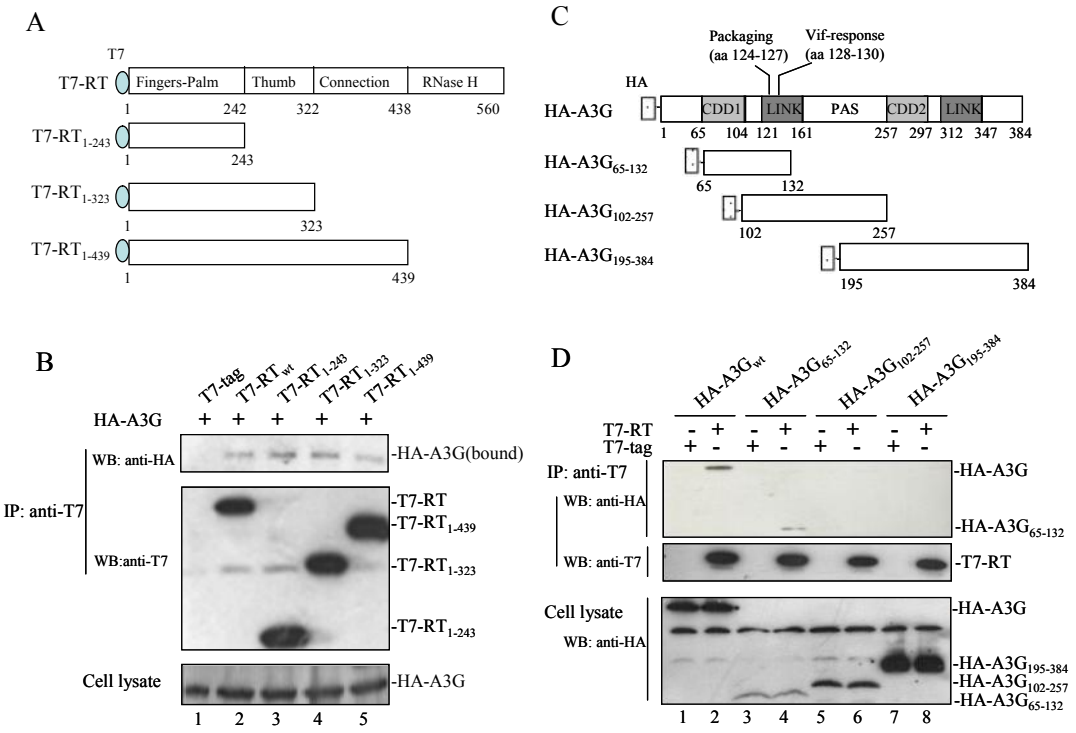


**Fig. 3.4 Mapping the binding domains in both RT and A3G required for their interaction. (**A) A schematic representation of the different T7-tagged RT wt/mutant constructs used in the domain-mapping experiments. Full-length T7-RT is shown at the top. The numbers indicate the amino acid positions in RT. The domains are marked in the full-length RT. Different RT truncated mutants are shown at the bottom. (B) Interaction of HA-A3G with T7-RT wt/mut. HA-A3G was co-transfected with T7-RTwt/mut in 293T cells for 48 hours. The association of A3G with truncated RT was analyzed by Co-IP with an anti-T7 antibody followed by WB with an anti-HA antibody (upper panel). The immunoprecipitated T7-RTwt/mut were detected by an anti-T7 antibody (middle panel). The HA-A3G expression levels in the cell lysates was evaluated by WB with anti-HA antibody (lower panel). (C) A schematic representation of the different HA-A3G wt/mutant constructs used in the domain-mapping experiments. Full-length HA-A3G is shown at the top. The numbers indicate the amino acid positions in A3G. The domains marked are the cytidine deaminase domain (CDD), the linker (LINK), and the pseudoactive site (PAS). Different A3G truncated mutants are shown at the bottom. (D) Interaction of T7-RT with HA-A3G wt/mut was detected in 293T cells co-transfected with SVCMVin-T7-RT plasmid and each of A3G mutants. After 48 hours of transfection, the interaction of each A3G truncated mutant with RT was analyzed by Co-IP with anti-T7 antibody followed by WB with an anti-HA antibody (upper panel). The immunoprecipitated T7-RT was detected by anti-T7 antibody (middle panel). The expression levels of HA-A3Gwt/mutant in the cell lysates was detected with an anti-HA antibody (lower panel). The images represent the results of three independent experiments.

sufficient for binding to A3G.

Similarly, to map the regions in A3G required for the A3G/RT interaction, we constructed a panel of A3G N- and/or C-terminal deletion mutants based on the locations of the two cytidine deaminase domains (CDDs) in A3G (43, 141, 147), including HA-A3G$_{65-132}$, HA-A3G$_{102-257}$, and HA-A3G$_{195-384}$ (Fig. 3.4C). Each of these mutants was co-transfected with a T7-RT or T7-tag plasmid into 293T cells. In parallel, HA-A3Gwt was included in the experiments. As shown in Figure 3.4D, the expression of the different A3G mutants varied (lower panel). Interestingly, despite the low level of expression, the mutant HA-A3G$_{65-132}$ was able to bind to RT efficiently (Fig. 3.4D, lane 4). In contrast, the truncated mutants HA-A3G$_{102-257}$ and HA-A3G$_{195-384}$ did not bind to RT (Fig. 3.4D, lanes 6 and 8). Collectively, these data indicate that the N-terminal domain of A3G that encompasses the amino acids 65 to 132 and contains the first CDD and part of the linker region is the necessary region for A3G to bind to HIV-1 RT.

### 3.2.5 The RT-binding polypeptide A3G$_{65-132}$ inhibits both the A3G/RT interaction and the effect of A3G on HIV-1 reverse transcription

Because A3G$_{65-132}$ is able to bind to HIV-1 RT, it is possible that this peptide could compete with wild-type A3G for RT binding. To test this possibility, we performed competition Co-IP experiments in 293T cells by co-expressing T7-RT and HA-A3G$_{wt}$ with HA-A3G$_{65-132}$, HA-A3G$_{102-257}$, and HA-A3G$_{195-384}$. After the Co-IP assay with anti-T7 precipitation, followed by WB with an anti-HA antibody, we found that the presence of the RT-binding peptide A3G$_{65-132}$ significantly disrupted the binding of HA-A3Gwt with RT (Fig. 3.5A, top panel, lane 3). In contrast, the presence of equal amounts of HA-A3G$_{102-257}$ or higher amounts of HA-A3G$_{195-384}$ showed no

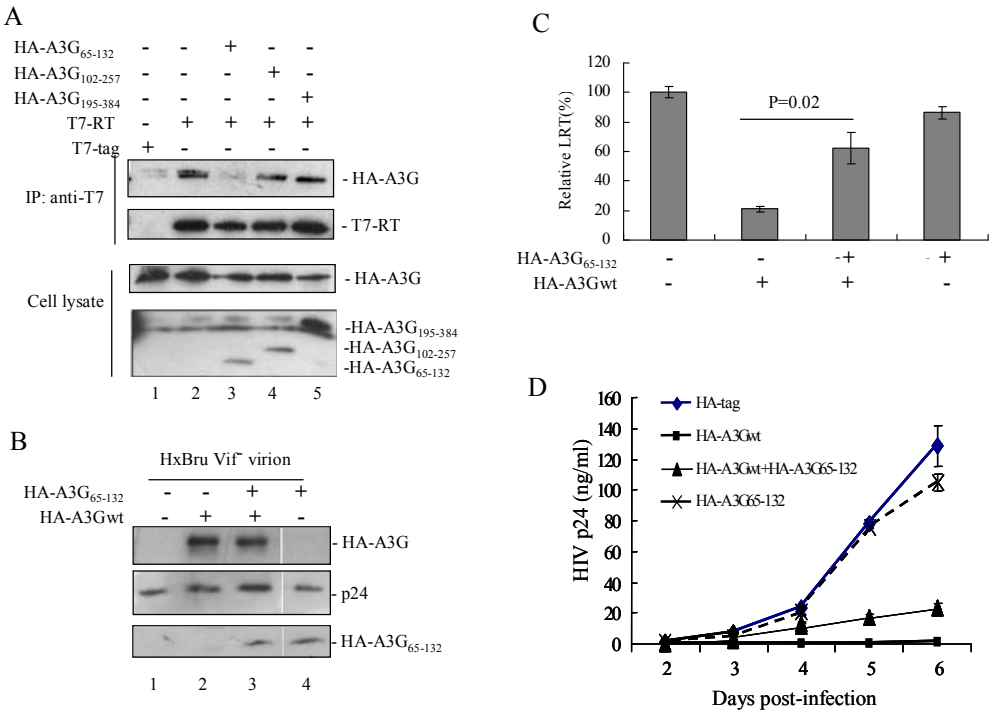


**Fig. 3.5 A3G$_{65-132}$ disrupts both the A3G/RT interaction and attenuates A3G's inhibitory effect on HIV-1 reverse transcription.** (A) A3G$_{65-132}$ blocks the binding of A3Gwt with HIV-1 RT. HA-A3Gwt, SVCMVin T7-RT, and each HA-A3G truncated mutant plasmids were co-transfected into 293T cells for 48 hours. The interaction between HA-A3Gwt and T7-RT was analyzed by Co-IP with anti-T7 antibody followed by WB with an anti-HA antibody (upper panel). The immunoprecipitated T7-RT was visualized by WB with anti-T7 antibody (second panel). The expression of HA-A3Gwt in the cell lysates was detected with anti-A3G antibody (third panel). HA-A3G mutants were detected with an anti-HA antibody (lower panel). (B) To evaluate the virus incorporation of A3G in presence of HA-A3G$_{65-132}$, the HxBru-Vif$^-$ provirus was co-transfected with HA-A3Gwt or HA-A3G$_{65-132}$ alone or the HA-A3Gwt and HA-A3G$_{65-132}$ expression plasmids. After 48 hrs of co-transfection, virions were collected by ultracentrifugation, lysed and loaded on SDS-PAGE. Then the presence of A3G, viral protein Gag p24 and A3G$_{65-132}$ in each viral sample was analyzed by WB with anti-A3G (upper panel), anti-p24(middle panel) and anti-HA(lower panel) antibodies. (C) and (D) To test the effect of A3G$_{65-132}$ on HIV-1 reverse transcription and viral replication, equal amounts of viruses (normalized by p24 ELISA) were used to infect CD4$^+$ C8166 T cells. Twelve hours post-infection, total DNA was extracted from the infected cells. The level of HIV-1 LRT was analyzed by real time-PCR(C). Meanwhile, at different time points after infection, the supernatants from the infected cell cultures were collected, and viral replication was monitored by measuring the level of the HIV-1 Gag p24 antigen in the supernatant (D). A and B show representative WB results from three independent experiments. The value presented in C is the means and standard deviation from three independent experiments. P values determined by *t*-test are shown above the bars of compared groups. The HIV p24 values in D presented are the means and range of values from two independent experiments.

inhibition effect on the A3G/RT interaction (Fig. 3.5A, lanes 4 and 5). This binding difference among each sample was not due to the variation of HA-A3Gwt and T7-RT expression because similar amounts of HA-A3Gwt and T7-RT were detected in different samples (Fig. 3.5A, two middle panels). Taken together, these data indicated that $A3G_{65-132}$ did not influence the expression of A3Gwt and RT but specifically competed with HA-A3Gwt to bind to HIV-1 RT.

Because $A3G_{65-132}$ blocks the binding of A3G to RT, we asked whether HA-$A3G_{65-132}$ could impact the antiviral activity of A3Gwt. To test this possibility, we produced $Vif^-$ HIV-1 from 293T cells by co-transfecting the HxBru-$Vif^-$ provirus with HA-A3Gwt or HA-$A3G_{65-132}$ alone or with HA-A3Gwt and HA-$A3G_{65-132}$ expression plasmids together. After harvesting the viruses, the amount of A3Gwt packaged into the viruses was measured by WB. The results showed that both A3Gwt and HA-$A3G_{65-132}$ were able to be incorporated into the virus (Fig. 3.5B, lane 2 to 4). Meanwhile, a HA-tagged Vpx ($SIVmac_{239}$) was unable to be packaged into the virus (data not shown) (317), thus demonstrating the specificity of HA-$A3G_{65-132}$ incorporation. Interestingly, the association of the HA-$A3G_{65-132}$ polypeptide did not appear to affect the packaging of A3Gwt (Fig. 3.5B, compare lane 3 to 2). To further test the effect of A3Gwt and HA-$A3G_{65-132}$ on virus infection, each virus stock shown in Figure 3.5B was used to infect C8166 T cells and after 12 hours, the viral reverse transcription was evaluated by real-time PCR. The results showed that in the cells infected by the $Vif^-$ viruses containing only A3Gwt, the level of LRT was reduced to 20%, which was similar to the results described in Figure 3.1A. In contrast, after cells were infected by the virus produced in the presence of both HA-A3Gwt and HA-$A3G_{65-132}$, the detected LRT level reached to approximately 60% of the wild-type virus infection level without A3Gwt (Fig. 3.5C, compare bar 3 to 1). Meanwhile, the

effect of HA-A3G$_{65-132}$ alone was also tested and showed no significant inhibition on HIV-1 reverse transcription (Fig. 3.5C, bar 4). Furthermore, we also monitored viral replication after infection by each viral stock indicated in Figure 3.5B. Results showed that the virus produced in the presence of A3Gwt lost infection ability (Fig. 5D). Interestingly, the data also revealed that the virus produced in 293T cells expressing both A3Gwt and HA-A3G$_{65-132}$ was able to induce a low-level infection that reached to approximately 15% of the wild type infection level (Fig. 5D). All of these results indicate that the presence of A3G$_{65-132}$ polypeptide is able to inhibit the anti-HIV effect mediated by A3G.

**3.3 Discussion**

Several intrinsic anti-HIV factors, including TRIM5α, A3G, BST-2, and SAMHD1, have been identified recently (287, 296, 315). Among them, A3G is a member of the cytidine deaminase family of nucleic acid-editing enzymes which have been found to confer broad protection against retroviruses, including HIV-1, and limit the cross-species transmission of these pathogens (203, 296). It is well known that one of the main functions of A3G is to terminate HIV infection by deaminating cytosine residues to uracil in the minus viral DNA strand during reverse transcription, consequently resulting in G to A mutations in the HIV-1 provirus (120, 178, 198, 365). In addition, a number of other studies have reported that A3G also inhibits HIV-1 reverse transcription soon after Vif$^-$ virus entry into the cells, and this anti-reverse transcription activity was not correlated with the deaminase activity of the protein (28, 29, 131, 237, 354), indicating that A3G exerts a multifaceted antiviral effect against HIV-1 infection. However, until now, it is still unclear whether A3G requires binding to HIV-1 RT to disrupt its function. In this chapter, we have demonstrated that A3G

specifically binds to HIV-1 RT in the viruses, and their interaction did not require other HIV-1 proteins or viral RNA. In addition, our deletion analyses indicate that a region of A3G (residues 65-132) containing the first CDD and part of the linker region, and the RT fingers-palm domain were required for their interaction. Interestingly, the presence of the $A3G_{65-132}$ polypeptide was shown to be able to block the A3G/RT interaction and attenuate the anti-HIV effect of A3G. Thus, this study provides evidence for an interaction between A3G and HIV-1 RT, which may be a necessary step for A3G to inhibit HIV-1 reverse transcription.

Previous studies showed that A3G was able to interrupt several steps of HIV-1 reverse transcription, including the inhibition of $tRNA^{lys3}$ primer annealing (111-113), the blocking of strand transfers (185, 206) and/or the suppression of $tRNA^{lys3}$ cleavage and removal (206). By studying the properties of A3G using purified A3G and RT proteins, Iwatani et al. proposed a 'roadblock' mechanism to explain the inhibition of A3G on all RT-catalyzed DNA elongation reactions (143). Their study indicated that A3G binds to nucleic acid with a higher affinity than RT, which consequently blocks the movement of RT along the template. Conversely, our study provides evidence for the direct interaction of A3G with HIV-1 RT, and an RT-binding peptide derived from A3G interfered with both the ability of A3G to bind to RT and inhibit HIV-1 reverse transcription. This observation raises the possibility that A3G binding to RT may be one of the prerequisite steps for its inhibitory effect on HIV-1 reverse transcription. Several mechanisms may account for its inhibitory effect. The binding of A3G to RT could interfere with the access of RT to the substrate or physically inhibit the enzymatic activities of RT. Interestingly, an earlier study reported an interaction between A3G and RT in the hepatitis B virus (HBV) (239). This study indicated that A3G binding to HBV RT was required for the incorporation of A3G into HBV

nucleocapsids. In HIV-1 infection, several previous studies clearly showed that A3G virus incorporation is mediated by the NC domain of the Gag protein and/or viral RNA (5, 76, 363). We also examined the effect of RT on the incorporation of A3G into the virus, and the results suggest that the content of A3G in the HIV-1 virions was not significantly reduced when RT was deleted in our single-cycle replication virus (data not shown). This finding suggests that the interaction of A3G with HIV-1 RT may occur after A3G is already within the virus. It should be noted that both our study and the study by Nguyen, D. et al. (239) revealed that A3G binding to both HBV and HIV-1 RT did not require the presence of the viral genomic RNA (Fig. 3.3A).

Through the deletion analysis, we mapped the RT-binding region in the A3G encompassing residues 65 to 132, which partially overlaps with the region essential for A3G packaging (43, 141, 191). This finding suggests that RT-binding region may partially overlap with the NC-binding region in A3G. These results led to the speculation that at the initial stage of HIV-1 assembly, A3G may be first associated with HIV-1 NC and/or RNA. At this stage, the incorporation of A3G does not necessarily require the presence of RT. Consistently, our data also revealed that the presence of the RT-binding polypeptide $A3G_{65\text{-}132}$ does not significantly impair the incorporation of $A3G_{wt}$ into the virus (Fig. 3.5B). During viral maturation and Gag/Gag-Pol proteolytic processing, A3G may be released from Gag and/or Gag-Pol precursor and targets HIV-1 RT in the virus. This highly regulated order of binding may be necessary for an efficient packaging of A3G and, consequently, its action on viral reverse transcription. This speculation is also supported by the fact that the interaction between A3G and NC does not affect reverse transcription (143). Moreover, our results showed that the RT processing in the virus was not affected by A3G (Fig. 3.2B and 3.2C). This data suggests that A3G may bind to RT after RT is cleaved from

the precursor and forms the p66/p51 heterodimer. However, we still do not have direct evidence to support this hypothesis, and further investigation will be required to elucidate these mechanisms.

A number of peptides have demonstrated therapeutic potential against HIV-1 replication, and some of them target HIV-1 RT (8). A peptide derived from HIV-1 NCp7 reduced the viral DNA level in a dose-dependent manner through the inhibition of the NCp7/RT interaction (80). In this study, we identified a polypeptide, $A3G_{65-132}$, which could compete with A3Gwt for the interaction with RT. Intriguingly, the infection experiments showed that when $CD4^+$ T cells were infected by viruses produced in the presence of both the A3Gwt and $A3G_{65-132}$ peptide, the reverse transcription level was significantly higher than that in cells infected with viruses produced in the presence of only A3Gwt (Fig. 3.5C). In contrast, the viral reverse transcription was not affected when the infecting viruses were produced in the presence of the $A3G_{65-132}$ peptide alone. These results clearly indicate that even though the $A3G_{65-132}$ peptide was able to bind to RT efficiently, it did not inhibit its function; however, its presence was able to compete with A3Gwt and dominantly interfere with its anti-reverse transcription activity. However, we also could not eliminate the possibility that A3G65-132 may bind to A3Gwt and disrupt its ability to interact with HIV RT, which will require further investigation.

Overall, these observations provide evidence for the requirement of the A3G/RT interaction for the inhibition of A3G on HIV-1 reverse transcription. Also, our study suggests that RT binding through the binding motif itself is not sufficient to disrupt the activity of RT, and the other domains of A3G are also required. It is worth noting that, the previously described virion incorporation domain (aa 124-127) and a Vif-binding motif (aa128-130) are present in both the RT-binding peptide $A3G_{65-132}$ and a

RT-unbound $A3G_{102-257}$ (Fig. 3.4D), suggesting that these two functional domains may not be sufficient for A3G binding to HIV-1 RT. Additionally, we also observed that even though $A3G_{65-132}$ significantly inhibited A3G's effect on HIV reverse transcription (Fig. 3.5C), the presence of $A3G_{65-132}$ could only modestly increase viral production (Fig. 3.5D). At this point, we still do not know whether the presence of $A3G_{65-132}$ had less effect on A3G-induced viral hypermutation. Hence, more studies are required to address these questions. Also, more detailed analysis will be required to define the critical amino acid(s) and/or motifs within $A3G_{65-132}$ that are required for its interaction with RT.

Until now, A3G has been reported to bind to the following four HIV-1 proteins: NC, Vif, IN and RT (158, 191, 192). Among those, the A3G-binding viral proteins Vif, NC and IN have all been shown to interact with RT and promote the efficiency of reverse transcription to varying levels (40, 123, 127, 158, 181). Thus, an unanswered question is whether A3G-mediated inhibition of reverse transcription could be due to the disrupting effect of their associations with RT. In our study, we have ruled out the involvement of IN and Vif, because in the absence of Vif and IN, A3G still significantly inhibited reverse transcription (Fig. 3.1D). However, we still do not know if A3G binding to RT could interfere with the NC/RT interaction, and this question has yet to be answered. Additionally, it would also be interesting to investigate whether the A3G/RT interaction could contribute to A3G-induced hypermutation during HIV replication, and if this is the case, whether $A3G_{65-132}$ could affect the rate of A3G-induced hypermutation. Overall, our results have demonstrated the A3G/RT interaction and its impact on HIV-1 reverse transcription. Further investigation of this interaction will elucidate our understanding of the mechanism underlying the antiviral action of A3G, which will contribute to the design of new

anti-HIV strategies.

# CHAPTER 4

## Characterization of the Anti-HIV Activity Mediated by Various R88-APOBEC3G Mutant Fusion Proteins

### 4.1 Introduction

During wild-type HIV-1 infection, the antiviral effects of A3G are counteracted by the viral protein Vif. It is well known that Vif can directly bind to A3G and significantly prevent virion incorporation of A3G by accelerating A3G ubiquitination and proteasomal degradation, thus decreasing the intracellular concentration of A3G (65, 155, 203, 204, 297, 310, 361, 362). In addition, other studies suggest that Vif can prevent A3G incorporation into virions independent of the reduction in A3G intracellular levels (155, 156, 203, 297). Indeed, Opi et al. showed that HIV-1 Vif efficiently inhibits the virion packaging and antiviral activity of a degradation-resistant A3G mutant (249).

Given that A3G possesses potent anti-HIV activity and its action is counteracted by HIV-1 Vif protein, considerable interest has been focused on restoring A3G's antiviral activity during wild-type HIV-1 infection. One way to overcome the Vif-mediated inhibition is to disrupt the Vif-A3G interaction. Previous studies have shown that a single amino-acid substitution at position 128 of A3G (representing a change of an aspartic acid [D] to a lysine [K]) blocked the Vif-A3G interaction and rescued the antiviral activity of A3G (32, 141, 176, 199, 290, 352). This finding demonstrated the feasibility of designing pharmaceutical agents that could block Vif binding to A3G. Interestingly, while the three amino acid motif comprised of aspartic acid, proline, aspartic acid (DPD) at positions 128 to 130 of A3G was identified as a crucial region for the interaction between A3G and HIV-1 Vif (141), a YYFW (124-127) region that is adjacent to the N-terminus of the DPD motif was found to be

critical for the virion packaging of A3G. Such close alignment of these two functional domains within A3G makes it difficult to target the DPD motif with a pharmaceutical agent without affecting A3G packaging. Thus, other approaches, including delivering A3G into HIV-1 particles independent of the blockage by Vif and subsequently inactivating HIV-1 infectivity, could hold promise as a potential HIV therapeutic approach.

In our previous study, R88-A3G fusion protein, which was made by fusing A3G to a virus-targeting polypeptide (R14-88) derived from HIV-1 Vpr protein (356), was able to overcome the HIV-1 Vif barrier and efficiently deliver A3G into the virus (14). Moreover, the study demonstrated that expression of the R88-A3G fusion protein in $Vif^+$ HIV-1-producing cells drastically inhibited progeny virus infection in different cell types including $CD4^+$ C8166 T cells and human primary PBMCs (14). As noticed, R88-A3G protein was still sensitive to Vif-induced degradation. To develop a more potent anti-HIV R88-A3G fusion molecule, in current chapter, different A3G mutants were introduced into the R88-A3G fusion system and their anti-HIV properties were characterized. It is hypothesized that through point mutation, the optimized R88-A3G can gain resistance to Vif inducted-degradation and exhibit advanced anti-HIV effect than wild-type R88-A3G. Following objectives were designed to evaluate the hypothesis:

1. Generation and characterization of different R88-A3G mutants, including their sensitivity to Vif-induced degradation, intracellular localization, virion encapsidation and inhibitory effects against $Vif^+$ HIV-1.
2. Detailed study on the antiviral effect mediated by representative mutant R88-$A3G_{P129A}$ in susceptible cell populations.

## 4.2 Results

### 4.2.1 Expression of different R88-A3G variants and their resistance to Vif-mediated degradation

Our previous study demonstrated that the fusion protein R88-A3Gwt comprised of an A3G and a virion-targeting polypeptide (R14-88) significantly inhibited HIV-1 infection even in the presence of Vif (14). To develop a more potent anti-HIV R88-A3G fusion molecule and test the requirement of A3G enzymatic activity for the anti-HIV effect of R88-A3G fusion protein, we introduced several A3G mutants into the CMVin-R88-A3G, including R88-A3G$_{Y124A}$, R88-A3G$_{D128K}$, R88-A3G$_{P129A}$ and R88-A3G$_{E259Q}$ (Fig. 4.1A). Among these mutants, D128K and P129A, which are located in the previously-described HIV Vif-binding region D$^{128}$PD$^{130}$, were intended to block the Vif-A3G interaction (141, 352). The R88-A3G$_{Y124A}$ contains a mutation located in a Y$^{124}$YFW$^{127}$ region that is important for the packaging of A3G into HIV-1 particles. This mutant has been previously shown to lose the virion incorporation ability (141). We also included a C-terminal cytidine deaminase domain mutant, R88-A3G$_{E259Q}$ (35, 292, 299), to test the importance of the enzymatic function of A3G in the antiviral activity of R-A3G.

We next tested the expression of different A3G mutants and their resistance to Vif-mediated degradation. It is known that HIV-1 Vif targets A3G to the proteasome for degradation, and that this targeting results in reduced intracellular levels of A3G, consequently inhibiting A3G packaging into virions (155, 203, 204, 297, 310). In this study, we cotransfected individual the R88-A3G with HIV-1 Vif (pcDNA-hVif) plasmids into 293T cells. At 48 hours post-transfection, the expression of each protein in 293T cells was analyzed by [$^{35}$S]methionine pulse-chase radiolabeling and immunoprecipitation with anti-Vpr antibodies as described previously (14). Our

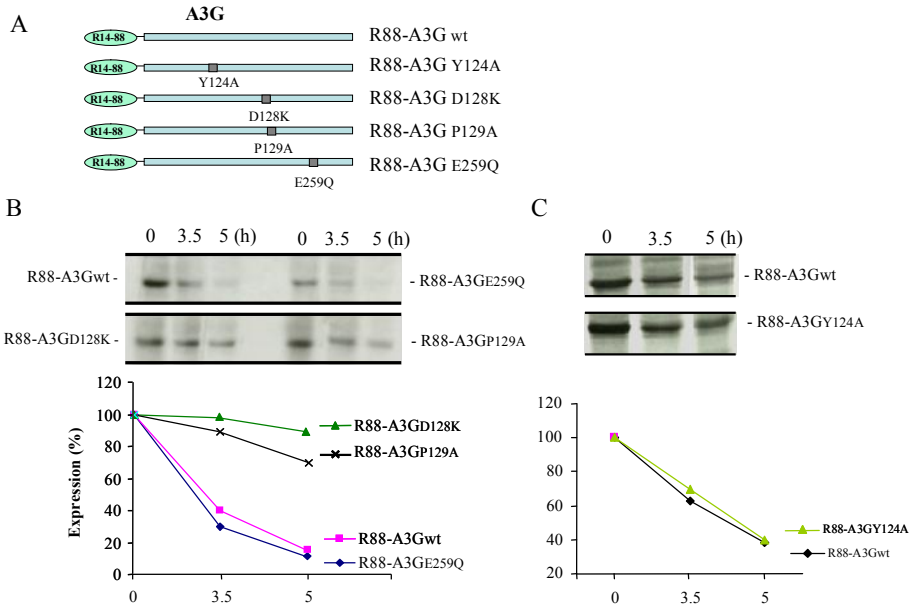


**Fig. 4.1 The expression of R88-A3G mutants and their resistance to Vif-mediated degradation.** (A) Schematic representation of R88-A3G mutants at the cytidine deaminase activity site (E259Q), viral packaging site (P124A) and Vif-response site (D128K, P129A). (B and C) R88-A3G wild type or mutant plasmids were co-transfected with a pcDNA-hVif plasmid in 293T cells. At 48 hour post-transfection, cells were pulse-radiolabeled with [$^{35}$S]-methionine for 30 min and collected and lysed at 0, 3.5 and 5 hours. The level of R88-A3Gwt/mutant in each lysed cell sample was evaluated by anti-Vpr immunoprecipitation (upper panel). The level of degradation of wild type and mutant R88-A3Gs was quantified by laser densitometry (lower panel). The result is a representative of two independent experiments.

results show that, consistent with a previous study (14), R88-A3Gwt was rapidly degraded in the presence of Vif and had a half-life of approximately 3 hours (Fig. 4.1B). Similarly, R88-A3G$_{E259Q}$ and R88-A3G$_{Y124A}$ were also sensitive to Vif-inducted degradation (Fig. 4.1B and C). By contrast, the R88-A3G$_{D128K}$ and R88-A3G$_{P129A}$ mutants were found to be resistant to degradation and had half-lives of more than 5 hours (Fig. 4.1B). These results are consistent with previous observations for wild-type A3G (141, 291, 352) and imply that the Vif-resistant properties of R88-A3G$_{D128K}$ and R88-A3G$_{P129A}$ may affect their antiviral activities.

### 4.2.2 Inhibitory effects of different R88-A3G mutants on Vif$^+$ HIV-1 infectivity

To investigate the inhibitory effect of each R88-A3G mutant on Vif$^+$ HIV-1 infectivity, we produced virus stocks by co-transfecting pNL4.3/GFP$^+$/Vif$^+$ provirus with either wild type R88-A3G or different mutant expression vectors in 293T cells. 48 hours after transfection, progeny viruses were pelleted by ultracentrifugation and quantified by Gag-p24 measurements using an HIV-1 p24 ELISA kit. The virus production from different R88-A3G mutant-transfected cells did not differ significantly according to the p24 levels (data not shown). Equal amounts of the viruses (adjusted by HIV-1 Gag-p24 levels) were used to infect CD4$^+$ C88166 T cells, and the level of infection was determined by FACS analysis of the percentage of infected (GFP-positive) cells (Fig. 4.2). In the absence of any R88-A3G, approximately 64% of the cells were infected (Fig. 4.2A and B, b), while in the presence of R88-A3Gwt, only 19% of cells were found to be positive (Fig. 4.2A and B, c). Interestingly, R88-A3G$_{E259Q}$, a catalytically defective mutant, did not exhibit significant antiviral activity compared to R88-A3Gwt (Fig. 4.2A and B, g). These results indicate that, in the context of the R88-A3G fusion, the cytidine deaminase

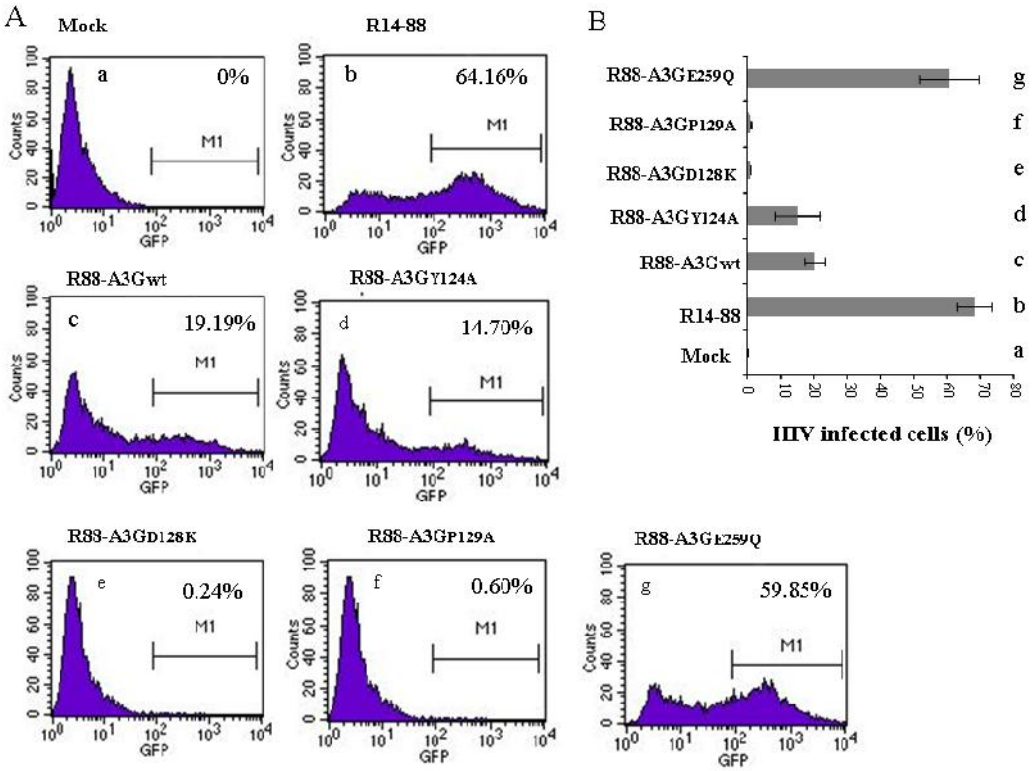


**Fig. 4.2 The inhibitory effects of R88-A3G mutants on Vif$^+$ virus infectivity.** Viruses were produced from 293T cells transfected with 3µg HIV-1 pNL4.3-GFP or co-transfected with 4µg R88-A3Gwt/mutant plasmid. Equal amounts of produced viruses (as adjusted by the Gag p24 level) were used to infect CD4$^+$ C8166 T cells. At 72 hours post-infection, the percentage of infected (GFP-positive) cells was measured by FACS analysis. (A) Representative FACS profiles. (B) Mean percentages of infected cells from each cell line (a-g) with standard errors from duplicated samples of the experiment.

mutant $A3G_{E259Q}$ was not active against HIV-1, even though it was efficiently incorporated into the virus (Fig. 4.3B, left panel). In contrast, the packaging-defective mutant R88-$A3G_{Y124A}$ (141) possessed anti-HIV activity as efficiently as the wild type R88-A3G (Fig. 4.2A and B, compare d to c). This result provides evidence that the fusion of a virion-targeting signal (R88) to $A3G_{Y124A}$ can rescue the antiviral activity of $A3G_{Y124A}$.

Two R88-A3G mutants, R88-$A3G_{D128K}$ and R88-$A3G_{P129A}$, showed significantly enhanced anti-HIV activities compared to R88-A3Gwt. The infection was almost completely blocked when the infecting virus was produced from R88-$A3G_{D128K}$- or R88-$A3G_{P129A}$-expressing cells (Fig. 4.2A and B, e and f). This result was expected because the two mutants have been shown to be resistant to inhibition by Vif (141, 199, 290, 352). Moreover, our data indicate that wild type R88-A3G is not fully Vif-resistant, and that introducing D128K or P129A into R-A3G could almost completely inhibit HIV-1 replication by overcoming the blockage of Vif. These results suggest that R88-$A3G_{D128K}$ and R88-$A3G_{P129A}$ are potent antiviral molecules.

### 4.2.3 Intracellular localization and virion incorporation of different R88-A3G mutants

The results discussed above show that different R88-A3G mutants possess varying anti-HIV activities. To better understand the mechanism underlying the actions of these mutants, we investigated their intracellular localization and virion incorporation. Previous studies showed that A3G localized predominantly in the cytoplasm and that the single amino acid substitutions within the region from amino acids 113 to 128 did not affect the cytoplasmic localization of A3G (309). Because A3G was fused to a HIV-1 Vpr peptide, a karyophilic protein that is predominantly

localized in the nucleus (190), we examined whether this fusion strategy changed the intracellular distribution of different A3G mutants. Each R88-A3G mutant was transfected into HeLa cells, and their intracellular localization was analyzed by an anti-A3G immunofluorescence assay. In parallel, plasmid expressing HA-tagged A3G (14) was also transfected into HeLa cells as a control. The results show that HA-A3G was evenly distributed in the cytoplasm (Fig. 4.3A). Similarly, wild-type R88-A3G and all R88-A3G mutants were predominantly localized in the cytoplasm (Fig. 4.3A). These results indicate that fusing R14-88 with A3G did not affect the intracellular localization of the fusion protein.

To examine the encapsidation of R-A3G mutants into the virus in the presence of HIV Vif, we transfected 293T cells with the HxBru-Vif$^{+}$ provirus and either the wild type or mutant (D128K, P129A or E259Q) CMVin-R88-A3G plasmids. At 48 hours post-transfection, viral particles were collected and concentrated by ultracentrifugation through a 20% sucrose cushion. Similar amounts of each virus (adjusted by the amount of HIV p24) were lysed and directly loaded into a 12% SDS-PAGE gel. The virion-associated R88-A3G and Gag-p24 proteins were detected by WB with rabbit anti-A3G and mouse anti-p24 antibodies. Consistent with our previous observations (14), a significant amount of R88-A3Gwt was shown to be packaged into Vif$^{+}$ HIV-1 virions (Fig. 4.3B, lane 2). Interestingly, the R88-A3G$_{D128K}$ and R88-A3G$_{P129A}$ mutants that are resistant to Vif-mediated degradation (Fig. 4.1B) were incorporated into viruses at much higher levels compared with R88-A3Gwt (Fig. 4.3B, compare lanes 3 and 4 with lane 2). The virion-incorporation level of the cytidine deaminase-deficient mutant R88-A3G$_{E259Q}$ was similar to that of wild type R88-A3G (Fig. 4.3B, lane 5). These data indicated that one explanation for the remarkable anti-HIV activities of R88-A3G$_{D128K}$ and R88-A3G$_{P129A}$ arises from their

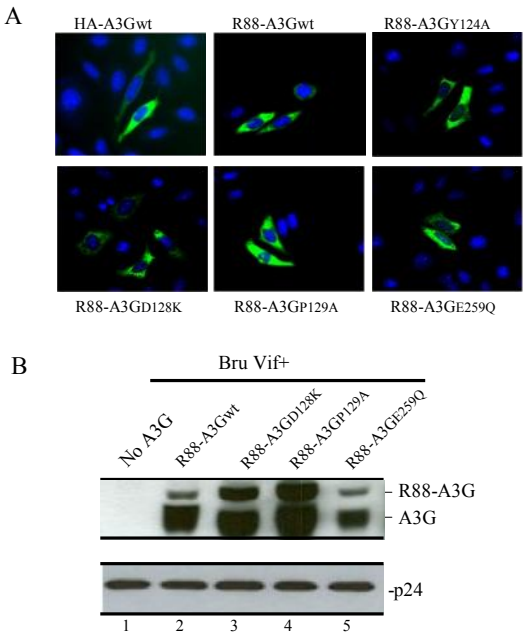


**Fig. 4.3 Intracellular localization and virion incorporation of different R88-A3G mutants**. (A) HeLa cells were transfected with equal amounts of HA-A3G or R88-A3Gwt/mutant plasmid DNA. 48 hours post-transfection, cells were fixed and treated with rabbit anti-A3G polyclonal antibody followed by incubation with FITC-conjugated anti-rabbit antibody and observed by fluorescence microscopy (20x objective). (B) 293T cells were transfected with HxBru-Vif$^{+}$ (3µg; lane 2) or co-transfected with HxBru-Vif$^{+}$ and 2µg of R88-A3Gwt/mutant (D128K, P129A or E259Q; lanes 3-6). After 48 hours, the produced virus particles were collected from the supernatant by ultracentrifugation through a 20% sucrose cushion. The virus lysate samples were loaded into a 12% SDS-PAGE gel and analyzed by WB with rabbit anti-A3G and anti-p24 antibodies as indicated. The result is a representative of two independent experiments.

high levels of virion incorporation.

### 4.2.4 Expression of R88-A3G$_{P129A}$ in CD4$^+$ C8166 T cells effectively blocks HIV-1 replication and spread

The results from the above-mentioned experiments showed that R88-A3G$_{D128K}$ and R88-A3G$_{P129A}$ exhibited the most effective antiviral activity when they were transiently over-expressed in HIV-producing 293T cells. To determine how these mutants affect HIV replication and spread when expressed in CD4$^+$ T cells, we generated CD4$^+$ T cell lines that stably expressed a low level of R88-A3G and R88-A3G$_{P129A}$ through a lentiviral vector system as previously described (14). Briefly, the CD4$^+$ C8166 T cells were transduced with an equal amount of R88-A3G- or R88-A3G$_{P129A}$-expressing vector particles (300ng of Gag-p24), as described in materials and methods, and selected with puro (0.5μg/ml). Two C8166 T cell lines that stably expressed R88-A3Gwt or R88-A3G$_{P129A}$ were obtained. The expression of the fusion protein was detected by monitoring virion-incorporated R88-A3Gwt or R88-A3G$_{P129A}$ protein from highly concentrated HxBru-Vif$^+$ viruses produced in these two cell lines (data not shown). Prior to examining the effects of the R-A3Gwt/mutant on HIV replication, we evaluated the cell growth, cell cycle profile and CD4 receptor expression on the cell surface as described previously (14). The results showed that cell growth and the cell cycle profiles did not significantly differ in R88-A3Gwt, R88-A3G$_{P129A}$ or empty vector-transduced C8166 T cell lines (Fig. 4.4A and B). In addition, equivalent levels of the surface CD4 receptor were detected on these stable cell lines (Fig. 4.4C).

To determine whether the R88-A3G$_{P129A}$-transduced C8166 T cells exerted inhibitory effects on HIV-1 infection, we infected R88-A3Gwt, R88-A3G$_{P129A}$ and

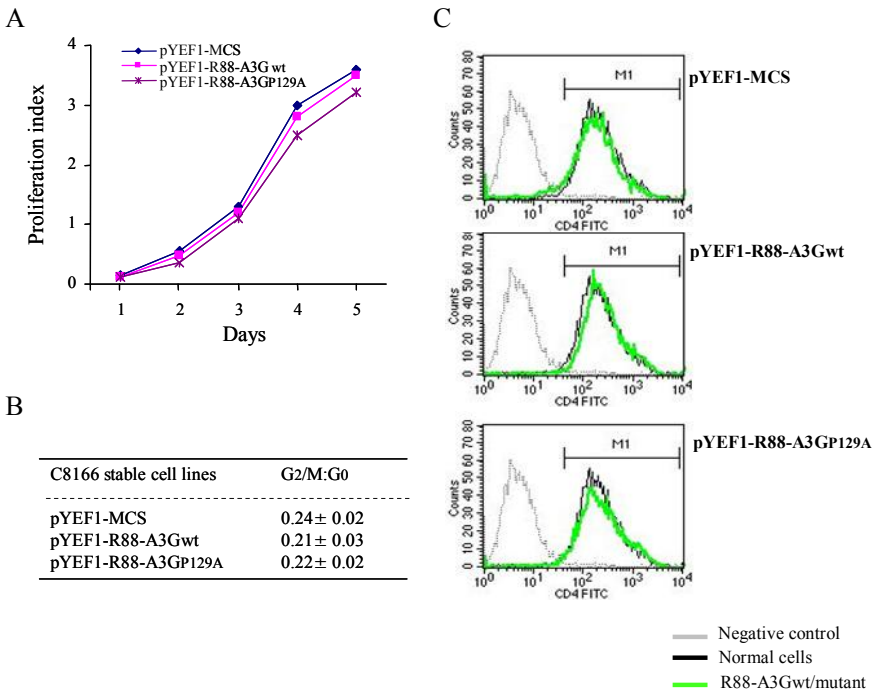


| C8166 stable cell lines | G2/M:G0 |
|---|---|
| pYEF1-MCS | 0.24± 0.02 |
| pYEF1-R88-A3Gwt | 0.21± 0.03 |
| pYEF1-R88-A3GP129A | 0.22± 0.02 |

**Fig. 4.4 Generation and biological characterization of CD4$^+$ T cells stably expressing R88-A3G$_{P129A}$.** C8166 T cells (0.5x10$^6$) were transduced with an empty vector (pYEF1-MCS) or lentiviral vectors containing either R88-A3Gwt (pYEF1-R88-A3Gwt) or R88-A3G$_{P129A}$ (pYEF1-R88-A3G$_{P129A}$) and selected with 0.5μg/ml puro to produce puro-resistant cell populations. (A) To assess the growth of vector- and R88-A3Gwt/mut-transduced C8166 T cells, a WST assay was performed to determine the cell viability at several time points. (B) The cell-cycle profiles of vector- and R88-A3G-transduced C8166 T cells were analyzed by staining with 30μg/ml of PI followed by flow cytometry to measure cellular DNA content. (C) CD4 receptor expression levels in vector- and R88-A3Gwt/mut-transduced C8166 T cells were analyzed by an anti-CD4 staining and flow cytometry assay.

empty vector-transduced C8166 T cell lines in parallel with equal amounts of pNL4.3-GFP virus (14). Viral replication was monitored by measuring the level of the HIV-1 Gag-p24 antigen in the supernatant for a 24-day period (Fig. 4.5A). In addition, the presence of HIV-1 infected cells (GFP-positive) at day six was determined using fluorescence microscopy (Fig. 4.5B). The results showed that the empty vector control cell line supported $Vif^+$ pNL4.3-GFP virus replication, which peaked after six days of infection. In the R-A3Gwt-transduced cell line, $Vif^+$ pNL4.3-GFP robust virus replication began at day 12 and peaked at day 16 (Fig. 4.5A and B). Interestingly, no HIV-1 replication was detected during the 24 days of observation in cells expressing R88-$A3G_{P129A}$ (Fig. 4.5A and B). These data indicate that R88-$A3G_{P129A}$ expressed in highly susceptible $CD4^+$ T cells was capable of providing long-term inhibition of $Vif^+$ HIV-1 replication.

To further test the effect of R88-A3Gwt and R88-$A3G_{P129A}$ on HIV transmission, the supernatant from the initial infection culture (passage 1) was collected at 72 hours post-infection. Similar volumes (1 ml) of infectious supernatants were used to infect normal (Fig. 4.5C, upper panel) or fresh R88-A3Gwt or R88-$A3G_{P129A}$-expressing C8166 T cells (Fig. 4.5C, lower panel). After infection, we performed an HIV-1 p24 ELISA to determine the infectivity of the progeny virus by measuring HIV-1 Gag-p24 levels in the supernatants from the corresponding cultures at days 7 and 11 post-infection. The results show that the infectivity of the progeny virus from R88-A3Gwt-transduced cells was reduced approximately fivefold compared with the virus from empty vector-transduced cells in normal C8166 cells (passage 2; Fig. 4.5C, upper panel). However, when the viral infection was carried out in freshly R88-A3Gwt-transduced cells (passage 2; Fig. 4.5C, lower panel), no infection was detected until day 11. Interestingly, there were no escaped infectious viruses produced

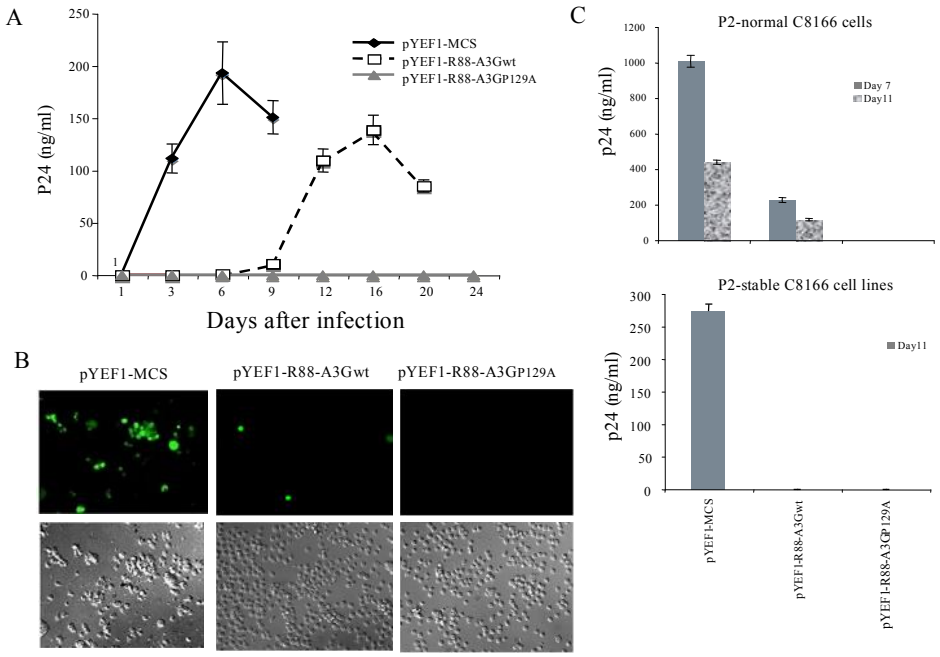


**Fig. 4.5 The R88-A3G$_{P129A}$-transduced CD4$^+$ C8166 T cells significantly inhibited HIV-1 infection.** Equal amounts of pNL4.3-GFP virus were used to infect vector-, R88-A3Gwt- or R88-A3G$_{P129A}$-transduced C8166 cell lines. (A) At different time points, virion-associated Gag p24 levels in the supernatant were measured by anti-p24 ELISA. (B) After 6 days of infection, the numbers of infected (GFP-positive) cells were visualized under fluorescence microscopy. (C) Identical volumes of 72-hour infectious supernatants were used to infect nontransduced (upper panel) or transduced C8166 cells (lower panel; passage 2). Levels of HIV-1 Gag p24 antigen in supernatants from passage 2 were then measured by an HIV p24 ELISA assay at days 7 and 11 post infection. The result shown is representative of two independent experiments. Mean with standard errors were calculated from the duplicated samples of one experiment.

in R88-A3G$_{P129A}$-expressing cells at passage 1. Therefore, no infection was observed at passage 2 post infection in either normal or freshly R88-A3G$_{P129A}$-transduced cells (passage 2; Fig. 4.5C). Taken together, these results further demonstrate that the presence of R88-A3G in CD4$^+$ T cells significantly inhibited HIV infection, and that R88-A3G$_{P129A}$ was able to completely block HIV infection and spread in CD4$^+$ C8166 T cells.

### 4.2.5 R88-A3G$_{P129A}$ inhibits HIV-1 replication in human PBMCs and macrophages

Human CD4$^+$ T cells and macrophages are the main HIV-1 infection target cells *in vivo*. Thus, it is important to introduce R88-A3G$_{P129A}$ into these primary cells and test its inhibitory effect on HIV infection. Here, we utilized an adeno-associated virus(AAV)-based vector, AAV2/5, to introduce the R88-A3G$_{P129A}$ gene into primary PBMCs and macrophages. Previous studies confirmed that the production and transduction of the AAV vector were not inhibited by A3G (49, 229). To produce AAV2/5-expressing R88-A3G$_{P129A}$, we first replaced the *lac*Z gene in an AAV2-*lac*Z vector (18, 26) with a cDNA encoding R88-A3G$_{P129A}$ (Fig. 4.6A). AAV2/5-*lac*Z and AAV2/5-R88-A3G$_{P129A}$ particles were subsequently produced by transfecting 293 cells with AAV2-*lac*Z or AAV2-R88-A3G$_{P129A}$, the pACK2/5 packaging plasmid, and the helper plasmid pAd.DELTA F6. The recombinant AAV2/5 vector particles were collected, purified by $CsCl_2$ gradients and titrated by TaqMan PCR as described in the material and methods section. To determine the transduction efficiency of AAV2/5 in C8166 T cells, human PBMCs and macrophages, we transduced these cells with the AAV2/5-R88-A3G$_{P129A}$ vector ($10^6$ vp/cell). After 3 days, the levels of R88-A3G$_{P129A}$ and the total cellular A3G mRNA were quantified by reverse transcription followed by

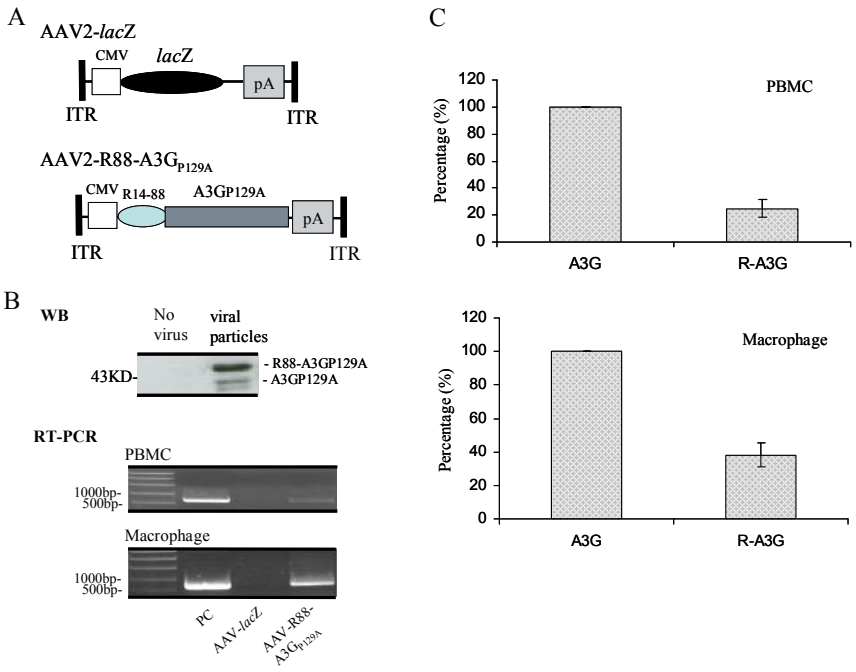


**Fig. 4.6 AAV2/5 vectors delivered R88-A3G$_{P129A}$ into C8166 T cells, human PBMCs and macrophages.** (A) Structures of AAV2-*lacZ*-transgene vectors. AAV2-R88-A3G$_{P129A}$ vector was constructed by substituting the *lacZ* gene with R88-A3G$_{P129A}$ between the CMV promoter and the poly(A) sequence. The entire vector DNA is flanked by the AAV2 inverted terminal repeats ITRs. (B) C8166 T cells were transduced with AAV2/5-*lacZ* or AAV2/5-R88-A3G$_{P129A}$ vectors at $10^6$ vp/cell. 72 hours after transduction, cells were infected with the pNL4.3-GFP HIV virus. 7 days after infection, viruses were pelleted from the supernatant, lysed and loaded into a 10% SDS-PAGE gel and analyzed by WB using anti-A3G antibody (upper panel). Total RNA was isolated from AAV2/5-*lacZ* or AAV2/5-R88-A3G$_{P129A}$-transduced human PBMCs and macrophages at 72 hours after transduction. The samples were analyzed by reverse transcription-PCR for the presence of R88-A3G$_{P129A}$ mRNA. The AAV2-R88/A3G$_{P129A}$ plasmid was used as a template for positive control (PC). (C) Real-time PCR analysis to determine R88-A3G$_{P129A}$ mRNA expression level. Cellular mRNA was extracted from PBMCs and macrophages, and subjected to reverse transcription. The reverse transcribed DNA from each sample was then amplified by real time-PCR to quantify R88-A3G$_{P129A}$ (R-A3G) and the total A3G (A3G) mRNA levels. The total A3G mRNA level was arbitrarily set at 100%. The result is a representative of two independent experiments.

PCR (Fig. 4.6B) and the real-time PCR analysis (Fig. 4.6C). The results showed that R88-A3G$_{P129A}$ specific mRNA was detected in PBMCs and in macrophages (Fig. 4.6B, middle and lower panels), and the data from quantitative real-time PCR revealed that the R88-A3G$_{P129A}$ mRNA level in PBMCs was approximately 23% of total A3G mRNA level (Fig. 4.6C, upper panel). Interestingly, the R88-A3G$_{P129A}$ mRNA level in macrophages reached nearly 40% of the total A3G mRNA level (Fig. 4.6C, lower panel). These results indicate that by using AAV2/5 delivery vector, R88-A3G$_{P129A}$ can be efficiently introduced into primary PBMCs and macrophages. Moreover, by using WB with an anti-A3G antibody, we could directly detect R88-A3G$_{P129A}$ fusion protein and its cleaved product, A3G$_{P129A}$, in HIV progeny viruses produced from AAV2/5-R88-A3G$_{P129A}$-transduced C8166 T cells infected with HIV-1 (Fig. 4.6B, upper panel).

We next tested whether AAV2/5-R88-A3G$_{P129A}$ transduced C8166 T cells and human PBMCs were resistant against HIV-1 infection. First, we transduced C8166 T cells and PHA-stimulated human PBMCs with AAV2/5-R88-A3G$_{P129A}$ or AAV2/5-*lacZ* particles ($10^6$ vp/cell) for 3 days. The cells were subsequently infected with equal amounts (adjusted by amounts of HIV Gag p24) of T-tropic HIV-1 (pNL4.3-GFP). At day 3 (for C8166 T cells) or 6 (for PBMCs), supernatants were collected and the HIV-1 replication level was monitored by measuring HIV-1 Gag p24 antigen levels. The results showed that in both R88-A3G$_{P129A}$-expressing C8166 T cells and human PBMCs, HIV-1 replication was reduced approximately two- to threefold compared with that in AAV2/5-*lacZ*-transduced cells (Fig. 4.7A and B).

To further test the effect of R88-A3G$_{P129A}$ on HIV replication in macrophages, we transduced macrophages from two different donors with the same AAVs. After three days, the transduced cells were infected with a macrophage-tropic pNL4.3-Bal virus

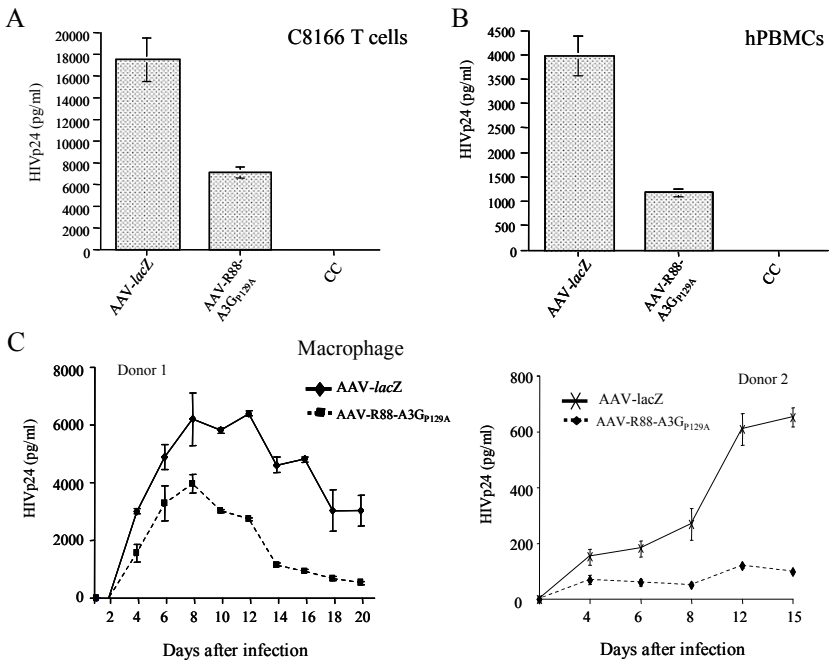


**Fig. 4.7 AAV2/5-R88-A3G$_{P129A}$ transduced CD4$^+$ C8166 T cells, human PBMCs and macrophages were significantly resistant to HIV-1 replication.** C8166 cells (A), PHA-stimulated human PBMCs (B), and M-CSF stimulated human macrophages (C, donor 1 and 2) were transduced with AAV2/5-*lacZ* or AAV2/5-R88-A3G$_{P129A}$ vectors for 72 hours and infected with pNL4.3-GFP$^+$, nevirapine-resistant HIV-1 or the pNL4.3-Bal virus strain. At different time points after infection, the supernatants from the infected cell cultures were collected, and viral replication was monitored by measuring the level of the HIV-1 Gag p24 antigen. The result shown is representative of two independent experiments. Means with standard errors are calculated from the results of duplicated samples from one experiment.

as previously described (12, 28, 217). At different time points after infection, supernatants from each infected cell culture were collected, and the viral infection level was monitored using an anti-p24 ELISA. The data from Figure 4.7C show that HIV-1 replication was inhibited in AAV2/5- R88-A3G$_{P129A}$-transduced macrophages. From donor 1, HIV-1 replication in AAV2/5-*lacZ*-transduced macrophages peaked at days 8 to 12. In AAV2/5-R88-A3G$_{P129A}$-transduced macrophages, HIV-1 infection peaked at day 8, while viral replication was reduced by approximately 40%. Of interest, after 8 days of infection, the HIV-1 infection level in AAV2/5-R88-A3G$_{P129A}$-transduced macrophages rapidly decreased to a low level (Fig. 4.7C, left panel), suggesting that either HIV-1 infection could not persist or the progeny viruses were unable to initiate efficient subsequent infections. In macrophages from donor 2, HIV-1 infection was significantly less productive (approximately 10-fold decrease in HIV Gag p24 production) than that in macrophages from donor 1 (Fig. 4.7C, compare right panel with left panel). Interestingly, in AAV2/5-R88-A3G$_{P129A}$-transduced macrophages, it appeared that HIV-1 could not initiate a productive infection up to 15 days (Fig. 4.7C, right panel). All of these results indicate that AAV2/5-mediated introduction of R88-A3G$_{P129A}$ in primary PBMCs and macrophages are sufficient to inhibit HIV-1 infection.

### 4.3 Discussion

In this chapter, we investigated the anti-HIV activity of different R88-A3G mutant fusion proteins including the A3G virus-packaging mutant Y124A, the deaminase- defective mutant E259Q and the Vif-binding defective mutants D128K and P129A. We showed that, while all R-A3G mutants could be efficiently incorporated into Vif$^+$ HIV-1 particles, the highest virion-incorporation levels were

observed for R88-A3G$_{D128K}$ and R88-A3G$_{P129A}$ mutants, due to their resistance to Vif-mediated degradation. In addition, the results show that A3G deaminase activity was required for R88-A3G antiviral activity. Most importantly, we demonstrated that introducing R88-A3G$_{P129A}$ into $CD4^+$ C8166 T cells, PBMCs and macrophages through AAV2/5-mediated transduction could significantly inhibit HIV-1 infection. All of these data provide further evidence for a potent A3G-based gene therapy approach to inhibit HIV-1 infection.

In the absence of HIV Vif, A3G can be efficiently incorporated into viral particles and interrupt HIV infectivity by introducing dC-to-dU mutations in the minus viral DNA strand during reverse transcription in target cells (120, 178, 198, 203, 365). Although the cytidine deaminase activity mediated by A3G plays an important role in restricting HIV-1 infection, the deaminase-independent antiviral activity of A3G remains controversial. Several studies have suggested that the antiviral function of A3G can be dissociated from its cytidine deaminase activity (28, 237, 299). However, other studies have shown that a specific deaminase-defective mutant of A3G, E259Q, has little or no antiviral activity (35, 217, 231, 292). To exclude the possibility that E259Q could impair the virus-packaging ability of A3G, we introduced E259Q into R88-A3G and tested its virus incorporation and antiviral activity. Our results indicate that although this fusion protein was effectively incorporated into viruses (Fig. 4.3), it did not exhibit any antiviral effect (Fig. 4.2). This data suggests that the anti-HIV activity of R88-A3G is deaminase-dependent.

Previous studies identified a four amino acid region (residues $Y^{124}YFW^{127}$) immediately adjacent to the Vif-binding site ($D^{128}PD^{130}$) as a critical region for A3G virion incorporation (141). Moreover, the authors showed that the mutant Y124A located in this region lost its anti-HIV activity, presumably due to its inability to be

targeted into the virus. In the present study, we fused this $A3G_{Y124A}$ to the R88 peptide and found that the anti-HIV activity of this fusion protein was rescued to a similar level as the wild type R88-A3G (Fig. 4.2). These data indicate that R88 is sufficient to complement the virus-packaging defect of A3G (Fig. 4.2B), and that the Y124A mutation does not affect the antiviral property of R88-A3G. Of note, approximately 275 Vpr molecules were estimated to be incorporated into each HIV-1 particle (223), but only 0.3-0.8 active A3G molecules were present in each $Vif^+$ particle and 4-9 A3G molecules were present in Vif-negative particles (35, 246, 351). Thus, it is expected that R88 is capable of delivering R88-$A3G_{Y124A}$ into HIV particles and fully rescuing its antiviral effect.

Another interesting observation in this study was that, while the R88-mediated virion incorporation pathway could allow R88-A3Gwt to overcome the physical blockage of Vif, the encapsidation of R88-A3Gwt was still significantly affected by the presence of Vif (Fig. 4.3B). This is due to the fact that R88-A3Gwt is still sensitive to Vif-mediated degradation, resulting in a relatively low level of intracellular R88-A3G available for viral encapsidation. Fortunately, this defect in R-A3Gwt can be complemented by introducing the Vif binding mutations D128K or P129A into this fusion protein. Our results demonstrate that the virion incorporation levels of R88-$A3G_{D128K}$ and R88-$A3G_{P129A}$ were significantly higher than that of R88-A3Gwt (Fig. 4.3B). Here, we also compared the antiviral activities of wild type R88-A3G and the different mutants, and found that fusing R88 to A3Gwt could not completely inhibit viral replication, and R88-$A3G_{D128K}$ and R88-$A3G_{P129A}$ exhibited a much stronger anti-HIV effect compared with R88-A3Gwt (Fig. 4.2 and Fig. 4.4). Although these two Vif-binding-defective mutants were efficiently incorporated into the virus, we still could not conclude that their remarkable anti-HIV activity could be

attributed to higher levels of virion-incorporation. In case HIV Vif located within the virus could directly interfere with A3G's biological activity, it would be expected that the action of R88-A3G$_{D128K}$ and R88-A3G$_{P129A}$ would not be affected by Vif. Indeed, a previous study provided evidence that the production of infectious Vif$^{+}$ virus does not dependent on the reduced level of A3G from virus-producing cells (156), suggesting that the presence of Vif in virus may directly interfere with A3G's biological activity. Interestingly, Santa-Marta et al, also showed that HIV Vif can directly inhibit A3G-mediated hypermutation in bacteria (282). Because no ubiquitin-proteasome system is present in bacteria, these observations argue in favor of a direct effect of Vif on the enzymatic activity of A3G.

To further explore the feasibility of using this approach as a gene therapy strategy, we first introduced R88-A3Gwt and R88-A3G$_{P129A}$ into CD4$^{+}$ C8166 T cells using a lentiviral vector followed by puro selection. The selected cell lines were subsequently used to test the effect of these fusions on HIV-1 replication and spread. Our results show that the presence of R88-A3Gwt was sufficient to attenuate virus replication; however, after 12 days, the virus started to replicate again (Fig. 4.5). Intriguingly, in R88-A3G$_{P129A}$-expressing CD4$^{+}$ T cells, HIV-1 infection was completely blocked, and no sign of viral infection during the 24-day period could be detected. These results clearly demonstrate that introducing R88-A3G$_{P129A}$ in CD4$^{+}$ T cells efficiently inhibits HIV replication, although the long-term effect of the expression of this mutant requires further investigation. We still cannot exclude the possibility that HIV-1 could develop resistance against the antiviral effect of R88-A3G$_{P129A}$, because previous work has shown that changes in amino acid 14-17 of Vif could modify its interaction with A3G$_{D128K}$ and inhibit the activity of the mutant (291). However, it would be very difficult for the HIV to develop simultaneous resistance against the

actions of both R88 and $A3G_{P129A}$.

Another important question is how to introduce the R88-A3G fusion protein into human PBMCs and macrophages to investigate its impact on HIV replication. Here, we used an AAV vector system, which is currently the only nonpathogenic viral vector that can transduce genes into a number of tissues and cells, including dendritic cells, PBMCs and macrophages, without causing toxicity. In addition, the AAV vector system may direct long-term transgene expression (83, 88, 93, 128, 182, 266, 350). Importantly, two previous studies have shown that the production and transduction of AAV are not affected by the presence of A3G (49, 229), which makes it an ideal vector to deliver R88-A3G into primary cells. Indeed, our results show that AAV2/5 was able to quite efficiently introduce R88-$A3G_{P129A}$ into human PBMCs and macrophages. The quantitative real-time PCR analysis revealed that the R88-$A3G_{P129A}$ mRNA level was approximately 23% of total A3G mRNA level in PBMCs and reached at nearly 40% of the total A3G mRNA level in macrophages (Fig. 4.6B and C). Therefore, it is conceivable that an AAV2/5-R88-$A3G_{P129A}$ vector system can provide protection against HIV-1 infection. Interestingly, a recent study has shown that AAV5, rather than AAV2, can more effectively transduce human primary $CD4^+$ T cells, macrophages and dendritic cells (349). Thus, it will be interested to test whether AAV5 could also be more efficient than AAV2/5 to transduce R88-A3G into primary PBMCs and macrophages, and provide effective protection against HIV infection. Overall, this study has developed more potent anti-HIV R88-A3G fusion molecules by mutagenesis, and provided evidence for the feasibility of using R88-A3Gmutant as a gene therapy candidate to inhibit HIV infection and spread, particularly against HIV-1 mucosal infection during sexual transmission. More studies are required to characterize and optimize this anti-HIV gene therapy approach.

# CHAPTER 5

## Expression of R88-APOBEC3G$_{D128K}$ Inhibits HIV-1 Replication in Actively and Latently Infected Cells

### 5.1 Introduction

The introduction of HAART has been able to improve the life quality and enhance life expectancy of HIV-1 patients. However, problems associated with the antiretroviral drugs such as side effects and multi-drug resistance have emerged. Among them, drug resistance is a major cause of treatment failure. A study from Europe showed that drug-resistant strains of HIV-1 were present in approximately 80% of HIV-1 patients who were experiencing treatment failure (97). Also, in one of six-year study, it was found that about 80% of patients had their medications switched repeatedly due to drug resistance, resulting in a cumulative failure rate of 38% (263). It has been showed that drug-resistant viruses are not necessarily less fit than wild-type counterparts, and the transmission of HIV drug resistance has been reported. Studies in United States and Canada showed that at least one drug resistance mutation has been found in 17~20% of treatment-naive patients (45, 150). Hue et al. have identified the circulation of five drug-resistant viral clusters within an untreated population (138). Their study also revealed that these drug-resistant variants can persist at undetectable levels *in vivo*, providing a source for the spread/transmission of drug resistance. This transmitted resistance leads to fewer treatment options and reduced treatment efficacy. Therefore, before a new antiviral agent and/or strategy can be considered as sufficient and effective, it is necessary to evaluate its effectiveness against different drug-resistant strains of HIV-1.

Additionally, it is known that currently available antiviral therapies fail to eradicate the virus entirely from infected people, and virus persists mainly in resting

$CD4^+$ T cells and establishes a latent infection (60). Once HAART is discontinued, virus replication resumes from preexisting infected cells, leading to a rapid rebound of viremia in most patients. These latent reservoirs contain both wild type and drug-resistant strains of HIV-1 (67). They are long-lived and resistant to host immune response and antiviral treatment (62). It has been theoretically estimated that complete eradication of HIV-1 from an individual will require over 60 years of uninterrupted HAART (91). Thus, in order to fully recover, patients are required to adhere to lifelong therapies, which in turn are associated with long-term toxicities and metabolic disorders (23, 244). Considering these obstacles for HIV-1 eradication, there is growing demand for new therapeutic strategies to efficiently inhibit HIV-1 infection. Gene therapy approaches that target crucial steps of HIV-1 life cycle have been considered as viable alternative for HIV-1 control (161, 289). In addition, gene therapy may provide life-long protection, particularly if hematopoietic progenitor cells are targeted (232, 278).

The results from Chapter 4 proved that A3G-Vif axis was a potential antiviral target, and interrupting A3G-Vif interaction could restore A3G's antiviral activity and promote innate defense mediated viral control. As a logical extension, in the current chapter, the most potent A3G: R88-$A3G_{D128K}$, which was most resistant to Vif induced degradation and exhibited the strongest antiviral effect, was delivered into diverse HIV-1 susceptible cells via the suitable gene delivery system. Its action against both active and latent HIV-1 infection was fully characterized. It is hypothesized that R88-$A3G_{D128K}$ combined with suitable gene delivery system could provide a promising approach for anti-HIV-1 gene therapy. The following objectives were designed to test this hypothesis:

1. Generate a Dox-inducible lentiviral vector system for delivery of R88-$A3G_{D128K}$.

2. Evaluate the antiviral effect of R88-A3G$_{D128K}$ against active HIV-1 replication, including replication of drug-resistant strains.

3. Characterize the potential of R88-A3G$_{D128K}$ against latent HIV-1 infection.

## 5.2 Result

### 5.2.1. Generation of an inducible R88-A3G$_{D128K}$ expressing lentiviral vector system

To generate A3G-based anti-HIV gene therapy approach, we chose to use lentiviral vector due to its long-term expression ability. However, since A3G has intrinsic anti-retroviral effect, we needed to eliminate the inhibitory effect of A3G on lentiviral vector following transduction. First, we utilized an inducible lentiviral vector system pTRIPZ (pTZ)-RFP lentiviral vector, in which expression of transgenes RFP is under control of tetracycline response element (TRE) promoter. This promoter can be activated by the reverse tetracycline transactivator 3 (rtTA3) in the presence of Dox (Tet-ON system) (Fig. 5.1A). As shown in Fig. 5.1B (right), Dox bound to rtTA3 and promoted it binding to and activating RFP expression from TRE promoter. In the absence of Dox, the rtTA3 was in inactive state, which would not activate TRE promoter and induce RFP expression (Fig 5.1B, left).

Meanwhile, we replaced RFP with an R88-A3G$_{D128K}$ transgene in pTZ-RFP lentiviral vector and generated pTZ-R88-A3G$_{D128K}$. The regulated expression of R88-A3G$_{D128}$ and its virus incorporation were assessed after 293T cells were co-transfected with plasmids pTZ-R88-A3G$_{D128K,}$ Δ8.2 and pCMV VSV-G. 24 hours post transfection, cells were either treated with Dox or untreated for 48 hours and lysed. The level of R88-A3G$_{D128K}$ was examined by WB. Without Dox treatment, only a very low level of R88-A3G$_{D128K}$ was present in transfected cells. However, in

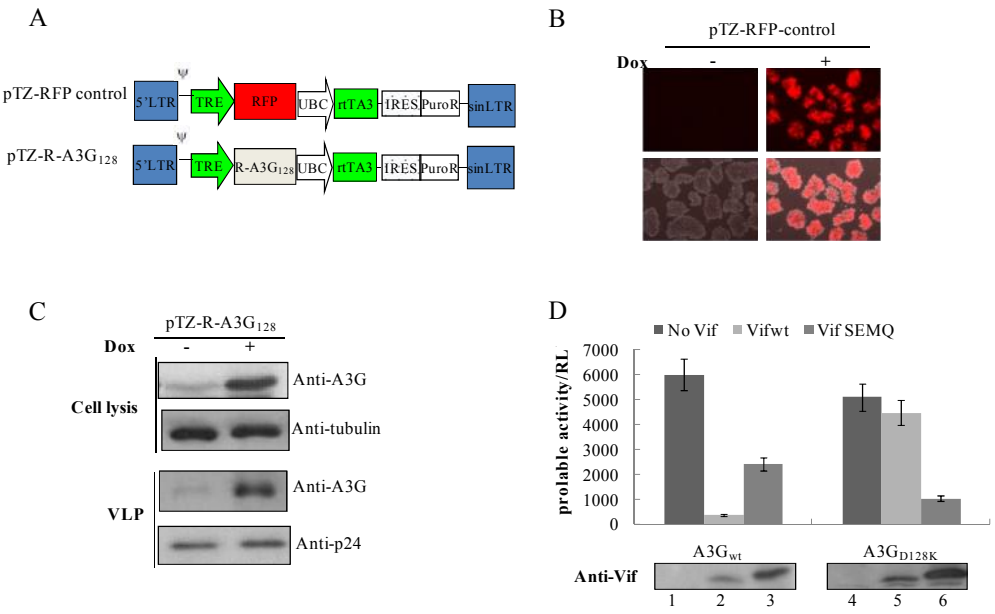


**Fig. 5.1 Regulated A3G expression in 293T cells.** (A) Schematic representation of pTRIPZ (pTZ) vectors for Dox-inducible transgenes expression. The expression of RFP or R88-A3G$_{D128K}$ in pTZ vectors was under the control of TRE, which is fused to the CMV minimal promoter. In the presence of Dox, reverse tetracycline transactivator 3 (rtTA3), whose expression is driven by the constitutively active Ubiquitin C promoter (UBC), binds to and activates expression from TRE promoters. The pTZ vectors contain the 5′ and 3′ long terminal repeats (LTR) with SIN deletion in the U3 region, packaging signal (Ψ), internal ribosome entry site (IRES), puromycin selectable marker (PuroR). (B) Inducible RFP expression in pTZ-RFP control transduced C8166 T cells. C8166 T cells were transducted with pTZ-RFP, and cultured in the absence (left panel) or presence (right panel) of 2μg/ml Dox. RFP expression was assessed at 72 hours by fluorescence microscopy. (C) Inducible A3G expression in transduced 293 T cells and produced viral like particles (VLPs). 293 T cells were co-transfected with pTZ-A3G, packaging plasmid Δ8.2, and VSV-G expression plasmid, and cultured in the absence or presence of 2μg/ml Dox. After 48 hours, VLPs were collected from supernatant by ultracentrifugation through a 20% sucrose cushion. The level of A3G in transduced cells and produced VLPs were measured by WB with anti-A3G antibody. As control, cell lysis and VLPs were probed with anti-tubulin and anti-p24 antibodies respectively. (D) Vif$_{SEMQ}$ mutant promotes the degradation of A3G$_{D128K}$. 293T cells were transfected with either ProLabel-A3G$_{wt}$ or ProLabel-A3G$_{D128K}$ plus control vector pcDNA3.1 (lane 1 and 4), Vif$_{wt}$ (lane 2 and 5), or Vif$_{SEMQ}$ (lane 3 and 6). Degradation of A3G in the transfected cells was determined by measuring ProLabel activity. Expression of Vif$_{wt}$ and Vif$_{SEMQ}$ were confirmed in the cell lysates by WB with anti-Vif antibody. The data are representative of three independent experiments.

presence of Dox, expression of R88-A3G$_{D128K}$ was highly induced (Fig 5.1C, upper panel). Meanwhile, encapsidation of R88-A3G$_{D128K}$ into VLPs was also measured. Consistent with the R88-A3G$_{D128K}$ expression in 293T cells, significant amount of R88-A3G$_{D128K}$ was detected in VLPs that were produced from Dox treated cells (Fig. 5.1C, lower panels). These results indicate that during lentiviral vector production, R88-A3G$_{D128K}$ expression and encapsidation can be minimized in the absence of Dox. However, following Dox induction, R88-A3G$_{D128K}$ was efficiently expressed and consequently packaged into VLPs.

Due to the incomplete suppression of TRE promoter (212), a very small amount of R88-A3G$_{D128K}$ was still expressed in the absence of Dox. This low amount of R88-A3G$_{D128K}$ was incorporated into VLPs (Fig. 5.1C), which may further impair vector's transduction efficiency. Here, we attempted to promote the degradation of R88-A3G$_{D128K}$ by introducing HIV-1 Vif$_{SEMQ}$. HIV-1 Vif$_{SEMQ}$ has been previously shown to be able to bind to human A3G$_{D128K}$ and induce its degradation (280, 291). Indeed, when Vif$_{SEMQ}$ was co-expressed with A3G$_{D128K}$ in 293T cells, the cellular level of A3G$_{D128K}$ protein was reduced by 5 times, as measured by ProLabel assay (Fig. 5.1D). However, A3G$_{D128K}$ was resistant to the degradation induced by wild-type Vif. Thus, by combining the inducible promoter and expression of Vif$_{SEMQ}$, we could minimize the presence of R88-A3G$_{D128K}$ during VLP production.

### 5.2.2. Characterization of transduction efficiency of pTZ-R88-A3G$_{D128K}$ vectors

As being described above, our results showed Dox-inducible promoter plus expression of Vif$_{SEMQ}$ could reduce the vector-mediated R88-A3G$_{D128K}$ expression. We next examined the transduction efficiency of pTZ-R88-A3G$_{D128K}$ vector produced in the absence of Dox and in presence of Vif$_{SEMQ}$. Briefly, 293 T cells were transfected

with pTZ-R88-A3G$_{D128K}$, packaging plasmid Δ8.2 and VSV-G expression plasmid, either in the presence or absence of plasmid Vif$_{SEMQ}$ and Dox. After 48 hours of transfection, VLPs were collected and quantified by measuring the amount of vector-associated p24. Then, equal amounts of different VLPs were used to tranduce CD4$^+$ C8166 T cells. 48 hours later, transduced cells were selected with puro, and only the ones expressing puro resistance gene from integrated pTZ-R88-A3G$_{D128K}$ vectors could survive. After 7 days of selection, the cell viability was assessed by PI staining and flow cytometry analysis (277). Results showed that 93.02% of C8166 T cells transduced with pTZ-R88-A3G$_{D128K}$ VLPs produced in the absence of Dox and presence of Vif$_{SEMQ}$ were resistant to puro (Fig. 5.2A, sample 5). As to the cells transduced with VLPs produced in the present of Dox and the absence of Vif$_{SEMQ}$, only 59.27% of them have survived (Fig. 5.2A, sample 2).

To assess the reproducibility of the results, we evaluated the performance of these VLPs on HeLa cells. HeLa cells were transduced with same panel of vectors, and selected with puro for 10 days to eliminate untransduced cells. Fig. 5.2B (upper part) showed the formation of puro-resistant colonies in transducted HeLa cell cultures. Significantly, among pTZ-R88-A3G$_{D128K}$ vectors (vector 2 to 5) transduced cells, more resistant colonies were formed in vector 5 transduced cell culture. We also counted the number of cells recovered from puro selection. Results showed that $7.6\times10^5$ cells were found in sample 5 (Fig. 5.2B, bar 5), while only $9\times10^4$ cells were found in sample 2 (Fig. 5.2B, bar 2).

To further quantify the transduction difference among individual vectors, we transduced C8166 T cells with the same panel of VLPs, and measured the integrated vector DNA copies related to cells by real-time PCR assay after 48 hours. Indeed, as shown in Fig. 5.2C, the highest transduction efficiency was observed with VLPs

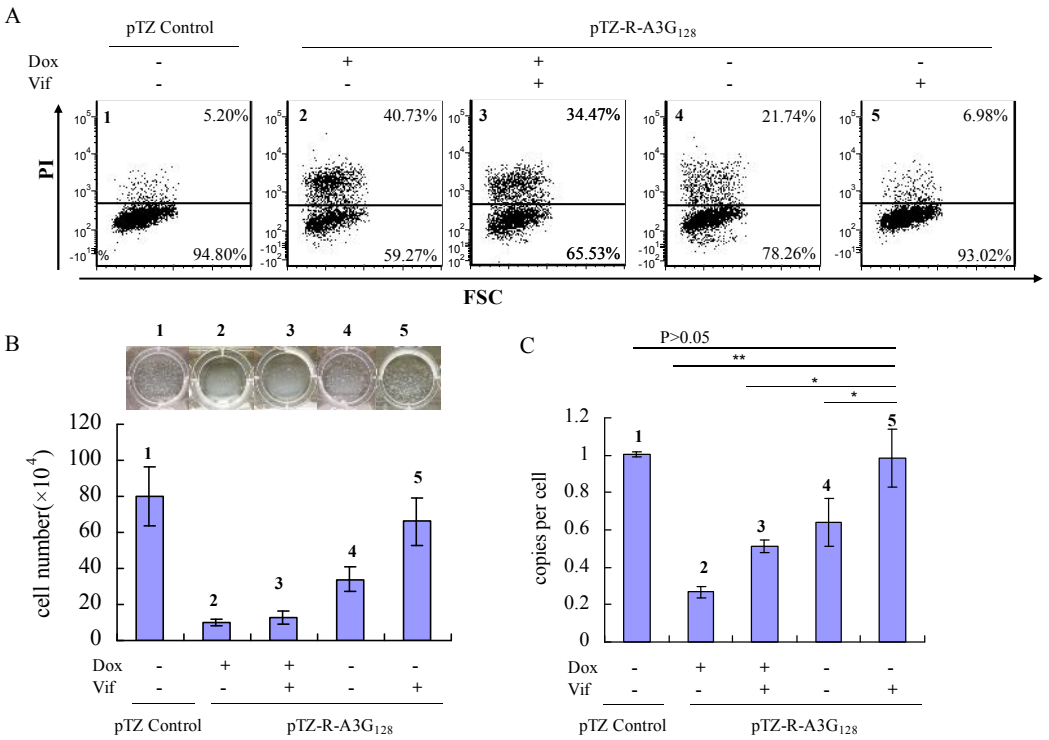


**Fig. 5.2 Evaluation of transduction efficiency of pTZ-R88-A3G$_{D128K}$ vectors.** VLPs containing pTZ-R88-A3G$_{D128K}$ were produced in the presence or absence of Dox (2μg/ml) and/or Vif$_{SEMQ}$ as indicated. Equal amounts of VLPs (normalized by p24 ELISA) were used to transduce target cells. (A) Transduced C8166 T cells were selected with puromycin (0.5μg/ml) for 7 days. After staining with propidum iodide (PI), cells were analyzed by flow cytometry. (B) Transduced HeLa cells were selected with puromycin (2μg/ml) for 10 days. Selective medium was replaced every 2 days to remove dead cells. Puromycin-resistant colonies were visualized under microscopy (upper panel). Total cell number from individual wells was counted with Trypan blue staining (lower panel). (C) Real time-PCR detecting U5-R sequence was performed on total DNA extracted from C8166 T cells at 2 days post transduction. The data were the averages of triplicates with the indicated standard deviations. Statistical significance was calculated using the student's *t*-test, and denoted as * for $p \leq 0.05$, ** for highly significant with $p \leq 0.01$. Results A and B were from one representative of two independent experiments.

produced in the absence of Dox and presence of $Vif_{SEMQ}$ (Bar 5), which showed a similar efficiency (approximately 1 copies/cell) to that of pTZ-RFP vector (Bar 1). In contrast, transduction efficiencies of the pTZ-R88-A3$G_{D128K}$ vectors produced either in the presence of Dox or absence of $Vif_{SEMQ}$ were compromised (Bars 2-4), and the lowest level was observed with vector produced in the presence of Dox and absence of $Vif_{SEMQ}$ (Bar 2, 0.27copies/cell). All of these results indicate that this Dox-inducible pTZ-R88-A3$G_{D128K}$ vector, produced in the presence of $Vif_{SEMQ}$ and absence of Dox, can be used to efficiently transduce $CD4^+$ C8166 T cell and HeLa cells.

### 5.2.3. Dox regulated R88-A3$G_{D128K}$ expression and antiviral effect in pTZ-R88-A3$G_{D128K}$ transduced $CD4^+$ C8166 T cells

To test whether C8166 T cells expressing R88-A3$G_{D128K}$ is resistant to HIV-1 infection, transduced C8166 T cells were treated with Dox at different concentrations (ranging from 0 to 2μg/ml), then infected with HIV-1 pNL-4.3 (MOI of 1). After 48 hours, viral replication was monitored by measuring the level of HIV Gag p24 in the supernatant. As shown in Fig. 5.3A, HIV-1 replication was inhibited at different concentrations of Dox and a maximal inhibition was shown with 1μg/ml Dox. Therefore, 1μg/ml was used as the optimal concentration for Dox induction in the following studies.

To check whether this antiviral effect is correlative to R88-A3$G_{D128K}$ expression, the presence of R88-A3$G_{D128K}$ protein in C8166 T cells was further measured. Due to the low level of expression, we failed to detect R88-A3$G_{D128K}$ protein in C8166 T cells by WB analysis (data not shown), instead, we measured the amount of R88-A3$G_{D128K}$ incorporated into viruses As shown in Fig. 5.3B, the presence of R88-A3$G_{D128K}$ was clearly detected in progeny viruses produced from Dox+ infected

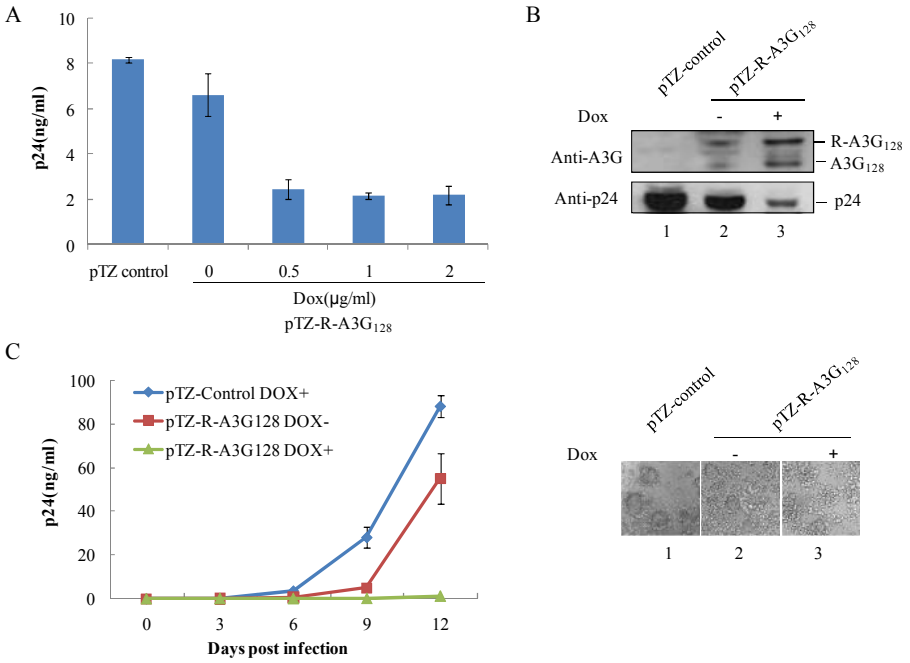


**Fig. 5.3 Dox regulated R88-A3G$_{D128K}$ expression and antiviral effect in pTZ-R88-A3G$_{D128K}$ transduced CD4$^+$ C8166 T cell line.** pTZ-control and pTZ-R88-A3G$_{D128K}$ transduced C8166 T cells were induced with Dox (1μg/ml or as indicated), and infected with pNL-4.3 at MOI of 1 (A, B) or MOI of 0.01 (C). (A) Levels of HIV-1 p24 in the supernatants were measured by p24 ELISA assay at 7 days post infection. (B) Virus produced from infection C8166 T cells was concentrated from the supernatant by ultracentrifugation. The presence of R88-A3G was analyzed by WB with anti-A3G antibody, and HIV-1 Gag protein was detected by anti-p24 antibody. (C) Virus replication was measured by p24 ELISA from the supernatant at different time intervals (left). HIV-1-induced syncytium formation was visualized under microscopy (right). Results were from one representative of two independent experiments.

cells (lane 3, upper panel). There was a low background level of R88-A3G$_{D128K}$ in non-Dox treated cells, which would be responsible for the slightly impaired viral replication in these cells.

To further evaluate the effect of R88-A3G$_{D128K}$ on viral replication and spread, we infected transduced C8166 T cells with HIV-1 pNL-4.3 at MOI of 0.01, and monitored viral replication for a prolonged period of time. As shown in Fig. 5.3C (left), HIV-1 replication in pTZ-R88-A3G$_{D128K}$ C8166 T cells cultured with 1μg/ml Dox were completely abolished, whereas in non-Dox treated cells HIV-1 replication still processed, even though viral replication kinetics was delayed as compared to it in pTZ-control C8166 T cells. Furthermore, HIV-1 induced cytopathic effect was blocked in pTZ-R88-A3G$_{D128K}$ C8166 T cells in the presence of Dox (Fig. 5.3C, right). Together, these results show that induced expression of R88-A3G$_{D128K}$ efficiently blocked HIV-1 replication and spread.

### 5.2.4. Inhibitory effect of pTZ-R88-A3G$_{D128K}$ against various drug-resistant HIV-1 strains

Transmission of drug resistance increases the difficulty for drug treatment and controlling the HIV pandemic. Thus, it was necessary to evaluate whether R88-A3G$_{D128K}$ expression was able to protect against infection caused by resistant strains of HIV-1. Here, we chose viruses resistant to different classes of currently used antiretroviral drugs, including AZT, 3TC, Nevirapine, Protease inhibitors (MK-639, XM323, A-80987, Ro31-8959, VX-478, and SC-52151) and Raltegavir. C8166 T cell lines inducibly expressing R88-A3G$_{D128K}$ or RFP were challenged with equal amounts of drug-resistant viruses. At different time intervals, viral replication was monitored by measuring Gag p24 level from supernatants. The results showed that for a 12-day

period, the empty vector transduced cell line was highly susceptible to all drug-resistant viruses, and viral replication peaked after 6 to 9 days of infection (Fig. 5.4). In contrast, cells expressing R88-A3G$_{D128K}$ showed no viral replication over a period of 12 days. These data indicate that the presence of R88-A3G$_{D128K}$ in highly susceptible CD4$^+$ T cells is able to completely block viral replication, including replication of drug-resistant viruses.

### 5.2.5. Expression of R88-A3G$_{D128K}$ in primary human cells inhibits active HIV-1 infection

CD4$^+$ T lymphocytes and macrophages are considered as two major targets for HIV-1 infection, thus it is important to determine whether R88-A3G$_{D128K}$ expression could inhibit viral replication in these cells. First, we purified primary CD4$^+$ T cells and macrophages cells from human PBMCs, and transduced them with pTZ-R88-A3G$_{D128K}$ or pTZ-control VLPs. 3 days following transduction, R88-A3G$_{D128K}$ DNA levels were measured by real-time PCR. We were able to detect R88-A3G$_{D128K}$ DNA in CD4$^+$ T cell and macrophage at 0.35 and 0.4 copies per cell, respectively (Fig. 5.5A), indicating successful transduction of R88-A3G$_{D128K}$ into primary cells.

To evaluate the antiviral effect of R88-A3G$_{D128K}$ in primary CD4$^+$ T cells, pTZ-R88-A3G$_{D128K}$ transduced CD4$^+$ T cells were induced with Dox for 2 days, followed by challenged with the nevirapine-resistant virus. At different time points, the level of Gag p24 from supernatants was measured by ELISA. Results from one representative donor showed that viral replication in R88-A3G$_{D128K}$ transduced CD4$^+$ T cells was inhibited by approximately two- to threefold when compared with control CD4$^+$ T cells (Fig. 5.5B, left). Next, we assessed R88-A3G$_{D128K}$ mediated antiviral

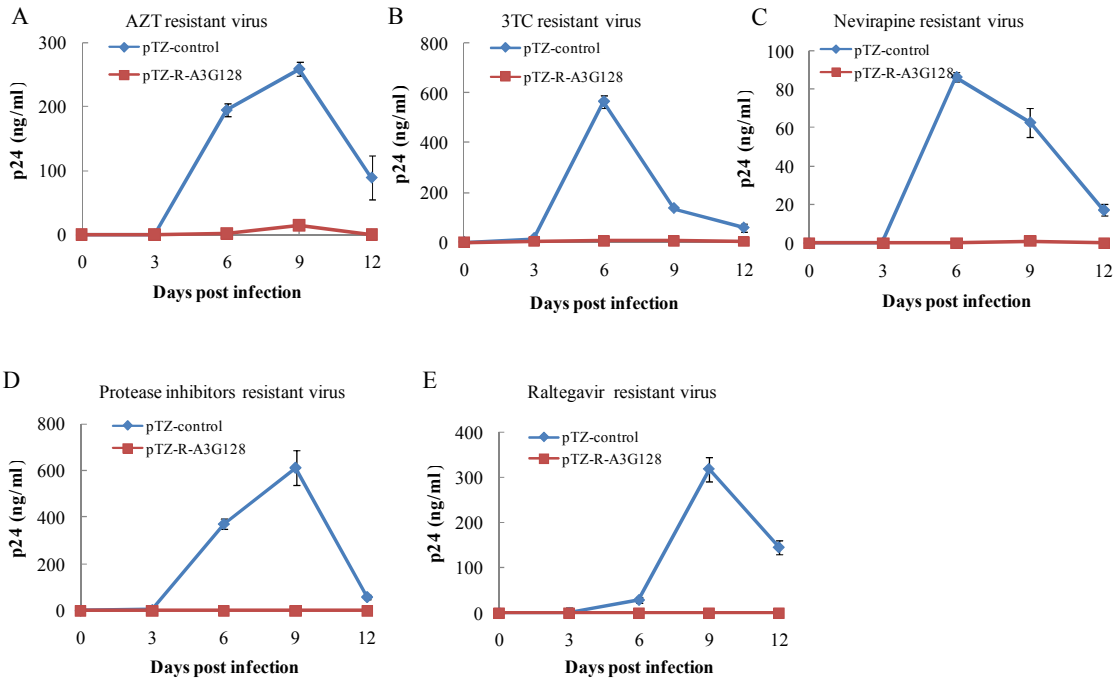


**Fig. 5.4 pTZ-R88-A3G$_{D128K}$ blocked the replication of drug resistant strains of HIV-1.** pTZ-R88-A3G$_{D128K}$ or pTZ-control transduced C8166 T cell lines were induced with Dox (1μg/ml) and infected with five drug resistant strains as indicated. Viral replication was monitored by measuring supernatant p24 level for 12 days. Protease inhibitors resistant virus is resistant to following drugs: MK-639, XM323, A-80987, Ro31-8959, VX-478, and SC-52151. Results were from one representative of two independent experiments.

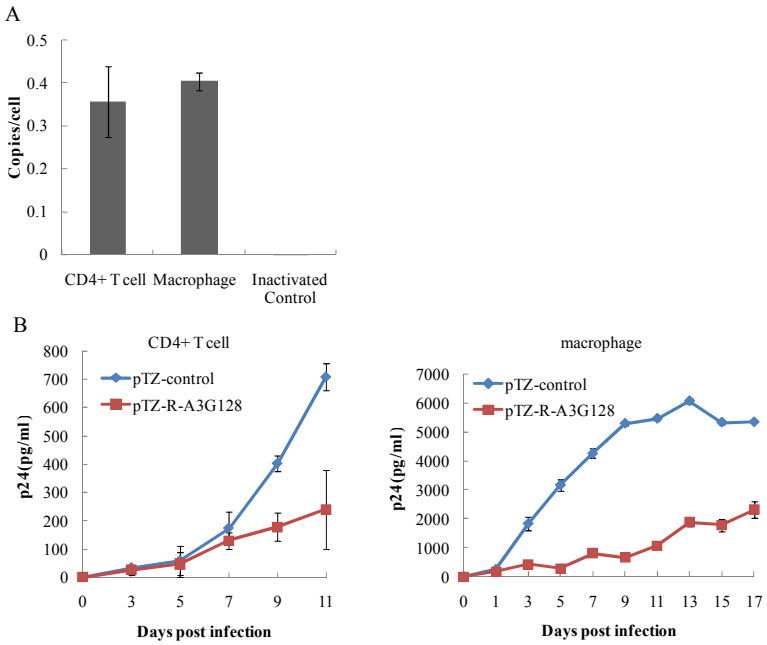


**Fig. 5.5 pTZ-R88-A3G$_{D128K}$ transduced primary cells were significantly resistant to HIV-1 replication.** (A) Primary CD4$^+$ T cells and macrophages were transduced with pTZ-R88-A3G$_{D128K}$ or pTZ-control vectors for 3 days. Total DNA was extracted from transduced cells and subjected to real-time PCR analysis to quantify R88-A3G levels. (B) Transduced CD4$^+$ T cells and macrophages were induced with Dox (1μg/ml), and infected with nevirapine-resistant and pNL4.3-Bal strains of HIV-1 at MOI 0.1, respectively. Viral replication was measured by p24 ELISA. Result A was from one representative of two donors. Results B was from one representative of three donors.

effect in macrophages. Transduced macrophages were induced with Dox and infected with pNL4.3-Bal virus, viral replication was monitored every two days. Data showed that viral replication in control vector transduced cells was peaked at day 13. In contrast, viral replication in R88-A3G$_{D128K}$ transduced cells was reduced by more than threefold, and failed to reach peak within 17 days of observation (Fig. 5.5B, right). Taken together, these results indicate that expression of R88-A3G$_{D128K}$ is capable of inhibiting active HIV-1 replication in primary CD4$^{+}$ T cells and macrophages.

### 5.2.6. Introduction of pTZ-R88-A3G$_{D128K}$ in HIV-1 latently infected cells disrupts the infectivity of progeny viruses

Given the fact that A3G mainly targets the newly produced viruses and disrupts their infectivity (198, 365), it would be of interest to investigate whether introducing R88-A3G$_{D128K}$ into HIV-1 latently infected cells could block the infectivity of progeny virus produced after latency reactivation. First, we transduced ACH-2 cells, a well-characterized HIV-1 latently infected cell line (94), with pTZ-R88-A3G$_{D128K}$ or pTZ-control vectors. Following Dox induction and phorbol-12-myristate-13-acetate (PMA) stimulation, the newly produced viruses were collected and quantified from supernatants by measuring Gag p24 level (Fig. 5.6A). Results showed that two days post infection, similar levels of progeny viruses were produced from pTZ-R88-A3G$_{D128K}$ and pTZ-control transduced ACH-2 cells (Fig. 5.6B), suggesting that R88-A3G$_{D128K}$ does not affect viral production from infected cells where latency is reversed.

Meanwhile, the infectivity of progeny viruses was evaluated. Equal amounts of progeny viruses produced from pTZ-R88-A3G$_{D128K}$ and pTZ-control transduced ACH-2 cells were used to infect normal C8166 T cells. After infection, we monitored

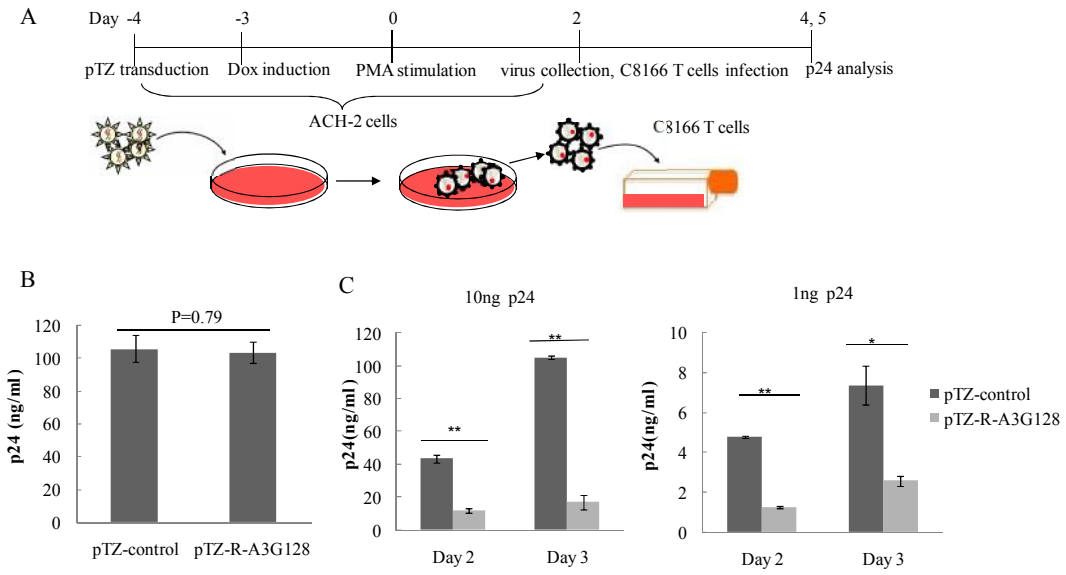


**Fig. 5.6 pTZ-R88-A3G$_{D128K}$ impaired the infectivity of virus produced from latently infected cells.** (A) Experimental set up. (B) HIV-1 viral production from pTZ-R88-A3G$_{D128K}$ or pTZ-control transduced ACH-2 cells was monitored at 48 hours post stimulation by measuring p24 level in cell culture supernatants. (C) High volumes (100µl, equals to 10ng p24) or low volumes (10µl, equals to 1ng p24) of cell free supernatants collected from stimulated pTZ-R88-A3G$_{D128K}$ and pTZ-control ACH-2 cells were used to infect C8166 T cells. Viral replication was measured at two and three days post infection. The data were the averages of triplicates with the indicated standard deviations. Statistical significance was calculated as described in Fig. 5.2C.

viral replication by measuring Gag p24 levels in the supernatants at day 2 and 3. Results showed that the infectivity of progeny viruses produced from R88-A3G$_{D128K}$ transduced ACH-2 cells was reduced by 3-6 folds, as compared with the viruses produced from the control vector transduced cells (Fig. 5.6C). Taken together, these results demonstrate that introducing R88-A3G$_{D128K}$ in latently HIV-1 infected cells dose not affect viral production from reactivated proviruses, but strongly disrupts the infectivity of newly produced viruses, and thereby blocks additional rounds of infection.

To further assess the effect of R88-A3G$_{D128K}$ on HIV-1 latent infection in primary cells, we employed a recently established primary cell model of HIV latency (175, 253, 321). In this model, latency can be established in resting CD4$^+$ T cells at post integration step, and activation of replication competent proviruses can be achieved by stimulation with appropriate inducing agents. Here, we infected unstimulated CD4$^+$ T cells with nevirapine-resistant virus (MOI 2.5) by spinoculation. 3 days later, the infected cells were activated by IL-2 and PHA treatment, followed by transduction with pTZ-R88-A3G$_{D128K}$ or pTZ-control vectors. Then we monitored the viral replication started from two days post transduction. As shown in Fig. 5.7B, viral replication was continuously increasing over 8 days. In the first 4 days, the difference of viral production between R88-A3G$_{D128K}$ and control vector transduced cells was not significant. But at day 6 and 8 post transduction, viral replication was clearly shown to be disrupted by R88-A3G$_{D128K}$, and three-fold reduced viral production was observed at day 8. In addition, we collected the supernatants from both R88-A3G$_{D128K}$ and control vector transduced cells at 3 days post transduction, and virus-containing supernatants were used to infect normal C8166 T cells to evaluate the infectivity of progeny viruses. Similar with progeny viruses from ACH-2 cells, infectivity of viruses

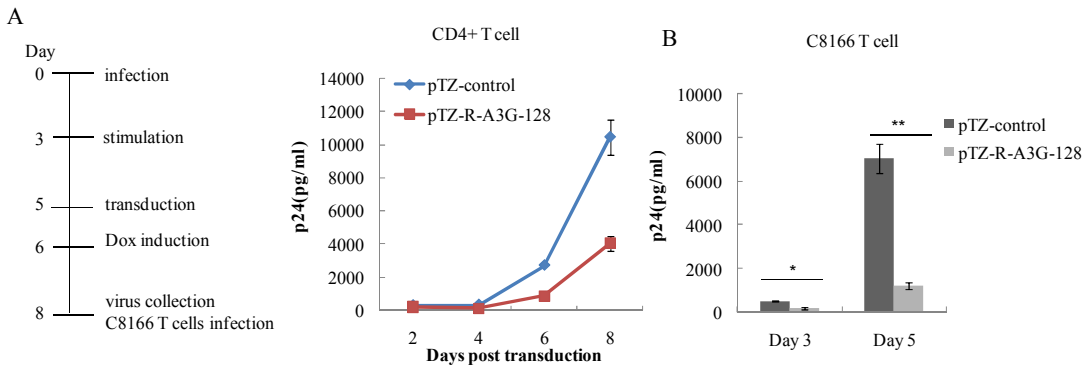


**Fig. 5.7 pTZ-R88-A3G$_{D128K}$ mediated inhibition of HIV-1 replication in primary latently infected cells.** (A) Unstimulated CD4+ T cells were infected with nevirapine-resistant viruses at day 0, and activated with IL-2 (100U/ml) and PHA (5µg/ml) at day 3. Activated cells were transduced with pTZ-R88-A3G$_{D128K}$ or pTZ-control vectors at day 5, and cultured in the presence of Dox (1µg/ml) and IL-2 from day 6. Supernatant was collected at indicated time points post transduction for p24 measurement. (B) C8166 T cells were infected with cell free supernatants from pTZ-R88-A3G$_{D128K}$ and pTZ-control transduced CD4$^+$ T cells collected at day 8. Viral replication was measured at three and five days post infection. The data were the averages of triplicates with the indicated standard deviations. Statistical significance was calculated as described in Fig. 5.2A.

produced from reactivated R88-A3G$_{D128K}$ transduced CD4$^+$ T cells was reduced by 3-6 folds (Fig. 5.7C). Taken together, data obtained from latent HIV infection model indicate that R88-A3G$_{D128K}$ could provide post infection protection and inhibit replication of reactivated virus.

## 5.3 Discussion

In the fight against HIV-1, a study showing that the Berlin patient was cured of HIV by a bone marrow transplant from a CCR5 homozygous null (CCR5–/–) HLA-matched donor (143), highlights the feasibility of developing therapeutics through gene modification. In the current chapter, we have established an anti-HIV gene therapy approach based on R88-tagged human A3G. Our study showed that stable expression of R88-A3G$_{D128K}$ in highly susceptible C8166 T cells significantly inhibit the replication of both laboratory-adapted and primary HIV-1 isolates that are resistant to several first-line antiviral drugs (Fig. 5.3 and 5.4). In addition, R88-A3G$_{D128K}$ is effective in HIV-1 latently infected cells, which renders the progeny viruses from these cells loss infectiousness (Fig. 5.6 and 5.7). Importantly, R88-A3G$_{D128K}$ exerts similar anti-HIV effects on human primary cell models.

Host restriction factors have become attractive candidates for gene therapy due to their potent antiviral activities (291, 338). Importantly, introduction of host restriction factors *in vivo*, unlike foreign proteins, could avoid immunogenicity associated with protein-based approaches. In Voit et al.'s study, for a prolonged period of exposure time, A3G$_{D128K}$ confers 198-fold and 100-fold protection against X4-tropic and R5-tropic viruses respectively, as compared to 3-fold and 64-fold protection provided by human-rhesus TRIM 5-α (335). Also, among proteins of APOBEC3 family, studies have shown that A3G exhibits advanced antiviral activities in human primary target

cells (45). Therefore, A3G is an attractive and potent candidate for anti-HIV gene therapy.

Given the fact that lentiviral vectors are capable of transducing both dividing and non-dividing cells and providing sustained gene expression, in this study we employed a Dox-inducible lentiviral vector to deliver anti-HIV gene R88-A3G$_{D128K}$. In this vector, the expression of transgenes is under the control of Dox. So during VLPs production, we could render transgene under silent condition and avoid the inhibitory effect of R88-A3G$_{D128K}$ following VLPs transduction (Fig. 5.1C). Once CD4$^+$ T cells were transduced by pTZ-R88-A3G$_{D128K}$, the transgene can be turned on or off dependent on the administration of Dox. Thus, the unexpected side effect of continuing expression of R88-A3G$_{D128K}$ can be limited or avoided. Still, we detected a trace amount of A3G expression in the vector producing cells in the absence of Dox (Fig. 5.1C), which led to modest inhibitory effect on pTZ-R88-A3G$_{D128K}$ vector transduction (Fig. 5.2). This Dox-independent basal expression was observed in other studies as well, such as expression of human cytidine deaminase in hematopoietic cells (171). To further reduce the leaking expression of R88-A3G$_{D128K}$, we co-expressed HIV-1 Vif$_{SEMQ}$ protein in the vector producing cells. This Vif mutant was able to bind to human A3G$_{D128K}$ and induce its degradation (280, 291). Indeed, when Vif$_{SEMQ}$ was co-expressed with A3G$_{D128K}$ in 293T cells, the cellular level of R88-A3G$_{D128K}$ protein was reduced by 5 times, as measured by ProLabel assay (Fig. 5.1D). As a consequence, the transduction efficiency of pTZ-R88-A3G$_{D128K}$ vector was increased to a similar level of control vector (Fig. 5.2).

In contrast to drastic anti-HIV effect of R88-A3G$_{D128K}$ in CD4$^+$ T cell line (Fig. 5.3 and 5.4), viral replication in R88-A3G$_{D128K}$ transduced primary CD4$^+$ T cells and macrophages were not completely inhibited (Fig. 5.5B). This varied antiviral effect

correlates to transduction efficiency of R88-A3G$_{D128K}$ in different types of cells. Transduced C8166 T cells were selected by puro to enrich for vector-containing cells. After selection, each cell contained at least one copy of R88-A3G$_{D128K}$. In contrast, in transduced primary cells, less than 50% of cells contained R88-A3G$_{D128K}$ as measured by real-time PCR (Fig. 5.5A) (286). Indeed, as predicted by Hosseini et al. that in the multicellular events model, viral replication completely stops only if therapeutics targeting A3G-Vif axis were delivered to nearly 100% cells (134). Meanwhile, another study pointed out that a single editing unit of incorporated A3G is capable of inactivating virus rather than causing sub-lethal mutations and increasing viral diversification (17). Therefore, partially impaired viral replication in primary cells is because of incomplete transduction of pTZ-R88-A3G$_{D128K}$ vector rather that insufficient R88-A3G$_{D128K}$ protein expression. In the future preclinical studies, we will put effort on enhancing the transduction efficiency in primary cells through modifying the lentiviral vector (31), or enrich the transduced cells by introducing selectable marker (eg, IL-2 receptor-α chain) followed by selection using corresponding beads (227).

The emergence of HIV-1 drug resistance occurs frequently after anti-HIV chemotherapy (119). Importantly, drug-resistant strains of HIV can be transmitted into susceptible individuals, resulting in suboptimal response to first-line therapy and treatment failure (130, 169). Therefore, an ideal new therapeutic strategy should possess activity against different existing drug-resistant strains of HIV. Herein, we chose representative viruses resistant to four classes of antiretroviral drugs (NRTI, NNRTIs, protease inhibitors and integrase inhibitors). Data showed that R88-A3G$_{D128K}$ transduced CD4$^{+}$ T cells were resistant to the replication of all these drug-resistant viruses (Fig. 5.4), highlighting the potential of R88-A3G$_{D128K}$ against

the re-infection and spread of HIV-1 drug resistant viruses.

Another challenge for HIV cure is that HIV-1 can establish a stable latent infection in resting $CD4^+$ T cells that persist in patients, even in those who are undergoing HAART (302). In order to eliminate these HIV-1 latent reservoirs, Wayengera has designed Zinc Finger Nucleases (ZFNs) targeting HIV-1 proviral genes, and used it to remove more that 80% of proviral HIV-1 DNA from latently infected cells (341). Yet, off-target effects are the major concerns of ZFNs which limit the use of this technique. Here, we showed that once R88-$A3G_{D128K}$ was introduced into latently infected ACH-2 cells, upon reactivation, the majority of produced progeny viruses were rendered to be non-infectious (Fig. 5.6C). Similar effect was also observed in primary cell system mimicking HIV-1 latent infection (Fig 5.7). It indicates that introducing R88-$A3G_{D128K}$ in HIV-1 latently infected cells is able to inhibit the dissemination of the progeny virus. Instead, these viruses would just present as antigenic particles to elicit host immune responses. Therefore, this A3G-based therapeutic approach can not only target actively HIV infected cells, but also target HIV-1 latently infected cells, contributing to the elimination of latent reservoirs.

Overall, studies from this chapter demonstrated the profound antiviral effect of R88-$A3G_{D128K}$ on both acute and chronic HIV-1 infection. If delivered during acute infection, R88-$A3G_{D128K}$ could block productive viral replication. As to latent infection, R88-$A3G_{D128K}$ does not preclude HIV reactivation in latent reservoirs, but prevents viral dissemination and further postpones the onset of AIDS. More importantly, R88-$A3G_{D128K}$ has shown to be effective against drug-resistant viruses. Besides their ability to productively replicate, these drug-resistant viruses also enter and persist in latent reservoir (220, 241). Our approach, but not antiretroviral drugs,

has the potential to target the reactivated resistant viruses, and prevents viral rebound. Taken together, our finding encourages further *in vivo* studies to characterize the action of R88-A3G$_{D128K}$ in appropriate animal model.

# CHAPTER 6

## General Discussion and Future Perspectives

### 6.1 Major findings

Given the increasing knowledge on cellular factors which allow host cells to resist HIV-1 infection, more and more researchers are focusing their attention on developing antiviral therapy based on host restriction factors. Compared to therapeutics targeting viral components, strategies targeting host restriction factors have unique advantages. Since these factors are naturally expressed in humans, they are relatively immutable and less immunogenic. The work presented in this thesis describes the antiviral action of restriction factor A3G and the effectiveness of A3G-based antiviral approach, which provides rationale for possible translation applications and development of novel therapeutics.

As shown in Chapter 3, the presence of A3G in virions disrupted reverse transcription of Vif⁻ HIV-1. We found that A3G interacted directly with HIV-1 RT in produced viruses and in co-transfected cells, which did not require viral genomic RNA bridging or other viral proteins. Although A3G bound to both p66 and p55 subunits of RT, their interaction neither affected the proteolytic processing of RT, nor facilitated A3G encapsidation. Nevertheless, A3G-RT interaction was shown to contribute to A3G-mediated inhibition of HIV-1 reverse transcription. Overexpression of the RT-binding polypeptide $A3G_{65-132}$ was able to disrupt their interaction, which consequently attenuated the anti-HIV effect of A3G on reverse transcription. This study highlights the contribution of A3G-RT interaction in A3G-mediated inhibition on HIV-1 reverse transcription.

In Chapter 4, to characterize the potential roles of critical residues in A3G mediated antiviral action, different A3G mutants were introduced into the R88-A3G

system. The results indicate that the antiviral effect of $A3G_{Y124A}$, a previously described packaging-defective mutant, was completely rescued when the mutant was fused with R88. Still, the introduction of the deaminase-defective mutant E259Q into R88-A3G did not affect virion incorporation, but abrogated its ability to inhibit HIV-1 infection. Meanwhile, we showed that introduction of Vif-binding mutants (D128K or P129A) enhanced the inhibitory effects of R88-A3G on $Vif^+$ virus infectivity. Expression of representive mutant R88-$A3G_{P129A}$ in $CD4^+$ C8166 T cells did not disturb cell growth, cell cycle profile and surface CD4 receptor expression, but completely blocked HIV-1 infection for at least 24 days. Similarly, a significant reduction of HIV-1 replication was observed in R88-$A3G_{P129A}$ transducted primary PBMCs and macrophages. These observations suggest that it is possible to develop a R88-A3G-based anti-HIV strategy.

The initial work presented in Chapter 4 aiming to optimize R88-A3G based anti-HIV approach was extended in Chapter 5. In this chapter, we developed a Dox inducible R88-$A3G_{D128K}$ lentiviral vector, and characterized its antiviral effect in detail. Results showed that expression and antiviral activities of R88-$A3G_{D128K}$ were highly regulated by Dox. In the presence of Dox, R88-$A3G_{D128K}$ transduced T cells were resistant to different drug resistant viruses, including AZT, 3TC, Nevirapine, Protease inhibitors and Raltegavir resistant viruses. Furthermore, we introduced R88-$A3G_{D128K}$ into HIV-1 latently infected ACH-2 cells, and showed that following reactivation, the infectivities of progeny viruses produced from R88-$A3G_{D128K}$ transduced ACH-2 cells were significantly impaired (3-6 fold reduced). Additionally, R88-$A3G_{D128K}$ exhibited similar anti-viral action in primary human cells. Altogether, data from this chapter indicate that R88-$A3G_{D128K}$ is a highly potent HIV-1 inhibitor, and a R88-$A3G_{D128K}$ based anti-HIV gene therapy is capable of blocking both active

and latent infections.

## 6.2 General discussion

### A3G as a potential target for anti-HIV therapy

The discovery of host restriction factors opens new avenues for HIV-1 therapeutic intervention. Increasing efforts have been conducted to develop more readily available and affordable therapeutics based on restriction factors. Although, no such antivirals have been tested in clinical trails yet, evidence from animal models and patients has highlighted their potential (215, 264, 306). Data from HIV/HCV-coinfected patients indicated that restriction factors A3G and BST-2 play critical roles in IFN-α-mediated suppression of HIV-1 replication *in vivo* (264).

In order to efficiently control HIV-1 infection and prevent HIV-associated disease, a rapid immune response is required (70). Besides antagonizing viral replication as a single host protein, A3G induces immune response to defend against HIV-1 infection (219). Uridines incorporated within A3G-edited viral DNAs induce the expression of natural killer (NK) cell-activating ligands through Vpr-mediated DNA-damage-response pathway, thereby activating NK cells to lysis HIV-infected cells (245). Meanwhile, A3G edited proviruses express aberrant (truncated or misfolded) viral proteins, which provide a pool of MHC-1-restricted viral antigens to activate HIV-1 specific $CD8^+$ cytotoxic T lymphocytes (CTLs) (42). Thus, this enzyme enhances the immunogenicity and promotes the recognition of HIV-infected cells by NK cells and CTLs (42, 245). Therefore, strategies aimed at enhancing A3G antiviral action may have the extra benefit of stimulating innate and adaptive immune response to target infected cells.

**The role of A3G against latency infection**

A major barrier to curing HIV-1 infection is the extensive latent reservoir that HIV-1 establishes as a reversibly non-productive infection in individual cells. The most well characterized reservoir is the resting $CD4^+$ T cells (201), also other cell types can be latently infected, including macrophages, microglia, astrocytes and hematopoietic progenitor cells (HPCs) (41). These cells are long-lived with an extremely slow decay rate, resulting in a lifelong persistence of virus in patients (201).

Since latent reservoirs are not expressing viral proteins, they are resistant to HAART and immune response (74). Once HAART is discontinued or activating signals are present, latency may be reversed and the cell may begin to produce viruses, leading to rebound viremia in patients. Moreover, recent study found that reactivation of drug-resistant latent viruses may contribute to the development of multidrug-resistance, and promote viral evolution through recombination with the superinfecting viruses (74).

Currently, considerable attention has been focused on finding ways to reactivate and deplete latent reservoirs. Although R88-$A3G_{D128K}$ itself is not able to eliminate the viral reservoirs, it can combine with latency reactivation compounds to target latent viruses. Since R88-$A3G_{D128K}$ acts to restrict second round infection, following reactivation compounds treatment, this protein can actively incorporate into viruses released from modified reservoirs and block additional rounds of viral replication. Therefore, viral rebound after latency reactivation can be avoided by introducing R88-$A3G_{D128K}$ into latent reservoirs. Moreover, since R88-$A3G_{D128K}$ does not disrupt the late stages of HIV-1 replication, latent HIV provirus can still be reactivated from modified cells and produce virus, thereby the reactivated reservoirs can be targeted by CTLs or killed by viral cytopathic effects. Results from Chapter 5 have shown that

R88-A3G$_{D128K}$ targets and blocks the replication of drug resistant viruses. Thus, it is capable for R88-A3G$_{D128K}$ to target drug-resistant latent viruses and prevent the generation of multi-drug resistance.

**Potential limitations of A3G based antiviral approach**

Since A3G is a host protein, its endogenous expression is regulated by cellular machineries. Here, we boosted its expression by introducing viral vector expressing R-A3G$_{D128K}$. It is uncertain whether side effect regarding the overexpression of A3G persists.

The constitutive and ubiquitous transgenic expression of another cytidine deaminase AID was associated with the development of various cancers in mouse models (55). In contrast to AID, A3G is a cytoplasmic protein that targets single-stranded DNA. It is unlikely for A3G to gain access to double-stranded cell genomic DNA (228). Indeed, a recent study showed that A3G has no effect on the mutation rate of transfected 293 cells. Meanwhile, data from our previous study and Chapter 4 proved that stable expression of A3G in C8166 cells does not cause cell cycle arrest or growth defects (14). Still, more safety studies are needed to exclude the possibility that A3G could induce mutations in genomic DNA, leading to cellular transformation.

The emergence of HIV resistance is the concern met by all antiretroviral therapeutics. Due to its high mutation rate, it is possible for HIV to evolve resistance against R88-A3G$_{D128K}$. However, no escape mutant has emerged in our study, and publication from Hache, et al. indicated that A3G was able to provide a lethal block to the replication of Vif-deficient HIV-1 for more than five weeks (116). However, the same study also showed that HIV was able to acquire a Vif-independent resistance

after six weeks constitutive culture, and the escape mutations were generated in 3/48 A3G-expressing T cell cultures (116). In order to provide strong and sustained protection from HIV-1 infection, we may combine R88-A3G$_{D128K}$ with other anti-HIV genes targeting different stages of HIV life cycle. This combinatorial anti-HIV gene therapy can enhance antiviral effect and reduce the likelihood of the emergence of HIV-1 escape mutants (19).

**Broad application of A3G based antiviral approach**

A3G exerts a strong antiviral effect against a diverse set of endogenous retroelements and exogenous viruses, such as HBV and HTLV-1 (132). HBV is the major causative agent of liver disease (52), and HTLV-1 is a oncogenic retrovirus associated with adult T cell leukemia, tropical spastic paraparesis and HTLV-1-associated myelopathy (21). Therefore, the development of an A3G based approach may have applications beyond the treatment of HIV-1 infection.

## 6.3 Future directions

For future application of A3G in anti-HIV therapies, it would be beneficial to further characterize the actions of A3G in viral replication. In Chapter 3, we studied the interaction between A3G and RT in the case of a Vif$^-$ HIV-1 infection. It is desirable to expand further studies to the case of Vif$^+$ HIV-1 infection, and determine if Vif could promote HIV-1 reverse transcription through disrupting A3G-RT interaction. It is also of interest to determine whether physical interaction between A3G and RT contributes to A3G getting access to single-strand DNA substrates. These proposed studies will promote better design and modification of A3G-based antiviral therapeutics.

In order to treat HIV-1 infection, R-A3G$_{D128K}$ can be delivered into HSCs isolated from HIV patients undergoing bone marrow transplantation using SIN-lentiviral vector system. HSCs are long-lived, and can differentiate into HIV-1 susceptible CD4$^+$ T cell and myeloid targets (161, 187). Such modification allows both HSCs and their progeny capable of inhibiting HIV-1 infection. Once these modified cells are transplanted back into patient, the host could be reconstituted with a hematopoietic system that is able to stably suppress HIV-1 replication. Thus, a functional cure of HIV-1 infection could be achieved. Moreover, a computational study by predicting the effect of A3G modified stem cells on *in vivo* HIV-1 replication, has highlighted the feasibility of A3G$_{D128K}$-based HSC therapy (133).

However, prior to conducting studies on humanized mice models or patients, it is important to ensure that lentiviral transduction and R-A3G$_{D128K}$ expression will not affect the potency of the HSCs. It would be necessary to check the proliferation ability and potential of modified HCSs, as well as the intrinsic function of differentiated cells. If no side effect is observed, further work can be carried out to determine the antiviral activity mediated by *ex vivo* modification of R-A3G$_{D128K}$ expressing HSCs.

Additionally, the potential of R-A3G$_{D128K}$ against mucosal HIV transmission is another area deserving further study. By using viral vectors or non-viral gene delivery vectors (189), R-A3G$_{D128K}$ expressing gene can be delivered into vaginal tissues where HIV-1 target cells are present. During early HIV infection in the mucosa, R-A3G$_{D128K}$ protein can be incorporated into newly synthesized virions to exhibit its antiviral activities, thereby reducing sexual transmission of HIV-1. However, *in vivo* tissue environments are complex, so suitable animal models are required to test this hypothesis.

## 6.4 Conclusion

In conclusion, results from this thesis demonstrate one of the mechanisms that how A3G disrupts HIV-1 reverse transcription, and provide proof-in-principle that R88-A3G$_{D128K}$ could be a potential candidate for HIV-1 gene therapy approach. The next step is to target *in vivo* HIV-1 susceptible cell populations, and to determine the safety and therapeutic effect of the R88-A3G$_{D128K}$ based approach. It is expected that this approach could prevent the onset of AIDS in HIV infected individuals.

# REFERENCES


1. **Adolph, M. B., J. Webb, and L. Chelico.** 2013. Retroviral Restriction Factor APOBEC3G Delays the Initiation of DNA Synthesis by HIV-1 Reverse Transcriptase. PLoS One **8:**e64196.
2. **Aiken, C.** 2006. Viral and cellular factors that regulate HIV-1 uncoating. Curr Opin HIV AIDS **1:**194-9.
3. **Ako-Adjei, D., M. C. Johnson, and V. M. Vogt.** 2005. The retroviral capsid domain dictates virion size, morphology, and coassembly of gag into virus-like particles. J Virol **79:**13463-72.
4. **Albin, J. S., and R. S. Harris.** 2010. Interactions of host APOBEC3 restriction factors with HIV-1 in vivo: implications for therapeutics. Expert Rev Mol Med **12:**e4.
5. **Alce, T. M., and W. Popik.** 2004. APOBEC3G is incorporated into virus-like particles by a direct interaction with HIV-1 Gag nucleocapsid protein. J Biol Chem **279:**34083-6.
6. **Anderson, J., and R. Akkina.** 2008. Human immunodeficiency virus type 1 restriction by human-rhesus chimeric tripartite motif 5alpha (TRIM 5alpha) in CD34(+) cell-derived macrophages in vitro and in T cells in vivo in severe combined immunodeficient (SCID-hu) mice transplanted with human fetal tissue. Hum Gene Ther **19:**217-28.
7. **Anderson, J., and R. Akkina.** 2005. TRIM5alpharh expression restricts HIV-1 infection in lentiviral vector-transduced CD34+-cell-derived macrophages. Mol Ther **12:**687-96.
8. **Andreola, M. L.** 2009. Therapeutic potential of peptide motifs against HIV-1 reverse transcriptase and integrase. Curr Pharm Des **15:**2508-19.
9. **Ao, Z., K. Danappa Jayappa, B. Wang, Y. Zheng, S. Kung, E. Rassart, R. Depping, M. Kohler, E. A. Cohen, and X. Yao.** 2010. Importin alpha3 interacts with HIV-1 integrase and contributes to HIV-1 nuclear import and replication. J Virol **84:**8650-63.
10. **Ao, Z., K. R. Fowke, E. A. Cohen, and X. Yao.** 2005. Contribution of the C-terminal tri-lysine regions of human immunodeficiency virus type 1 integrase for efficient reverse transcription and viral DNA nuclear import. Retrovirology **2:**62.
11. **Ao, Z., G. Huang, H. Yao, Z. Xu, M. Labine, A. W. Cochrane, and X. Yao.** 2007. Interaction of human immunodeficiency virus type 1 integrase with cellular nuclear import receptor importin 7 and its impact on viral replication. J Biol Chem **282:**13456-67.
12. **Ao, Z., K. D. Jayappa, B. Wang, Y. Zheng, S. Kung, E. Rassart, R. Depping, M. Kohler, E. A. Cohen, and X. Yao.** 2010. Importin {alpha}3 interacts with HIV-1 integrase and contributes to HIV-1 nuclear import and replication. J Virol **84:**8650-63.
13. **Ao, Z., X. Yao, and E. A. Cohen.** 2004. Assessment of the role of the central DNA flap in human immunodeficiency virus type 1 replication by using a single-cycle replication system. J Virol **78:**3170-7.
14. **Ao, Z., Z. Yu, L. Wang, Y. Zheng, and X. Yao.** 2008. Vpr14-88-Apobec3G fusion protein is efficiently incorporated into Vif-positive HIV-1 particles and inhibits viral infection. PLoS ONE **3:**e1995.
15. **Aravind, L., and E. V. Koonin.** 1998. The HD domain defines a new superfamily of metal-dependent phosphohydrolases. Trends Biochem Sci **23:**469-72.
16. **Arhel, N.** 2010. Revisiting HIV-1 uncoating. Retrovirology **7:**96.
17. **Armitage, A. E., K. Deforche, C. H. Chang, E. Wee, B. Kramer, J. J. Welch, J. Gerstoft, L. Fugger, A. McMichael, A. Rambaut, and A. K. Iversen.** 2012. APOBEC3G-induced hypermutation of human immunodeficiency virus type-1 is typically a discrete "all or nothing" phenomenon. PLoS Genet **8:**e1002550.
18. **Auricchio, A., M. Hildinger, E. O'Connor, G. P. Gao, and J. M. Wilson.** 2001. Isolation of highly infectious and pure adeno-associated virus type 2 vectors with a single-step gravity-flow column. Hum Gene Ther **12:**71-6.
19. **Aviran, S., P. S. Shah, D. V. Schaffer, and A. P. Arkin.** 2010. Computational models of HIV-1 resistance to gene therapy elucidate therapy design principles. PLoS Comput Biol **6**.
20. **Ayyavoo, V., S. Mahalingam, Y. Rafaeli, S. Kudchodkar, D. Chang, T. Nagashunmugam, W. V. Williams, and D. B. Weiner.** 1997. HIV-1 viral protein R (Vpr) regulates viral replication and cellular proliferation in T cells and monocytoid cells in vitro. J Leukoc Biol **62:**93-9.
21. **Bai, X. T., and C. Nicot.** 2012. Overview on HTLV-1 p12, p8, p30, p13: accomplices in persistent infection and viral pathogenesis. Front Microbiol **3:**400.
22. **Baldauf, H. M., X. Pan, E. Erikson, S. Schmidt, W. Daddacha, M. Burggraf, K. Schenkova, I. Ambiel, G. Wabnitz, T. Gramberg, S. Panitz, E. Flory, N. R. Landau, S. Sertel, F. Rutsch, F. Lasitschka, B. Kim, R. Konig, O. T. Fackler, and O. T. Keppler.** 2012.

SAMHD1 restricts HIV-1 infection in resting CD4(+) T cells. Nat Med **18:**1682-7.

23. **Barbaro, G.** 2006. Metabolic and cardiovascular complications of highly active antiretroviral therapy for HIV infection. Curr HIV Res **4:**79-85.
24. **Barre-Sinoussi, F., J. C. Chermann, F. Rey, M. T. Nugeyre, S. Chamaret, J. Gruest, C. Dauguet, C. Axler-Blin, F. Vezinet-Brun, C. Rouzioux, W. Rozenbaum, and L. Montagnier.** 1983. Isolation of a T-lymphotropic retrovirus from a patient at risk for acquired immune deficiency syndrome (AIDS). Science **220:**868-71.
25. **Bell, N. M., and A. M. Lever.** 2013. HIV Gag polyprotein: processing and early viral particle assembly. Trends Microbiol **21:**136-44.
26. **Bello, A., K. Tran, A. Chand, M. Doria, M. Allocca, M. Hildinger, D. Beniac, C. Kranendonk, A. Auricchio, and G. P. Kobinger.** 2009. Isolation and evaluation of novel adeno-associated virus sequences from porcine tissues. Gene Ther **16:**1320-8.
27. **Bhattacharya, J., A. Repik, and P. R. Clapham.** 2006. Gag regulates association of human immunodeficiency virus type 1 envelope with detergent-resistant membranes. J Virol **80:**5292-300.
28. **Bishop, K. N., R. K. Holmes, and M. H. Malim.** 2006. Antiviral potency of APOBEC proteins does not correlate with cytidine deamination. J Virol **80:**8450-8.
29. **Bishop, K. N., M. Verma, E. Y. Kim, S. M. Wolinsky, and M. H. Malim.** 2008. APOBEC3G inhibits elongation of HIV-1 reverse transcripts. PLoS Pathog **4:**e1000231.
30. **Blanco-Melo, D., S. Venkatesh, and P. D. Bieniasz.** 2012. Intrinsic cellular defenses against human immunodeficiency viruses. Immunity **37:**399-411.
31. **Bobadilla, S., N. Sunseri, and N. R. Landau.** 2012. Efficient transduction of myeloid cells by an HIV-1-derived lentiviral vector that packages the Vpx accessory protein. Gene Ther**:**1-7.
32. **Bogerd, H. P., B. P. Doehle, H. L. Wiegand, and B. R. Cullen.** 2004. A single amino acid difference in the host APOBEC3G protein controls the primate species specificity of HIV type 1 virion infectivity factor. Proc Natl Acad Sci U S A **101:**3770-4.
33. **Bonvin, M., F. Achermann, I. Greeve, D. Stroka, A. Keogh, D. Inderbitzin, D. Candinas, P. Sommer, S. Wain-Hobson, J. P. Vartanian, and J. Greeve.** 2006. Interferon-inducible expression of APOBEC3 editing enzymes in human hepatocytes and inhibition of hepatitis B virus replication. Hepatology **43:**1364-74.
34. **Britan-Rosich, E., R. Nowarski, and M. Kotler.** 2011. Multifaceted counter-APOBEC3G mechanisms employed by HIV-1 Vif. J Mol Biol **410:**1065-76.
35. **Browne, E. P., C. Allers, and N. R. Landau.** 2009. Restriction of HIV-1 by APOBEC3G is cytidine deaminase-dependent. Virology **387:**313-21.
36. **Buckman, J. S., W. J. Bosche, and R. J. Gorelick.** 2003. Human immunodeficiency virus type 1 nucleocapsid zn(2+) fingers are required for efficient reverse transcription, initial integration processes, and protection of newly synthesized viral DNA. J Virol **77:**1469-80.
37. **Bukrinsky, M.** 2004. A hard way to the nucleus. Mol Med **10:**1-5.
38. **Campbell-Yesufu, O. T., and R. T. Gandhi.** 2011. Update on human immunodeficiency virus (HIV)-2 infection. Clin Infect Dis **52:**780-7.
39. **Campbell, R. S., and W. F. Robinson.** 1998. The comparative pathology of the lentiviruses. J Comp Pathol **119:**333-95.
40. **Cancio, R., S. Spadari, and G. Maga.** 2004. Vif is an auxiliary factor of the HIV-1 reverse transcriptase and facilitates abasic site bypass. Biochem J **383:**475-82.
41. **Carter, C. C., A. Onafuwa-Nuga, L. A. McNamara, J. t. Riddell, D. Bixby, M. R. Savona, and K. L. Collins.** 2010. HIV-1 infects multipotent progenitor cells causing cell death and establishing latent cellular reservoirs. Nat Med **16:**446-51.
42. **Casartelli, N., F. Guivel-Benhassine, R. Bouziat, S. Brandler, O. Schwartz, and A. Moris.** 2010. The antiviral factor APOBEC3G improves CTL recognition of cultured HIV-infected T cells. J Exp Med **207:**39-49.
43. **Cen, S., F. Guo, M. Niu, J. Saadatmand, J. Deflassieux, and L. Kleiman.** 2004. The interaction between HIV-1 Gag and APOBEC3G. J Biol Chem **279:**33177-84.
44. **Cen, S., Z. G. Peng, X. Y. Li, Z. R. Li, J. Ma, Y. M. Wang, B. Fan, X. F. You, Y. P. Wang, F. Liu, R. G. Shao, L. X. Zhao, L. Yu, and J. D. Jiang.** 2010. Small molecular compounds inhibit HIV-1 replication through specifically stabilizing APOBEC3G. J Biol Chem **285:**16546-52.
45. **Chan, P. A., K. Tashima, C. P. Cartwright, F. S. Gillani, O. Mintz, K. Zeller, and R. Kantor.** 2011. Short communication: Transmitted drug resistance and molecular epidemiology in antiretroviral naive HIV type 1-infected patients in Rhode Island. AIDS Res Hum Retroviruses **27:**275-81.

46. **Chelico, L., P. Pham, P. Calabrese, and M. F. Goodman.** 2006. APOBEC3G DNA deaminase acts processively 3' --> 5' on single-stranded DNA. Nat Struct Mol Biol **13:**392-9.
47. **Chelico, L., P. Pham, and M. F. Goodman.** 2009. Stochastic properties of processive cytidine DNA deaminases AID and APOBEC3G. Philos Trans R Soc Lond B Biol Sci **364:**583-93.
48. **Chelico, L., P. Pham, J. Petruska, and M. F. Goodman.** 2009. Biochemical basis of immunological and retroviral responses to DNA-targeted cytosine deamination by activation-induced cytidine deaminase and APOBEC3G. J Biol Chem **284:**27761-5.
49. **Chen, H., C. E. Lilley, Q. Yu, D. V. Lee, J. Chou, I. Narvaiza, N. R. Landau, and M. D. Weitzman.** 2006. APOBEC3A is a potent inhibitor of adeno-associated virus and retrotransposons. Curr Biol **16:**480-5.
50. **Chen, K. M., E. Harjes, P. J. Gross, A. Fahmy, Y. Lu, K. Shindo, R. S. Harris, and H. Matsuo.** 2008. Structure of the DNA deaminase domain of the HIV-1 restriction factor APOBEC3G. Nature **452:**116-9.
51. **Chertova, E., O. Chertov, L. V. Coren, J. D. Roser, C. M. Trubey, J. W. Bess, Jr., R. C. Sowder, 2nd, E. Barsov, B. L. Hood, R. J. Fisher, K. Nagashima, T. P. Conrads, T. D. Veenstra, J. D. Lifson, and D. E. Ott.** 2006. Proteomic and biochemical analysis of purified human immunodeficiency virus type 1 produced from infected monocyte-derived macrophages. J Virol **80:**9039-52.
52. **Chisari, F. V., M. Isogawa, and S. F. Wieland.** 2010. Pathogenesis of hepatitis B virus infection. Pathol Biol (Paris) **58:**258-66.
53. **Chiu, T. K., and D. R. Davies.** 2004. Structure and function of HIV-1 integrase. Curr Top Med Chem **4:**965-77.
54. **Chiu, Y. L., and W. C. Greene.** 2008. The APOBEC3 cytidine deaminases: an innate defensive network opposing exogenous retroviruses and endogenous retroelements. Annu Rev Immunol **26:**317-53.
55. **Chiu, Y. L., and W. C. Greene.** 2009. APOBEC3G: an intracellular centurion. Philos Trans R Soc Lond B Biol Sci **364:**689-703.
56. **Chiu, Y. L., and W. C. Greene.** 2006. Multifaceted antiviral actions of APOBEC3 cytidine deaminases. Trends Immunol **27:**291-7.
57. **Chiu, Y. L., H. E. Witkowska, S. C. Hall, M. Santiago, V. B. Soros, C. Esnault, T. Heidmann, and W. C. Greene.** 2006. High-molecular-mass APOBEC3G complexes restrict Alu retrotransposition. Proc Natl Acad Sci U S A **103:**15588-93.
58. **Cochrane, A. W., A. Perkins, and C. A. Rosen.** 1990. Identification of sequences important in the nucleolar localization of human immunodeficiency virus Rev: relevance of nucleolar localization to function. J Virol **64:**881-5.
59. **Cohen, M. S., G. M. Shaw, A. J. McMichael, and B. F. Haynes.** 2011. Acute HIV-1 Infection. N Engl J Med **364:**1943-54.
60. **Coiras, M., M. R. Lopez-Huertas, M. Perez-Olmeda, and J. Alcami.** 2009. Understanding HIV-1 latency provides clues for the eradication of long-term reservoirs. Nat Rev Microbiol **7:**798-812.
61. **Coker, H. A., and S. K. Petersen-Mahrt.** 2007. The nuclear DNA deaminase AID functions distributively whereas cytoplasmic APOBEC3G has a processive mode of action. DNA Repair **6:**235-243.
62. **Colin, L., and C. Van Lint.** 2009. Molecular control of HIV-1 postintegration latency: implications for the development of new therapeutic strategies. Retrovirology **6:**111.
63. **Colman, P. M., and M. C. Lawrence.** 2003. The structural biology of type I viral membrane fusion. Nat Rev Mol Cell Biol **4:**309-19.
64. **Conti, L., G. Rainaldi, P. Matarrese, B. Varano, R. Rivabene, S. Columba, A. Sato, F. Belardelli, W. Malorni, and S. Gessani.** 1998. The HIV-1 vpr protein acts as a negative regulator of apoptosis in a human lymphoblastoid T cell line: possible implications for the pathogenesis of AIDS. J Exp Med **187:**403-13.
65. **Conticello, S. G., R. S. Harris, and M. S. Neuberger.** 2003. The Vif protein of HIV triggers degradation of the human antiretroviral DNA deaminase APOBEC3G. Curr Biol **13:**2009-13.
66. **Craigie, R., and F. D. Bushman.** 2012. HIV DNA Integration. Cold Spring Harb Perspect Med **2:**a006890.
67. **Dahl, V., and S. Palmer.** 2009. Establishment of drug-resistant HIV-1 in latent reservoirs. J Infect Dis **199:**1258-60.
68. **Darlix, J. L., J. L. Garrido, N. Morellet, Y. Mely, and H. de Rocquigny.** 2007. Properties, functions, and drug targeting of the multifunctional nucleocapsid protein of the human

immunodeficiency virus. Adv Pharmacol **55:**299-346.
69. **de Silva, T. I., M. Cotten, and S. L. Rowland-Jones.** 2008. HIV-2: the forgotten AIDS virus. Trends Microbiol **16:**588-95.
70. **Deeks, S. G., and B. D. Walker.** 2007. Human immunodeficiency virus controllers: mechanisms of durable virus control in the absence of antiretroviral therapy. Immunity **27:**406-16.
71. **Delebecque, F., R. Suspene, S. Calattini, N. Casartelli, A. Saib, A. Froment, S. Wain-Hobson, A. Gessain, J. P. Vartanian, and O. Schwartz.** 2006. Restriction of foamy viruses by APOBEC cytidine deaminases. J Virol **80:**605-14.
72. **Di Marzio, P., S. Choe, M. Ebright, R. Knoblauch, and N. R. Landau.** 1995. Mutational analysis of cell cycle arrest, nuclear localization and virion packaging of human immunodeficiency virus type 1 Vpr. J Virol **69:**7909-16.
73. **Doehle, B. P., H. P. Bogerd, H. L. Wiegand, N. Jouvenet, P. D. Bieniasz, E. Hunter, and B. R. Cullen.** 2006. The betaretrovirus Mason-Pfizer monkey virus selectively excludes simian APOBEC3G from virion particles. J Virol **80:**12102-8.
74. **Donahue, D. A., S. M. Bastarache, R. D. Sloan, and M. A. Wainberg.** 2013. Latent HIV-1 can be reactivated by cellular superinfection in a Tat-dependent manner, which can lead to the emergence of multidrug-resistant recombinant viruses. J Virol **87:**9620-32.
75. **Donahue, J. P., M. L. Vetter, N. A. Mukhtar, and R. T. D'Aquila.** 2008. The HIV-1 Vif PPLP motif is necessary for human APOBEC3G binding and degradation. Virology **377:**49-53.
76. **Douaisi, M., S. Dussart, M. Courcoul, G. Bessou, R. Vigne, and E. Decroly.** 2004. HIV-1 and MLV Gag proteins are sufficient to recruit APOBEC3G into virus-like particles. Biochem Biophys Res Commun **321:**566-73.
77. **Douek, D. C., J. M. Brenchley, M. R. Betts, D. R. Ambrozak, B. J. Hill, Y. Okamoto, J. P. Casazza, J. Kuruppu, K. Kunstman, S. Wolinsky, Z. Grossman, M. Dybul, A. Oxenius, D. A. Price, M. Connors, and R. A. Koup.** 2002. HIV preferentially infects HIV-specific CD4+ T cells. Nature **417:**95-8.
78. **Douek, D. C., M. Roederer, and R. A. Koup.** 2009. Emerging concepts in the immunopathogenesis of AIDS. Annu Rev Med **60:**471-84.
79. **Douglas, J. L., K. Viswanathan, M. N. McCarroll, J. K. Gustin, K. Fruh, and A. V. Moses.** 2009. Vpu directs the degradation of the human immunodeficiency virus restriction factor BST-2/Tetherin via a {beta}TrCP-dependent mechanism. J Virol **83:**7931-47.
80. **Druillennec, S., C. Z. Dong, S. Escaich, N. Gresh, A. Bousseau, B. P. Roques, and M. C. Fournie-Zaluski.** 1999. A mimic of HIV-1 nucleocapsid protein impairs reverse transcription and displays antiviral activity. Proc Natl Acad Sci U S A **96:**4886-91.
81. **Duggal, N. K., and M. Emerman.** 2012. Evolutionary conflicts between viruses and restriction factors shape immunity. Nat Rev Immunol **12:**687-95.
82. **Durand, S., and A. Cimarelli.** 2011. The inside out of lentiviral vectors. Viruses **3:**132-59.
83. **During, M. J., R. Xu, D. Young, M. G. Kaplitt, R. S. Sherwin, and P. Leone.** 1998. Peroral gene therapy of lactose intolerance using an adeno-associated virus vector. Nat Med **4:**1131-5.
84. **Dyer, W. B., A. F. Geczy, S. J. Kent, L. B. McIntyre, S. A. Blasdall, J. C. Learmont, and J. S. Sullivan.** 1997. Lymphoproliferative immune function in the Sydney Blood Bank Cohort, infected with natural nef/long terminal repeat mutants, and in other long-term survivors of transfusion-acquired HIV-1 infection. AIDS **11:**1565-74.
85. **Engelman, A., G. Englund, J. M. Orenstein, M. A. Martin, and R. Craigie.** 1995. Multiple effects of mutations in human immunodeficiency virus type 1 integrase on viral replication. J Virol **69:**2729-36.
86. **Esnault, C., O. Heidmann, F. Delebecque, M. Dewannieux, D. Ribet, A. J. Hance, T. Heidmann, and O. Schwartz.** 2005. APOBEC3G cytidine deaminase inhibits retrotransposition of endogenous retroviruses. Nature **433:**430-3.
87. **Esnault, C., J. Millet, O. Schwartz, and T. Heidmann.** 2006. Dual inhibitory effects of APOBEC family proteins on retrotransposition of mammalian endogenous retroviruses. Nucleic Acids Res **34:**1522-31.
88. **Fan, D. S., M. Ogawa, K. I. Fujimoto, K. Ikeguchi, Y. Ogasawara, M. Urabe, M. Nishizawa, I. Nakano, M. Yoshida, I. Nagatsu, H. Ichinose, T. Nagatsu, G. J. Kurtzman, and K. Ozawa.** 1998. Behavioral recovery in 6-hydroxydopamine-lesioned rats by cotransduction of striatum with tyrosine hydroxylase and aromatic L-amino acid decarboxylase genes using two separate adeno-associated virus vectors. Hum Gene Ther **9:**2527-35.

89. **Farrow, M. A., and A. M. Sheehy.** 2008. Vif and Apobec3G in the innate immune response to HIV: a tale of two proteins. Future Microbiol **3:**145-54.
90. **Feng, Y., R. P. Love, and L. Chelico.** 2013. HIV-1 viral infectivity factor (Vif) alters processive single-stranded DNA scanning of the retroviral restriction factor APOBEC3G. J Biol Chem **288:**6083-94.
91. **Finzi, D., J. Blankson, J. D. Siliciano, J. B. Margolick, K. Chadwick, T. Pierson, K. Smith, J. Lisziewicz, F. Lori, C. Flexner, T. C. Quinn, R. E. Chaisson, E. Rosenberg, B. Walker, S. Gange, J. Gallant, and R. F. Siliciano.** 1999. Latent infection of CD4+ T cells provides a mechanism for lifelong persistence of HIV-1, even in patients on effective combination therapy. Nat Med **5:**512-7.
92. **Fitzpatrick, K., M. Skasko, T. J. Deerinck, J. Crum, M. H. Ellisman, and J. Guatelli.** 2010. Direct restriction of virus release and incorporation of the interferon-induced protein BST-2 into HIV-1 particles. PLoS Pathog **6:**e1000701.
93. **Flotte, T. R., S. A. Afione, C. Conrad, S. A. McGrath, R. Solow, H. Oka, P. L. Zeitlin, W. B. Guggino, and B. J. Carter.** 1993. Stable in vivo expression of the cystic fibrosis transmembrane conductance regulator with an adeno-associated virus vector. Proc Natl Acad Sci U S A **90:**10613-7.
94. **Folks, T. M., K. A. Clouse, J. Justement, A. Rabson, E. Duh, J. H. Kehrl, and A. S. Fauci.** 1989. Tumor necrosis factor alpha induces expression of human immunodeficiency virus in a chronically infected T-cell clone. Proc Natl Acad Sci U S A **86:**2365-8.
95. **Fornerod, M., M. Ohno, M. Yoshida, and I. W. Mattaj.** 1997. CRM1 is an export receptor for leucine-rich nuclear export signals. Cell **90:**1051-60.
96. **Friew, Y. N., V. Boyko, W. S. Hu, and V. K. Pathak.** 2009. Intracellular interactions between APOBEC3G, RNA, and HIV-1 Gag: APOBEC3G multimerization is dependent on its association with RNA. Retrovirology **6:**56.
97. **Gallego, O., L. Ruiz, A. Vallejo, B. Clotet, M. Leal, and V. Soriano.** 2002. Rate of virological treatment failure and frequencies of drug resistance genotypes among human immunodeficiency virus-positive subjects on antiretroviral therapy in Spain. J Clin Microbiol **40:**3865-6.
98. **Gallo, R. C.** 1999. Tat as one key to HIV-induced immune pathogenesis and Tat (correction of Pat) toxoid as an important component of a vaccine. Proc Natl Acad Sci U S A **96:**8324-6.
99. **Gallois-Montbrun, S., B. Kramer, C. M. Swanson, H. Byers, S. Lynham, M. Ward, and M. H. Malim.** 2007. Antiviral protein APOBEC3G localizes to ribonucleoprotein complexes found in P bodies and stress granules. J Virol **81:**2165-78.
100. **Ganser-Pornillos, B. K., M. Yeager, and W. I. Sundquist.** 2008. The structural biology of HIV assembly. Curr Opin Struct Biol **18:**203-17.
101. **Gao, F., E. Bailes, D. L. Robertson, Y. Chen, C. M. Rodenburg, S. F. Michael, L. B. Cummins, L. O. Arthur, M. Peeters, G. M. Shaw, P. M. Sharp, and B. H. Hahn.** 1999. Origin of HIV-1 in the chimpanzee Pan troglodytes troglodytes. Nature **397:**436-41.
102. **Ghanam, R. H., A. B. Samal, T. F. Fernandez, and J. S. Saad.** 2012. Role of the HIV-1 Matrix Protein in Gag Intracellular Trafficking and Targeting to the Plasma Membrane for Virus Assembly. Front Microbiol **3:**55.
103. **Giedroc, D. P., and P. V. Cornish.** 2009. Frameshifting RNA pseudoknots: structure and mechanism. Virus Res **139:**193-208.
104. **Gilbert, M. T., A. Rambaut, G. Wlasiuk, T. J. Spira, A. E. Pitchenik, and M. Worobey.** 2007. The emergence of HIV/AIDS in the Americas and beyond. Proc Natl Acad Sci U S A **104:**18566-70.
105. **Goff, S. P.** 1990. Retroviral reverse transcriptase: synthesis, structure, and function. J Acquir Immune Defic Syndr **3:**817-31.
106. **Goh, W. C., M. E. Rogel, C. M. Kinsey, S. F. Michael, P. N. Fultz, M. A. Nowak, B. H. Hahn, and M. Emerman.** 1998. HIV-1 Vpr increases viral expression by manipulation of the cell cycle: a mechanism for selection of Vpr in vivo. *Nat. Med.* **4:**65-71.
107. **Goldstone, D. C., V. Ennis-Adeniran, J. J. Hedden, H. C. Groom, G. I. Rice, E. Christodoulou, P. A. Walker, G. Kelly, L. F. Haire, M. W. Yap, L. P. de Carvalho, J. P. Stoye, Y. J. Crow, I. A. Taylor, and M. Webb.** 2011. HIV-1 restriction factor SAMHD1 is a deoxynucleoside triphosphate triphosphohydrolase. Nature **480:**379-82.
108. **Green, L. A., Y. Liu, and J. J. He.** 2009. Inhibition of HIV-1 infection and replication by enhancing viral incorporation of innate anti-HIV-1 protein A3G: a non-pathogenic Nef mutant-based anti-HIV strategy. J Biol Chem **284:**13363-72.
109. **Grewe, B., and K. Uberla.** 2010. The human immunodeficiency virus type 1 Rev protein:

menage a trois during the early phase of the lentiviral replication cycle. J Gen Virol **91:**1893-7.
110. **Groom, H. C., E. C. Anderson, and A. M. Lever.** 2009. Rev: beyond nuclear export. J Gen Virol **90:**1303-18.
111. **Guo, F., S. Cen, M. Niu, J. Saadatmand, and L. Kleiman.** 2006. Inhibition of formula-primed reverse transcription by human APOBEC3G during human immunodeficiency virus type 1 replication. J Virol **80:**11710-22.
112. **Guo, F., S. Cen, M. Niu, Y. Yang, R. J. Gorelick, and L. Kleiman.** 2007. The interaction of APOBEC3G with human immunodeficiency virus type 1 nucleocapsid inhibits tRNA3Lys annealing to viral RNA. J Virol **81:**11322-31.
113. **Guo, F., J. Saadatmand, M. Niu, and L. Kleiman.** 2009. Roles of Gag and NCp7 in facilitating tRNA(Lys)(3) Annealing to viral RNA in human immunodeficiency virus type 1. J Virol **83:**8099-107.
114. **Guyader, M., M. Emerman, P. Sonigo, F. Clavel, L. Montagnier, and M. Alizon.** 1987. Genome organization and transactivation of the human immunodeficiency virus type 2. Nature **326:**662-9.
115. **Hache, G., M. T. Liddament, and R. S. Harris.** 2005. The retroviral hypermutation specificity of APOBEC3F and APOBEC3G is governed by the C-terminal DNA cytosine deaminase domain. J Biol Chem **280:**10920-4.
116. **Hache, G., K. Shindo, J. S. Albin, and R. S. Harris.** 2008. Evolution of HIV-1 isolates that use a novel Vif-independent mechanism to resist restriction by human APOBEC3G. Curr Biol **18:**819-24.
117. **Hahn, B. H., G. M. Shaw, K. M. De Cock, and P. M. Sharp.** 2000. AIDS as a zoonosis: scientific and public health implications. Science **287:**607-14.
118. **Hallenberger, S., V. Bosch, H. Angliker, E. Shaw, H. D. Klenk, and W. Garten.** 1992. Inhibition of furin-mediated cleavage activation of HIV-1 glycoprotein gp160. Nature **360:**358-61.
119. **Harris, M., B. Nosyk, R. Harrigan, V. D. Lima, C. Cohen, and J. Montaner.** 2012. Cost-Effectiveness of Antiretroviral Therapy for Multidrug-Resistant HIV: Past, Present, and Future. AIDS Res Treat **2012:**595762.
120. **Harris, R. S., K. N. Bishop, A. M. Sheehy, H. M. Craig, S. K. Petersen-Mahrt, I. N. Watt, M. S. Neuberger, and M. H. Malim.** 2003. DNA deamination mediates innate immunity to retroviral infection. Cell **113:**803-9.
121. **Harris, R. S., J. F. Hultquist, and D. T. Evans.** 2012. The restriction factors of human immunodeficiency virus. J Biol Chem **287:**40875-83.
122. **Harris, R. S., S. K. Petersen-Mahrt, and M. S. Neuberger.** 2002. RNA editing enzyme APOBEC1 and some of its homologs can act as DNA mutators. Mol Cell **10:**1247-53.
123. **Hehl, E. A., P. Joshi, G. V. Kalpana, and V. R. Prasad.** 2004. Interaction between human immunodeficiency virus type 1 reverse transcriptase and integrase proteins. J Virol **78:**5056-67.
124. **Helseth, E., U. Olshevsky, C. Furman, and J. Sodroski.** 1991. Human immunodeficiency virus type 1 gp120 envelope glycoprotein regions important for association with the gp41 transmembrane glycoprotein. J Virol **65:**2119-23.
125. **Hemelaar, J., E. Gouws, P. D. Ghys, and S. Osmanov.** 2011. Global trends in molecular epidemiology of HIV-1 during 2000-2007. AIDS **25:**679-89.
126. **Henriet, S., G. Mercenne, S. Bernacchi, J. C. Paillart, and R. Marquet.** 2009. Tumultuous relationship between the human immunodeficiency virus type 1 viral infectivity factor (Vif) and the human APOBEC-3G and APOBEC-3F restriction factors. Microbiol Mol Biol Rev **73:**211-32.
127. **Herschhorn, A., and A. Hizi.** 2010. Retroviral reverse transcriptases. Cell Mol Life Sci **67:**2717-47.
128. **Herzog, R. W., J. N. Hagstrom, S. H. Kung, S. J. Tai, J. M. Wilson, K. J. Fisher, and K. A. High.** 1997. Stable gene transfer and expression of human blood coagulation factor IX after intramuscular injection of recombinant adeno-associated virus. Proc Natl Acad Sci U S A **94:**5804-9.
129. **Hladik, F., and M. J. McElrath.** 2008. Setting the stage: host invasion by HIV. Nat Rev Immunol **8:**447-57.
130. **Hogg, R. S., D. R. Bangsberg, V. D. Lima, C. Alexander, S. Bonner, B. Yip, E. Wood, W. W. Dong, J. S. Montaner, and P. R. Harrigan.** 2006. Emergence of drug resistance is associated with an increased risk of death among patients first starting HAART. PLoS Med **3:**e356.

131. **Holmes, R. K., F. A. Koning, K. N. Bishop, and M. H. Malim.** 2007. APOBEC3F can inhibit the accumulation of HIV-1 reverse transcription products in the absence of hypermutation. Comparisons with APOBEC3G. J Biol Chem **282:**2587-95.
132. **Holmes, R. K., M. H. Malim, and K. N. Bishop.** 2007. APOBEC-mediated viral restriction: not simply editing? Trends Biochem Sci **32:**118-28.
133. **Hosseini, I., and F. Mac Gabhann.** 2013. APOBEC3G-Augmented Stem Cell Therapy to Modulate HIV Replication: A Computational Study. PLoS One **8:**e63984.
134. **Hosseini, I., and F. Mac Gabhann.** 2012. Multi-scale modeling of HIV infection in vitro and APOBEC3G-based anti-retroviral therapy. PLoS Comput Biol **8:**e1002371.
135. **Hoxie, J. A., and C. H. June.** 2012. Novel cell and gene therapies for HIV. Cold Spring Harb Perspect Med **2**.
136. **Hrecka, K., C. Hao, M. Gierszewska, S. K. Swanson, M. Kesik-Brodacka, S. Srivastava, L. Florens, M. P. Washburn, and J. Skowronski.** 2011. Vpx relieves inhibition of HIV-1 infection of macrophages mediated by the SAMHD1 protein. Nature **474:**658-61.
137. **Hu, W. S., and S. H. Hughes.** 2012. HIV-1 reverse transcription. Cold Spring Harb Perspect Med **2**.
138. **Hue, S., R. J. Gifford, D. Dunn, E. Fernhill, and D. Pillay.** 2009. Demonstration of sustained drug-resistant human immunodeficiency virus type 1 lineages circulating among treatment-naive individuals. J Virol **83:**2645-54.
139. **Hulme, A. E., H. P. Bogerd, B. R. Cullen, and J. V. Moran.** 2007. Selective inhibition of Alu retrotransposition by APOBEC3G. Gene **390:**199-205.
140. **Hulme, A. E., O. Perez, and T. J. Hope.** 2011. Complementary assays reveal a relationship between HIV-1 uncoating and reverse transcription. Proc Natl Acad Sci U S A **108:**9975-80.
141. **Huthoff, H., and M. H. Malim.** 2007. Identification of amino acid residues in APOBEC3G required for regulation by human immunodeficiency virus type 1 Vif and Virion encapsidation. J Virol **81:**3807-15.
142. **Iwatani, Y., D. S. Chan, L. Liu, H. Yoshii, J. Shibata, N. Yamamoto, J. G. Levin, A. M. Gronenborn, and W. Sugiura.** 2009. HIV-1 Vif-mediated ubiquitination/degradation of APOBEC3G involves four critical lysine residues in its C-terminal domain. Proc Natl Acad Sci U S A **106:**19539-44.
143. **Iwatani, Y., D. S. Chan, F. Wang, K. S. Maynard, W. Sugiura, A. M. Gronenborn, I. Rouzina, M. C. Williams, K. Musier-Forsyth, and J. G. Levin.** 2007. Deaminase-independent inhibition of HIV-1 reverse transcription by APOBEC3G. Nucleic Acids Res **35:**7096-108.
144. **Jacks, T., M. D. Power, F. R. Masiarz, P. A. Luciw, P. J. Barr, and H. E. Varmus.** 1988. Characterization of ribosomal frameshifting in HIV-1 gag-pol expression. Nature **331:**280-3.
145. **Jacobo-Molina, A., and E. Arnold.** 1991. HIV reverse transcriptase structure-function relationships. Biochemistry **30:**6351-6.
146. **Jacotot, E., L. Ravagnan, M. Loeffler, K. F. Ferri, H. L. Vieira, N. Zamzami, P. Costantini, S. Druillennec, J. Hoebeke, J. P. Briand, T. Irinopoulou, E. Daugas, S. A. Susin, D. Cointe, Z. H. Xie, J. C. Reed, B. P. Roques, and G. Kroemer.** 2000. The HIV-1 viral protein R induces apoptosis via a direct effect on the mitochondrial permeability transition pore. J Exp Med **191:**33-46.
147. **Jarmuz, A., A. Chester, J. Bayliss, J. Gisbourne, I. Dunham, J. Scott, and N. Navaratnam.** 2002. An anthropoid-specific locus of orphan C to U RNA-editing enzymes on chromosome 22. Genomics **79:**285-96.
148. **Jegede, O., J. Babu, R. Di Santo, D. J. McColl, J. Weber, and M. Quinones-Mateu.** 2008. HIV type 1 integrase inhibitors: from basic research to clinical implications. AIDS Rev **10:**172-89.
149. **Jern, P., R. A. Russell, V. K. Pathak, and J. M. Coffin.** 2009. Likely role of APOBEC3G-mediated G-to-A mutations in HIV-1 evolution and drug resistance. PLoS Pathog **5:**e1000367.
150. **Johnson, J. A., J. F. Li, X. Wei, J. Lipscomb, D. Irlbeck, C. Craig, A. Smith, D. E. Bennett, M. Monsour, P. Sandstrom, E. R. Lanier, and W. Heneine.** 2008. Minority HIV-1 drug resistance mutations are present in antiretroviral treatment-naive populations and associate with reduced treatment efficacy. PLoS Med **5:**e158.
151. **Jouvenet, N., S. J. Neil, C. Bess, M. C. Johnson, C. A. Virgen, S. M. Simon, and P. D. Bieniasz.** 2006. Plasma membrane is the site of productive HIV-1 particle assembly. PLoS Biol **4:**e435.
152. **Kanki, P. J., K. U. Travers, M. B. S, C. C. Hsieh, R. G. Marlink, N. A. Gueye, T. Siby, I.**

**Thior, M. Hernandez-Avila, J. L. Sankale, and et al.** 1994. Slower heterosexual spread of HIV-2 than HIV-1. Lancet **343:**943-6.

153. **Kao, S., H. Akari, M. A. Khan, M. Dettenhofer, X. F. Yu, and K. Strebel.** 2003. Human immunodeficiency virus type 1 Vif is efficiently packaged into virions during productive but not chronic infection. J Virol **77:**1131-40.
154. **Kao, S., R. Goila-Gaur, E. Miyagi, M. A. Khan, S. Opi, H. Takeuchi, and K. Strebel.** 2007. Production of infectious virus and degradation of APOBEC3G are separable functional properties of human immunodeficiency virus type 1 Vif. Virology **369:**329-39.
155. **Kao, S., M. A. Khan, E. Miyagi, R. Plishka, A. Buckler-White, and K. Strebel.** 2003. The human immunodeficiency virus type 1 Vif protein reduces intracellular expression and inhibits packaging of APOBEC3G (CEM15), a cellular inhibitor of virus infectivity. J Virol **77:**11398-407.
156. **Kao, S., E. Miyagi, M. A. Khan, H. Takeuchi, S. Opi, R. Goila-Gaur, and K. Strebel.** 2004. Production of infectious human immunodeficiency virus type 1 does not require depletion of APOBEC3G from virus-producing cells. Retrovirology **1:**27.
157. **Karn, J., and C. M. Stoltzfus.** 2012. Transcriptional and posttranscriptional regulation of HIV-1 gene expression. Cold Spring Harb Perspect Med **2:**a006916.
158. **Kataropoulou, A., C. Bovolenta, A. Belfiore, S. Trabatti, A. Garbelli, S. Porcellini, R. Lupo, and G. Maga.** 2009. Mutational analysis of the HIV-1 auxiliary protein Vif identifies independent domains important for the physical and functional interaction with HIV-1 reverse transcriptase. Nucleic Acids Res **37:**3660-9.
159. **Keene, S. E., and A. Telesnitsky.** 2012. cis-Acting determinants of 7SL RNA packaging by HIV-1. J Virol **86:**7934-42.
160. **Khan, M. A., S. Kao, E. Miyagi, H. Takeuchi, R. Goila-Gaur, S. Opi, C. L. Gipson, T. G. Parslow, H. Ly, and K. Strebel.** 2005. Viral RNA is required for the association of APOBEC3G with human immunodeficiency virus type 1 nucleoprotein complexes. J Virol **79:**5870-4.
161. **Kiem, H. P., K. R. Jerome, S. G. Deeks, and J. M. McCune.** 2012. Hematopoietic-stem-cell-based gene therapy for HIV disease. Cell Stem Cell **10:**137-47.
162. **Kirchhoff, F.** 2010. Immune evasion and counteraction of restriction factors by HIV-1 and other primate lentiviruses. Cell Host Microbe **8:**55-67.
163. **Kleiman, L., R. Halwani, and H. Javanbakht.** 2004. The selective packaging and annealing of primer tRNALys3 in HIV-1. Curr HIV Res **2:**163-75.
164. **Kobinger, G. P., D. J. Weiner, Q. C. Yu, and J. M. Wilson.** 2001. Filovirus-pseudotyped lentiviral vector can efficiently and stably transduce airway epithelia in vivo. Nat Biotechnol **19:**225-30.
165. **Kogan, M., and J. Rappaport.** 2011. HIV-1 accessory protein Vpr: relevance in the pathogenesis of HIV and potential for therapeutic intervention. Retrovirology **8:**25.
166. **Kondo, E., F. Mammano, E. A. Cohen, and H. G. Gottlinger.** 1995. The p6gag domain of human immunodeficiency virus type 1 is sufficient for the incorporation of Vpr into heterologous viral particles. J Virol **69:**2759-64.
167. **Koning, F. A., E. N. Newman, E. Y. Kim, K. J. Kunstman, S. M. Wolinsky, and M. H. Malim.** 2009. Defining APOBEC3 Expression Patterns in Human Tissues and Hematopoietic Cell Subsets. J Virol **83:**9474-85.
168. **Kozak, S. L., M. Marin, K. M. Rose, C. Bystrom, and D. Kabat.** 2006. The anti-HIV-1 editing enzyme APOBEC3G binds HIV-1 RNA and messenger RNAs that shuttle between polysomes and stress granules. J Biol Chem **281:**29105-19.
169. **Kozal, M. J.** 2009. Drug-resistant human immunodefiency virus. Clin Microbiol Infect **15 Suppl 1:**69-73.
170. **Krisko, J. F., F. Martinez-Torres, J. L. Foster, and J. V. Garcia.** 2013. HIV restriction by APOBEC3 in humanized mice. PLoS Pathog **9:**e1003242.
171. **Lachmann, N., S. Brennig, N. Pfaff, H. Schermeier, J. Dahlmann, R. Phaltane, I. Gruh, U. Modlich, A. Schambach, C. Baum, and T. Moritz.** 2012. Efficient in vivo regulation of cytidine deaminase expression in the haematopoietic system using a doxycycline-inducible lentiviral vector system. Gene Ther**:**1-10.
172. **Laguette, N., and M. Benkirane.** 2012. How SAMHD1 changes our view of viral restriction. Trends Immunol **33:**26-33.
173. **Laguette, N., B. Sobhian, N. Casartelli, M. Ringeard, C. Chable-Bessia, E. Segeral, A. Yatim, S. Emiliani, O. Schwartz, and M. Benkirane.** 2011. SAMHD1 is the dendritic- and myeloid-cell-specific HIV-1 restriction factor counteracted by Vpx. Nature **474:**654-7.

174. **Lahouassa, H., W. Daddacha, H. Hofmann, D. Ayinde, E. C. Logue, L. Dragin, N. Bloch, C. Maudet, M. Bertrand, T. Gramberg, G. Pancino, S. Priet, B. Canard, N. Laguette, M. Benkirane, C. Transy, N. R. Landau, B. Kim, and F. Margottin-Goguet.** 2012. SAMHD1 restricts the replication of human immunodeficiency virus type 1 by depleting the intracellular pool of deoxynucleoside triphosphates. Nat Immunol **13:**223-8.

175. **Lassen, K. G., A. M. Hebbeler, D. Bhattacharyya, M. A. Lobritz, and W. C. Greene.** 2012. A flexible model of HIV-1 latency permitting evaluation of many primary CD4 T-cell reservoirs. PLoS One **7:**e30176.

176. **Lavens, D., F. Peelman, J. Van der Heyden, I. Uyttendaele, D. Catteeuw, A. Verhee, B. Van Schoubroeck, J. Kurth, S. Hallenberger, R. Clayton, and J. Tavernier.** 2010. Definition of the interacting interfaces of Apobec3G and HIV-1 Vif using MAPPIT mutagenesis analysis. Nucleic Acids Res **38:**1902-12.

177. **Le Tortorec, A., and S. J. Neil.** 2009. Antagonism to and intracellular sequestration of human tetherin by the human immunodeficiency virus type 2 envelope glycoprotein. J Virol **83:**11966-78.

178. **Lecossier, D., F. Bouchonnet, F. Clavel, and A. J. Hance.** 2003. Hypermutation of HIV-1 DNA in the absence of the Vif protein. Science **300:**1112.

179. **Levesque, K., Y. S. Zhao, and E. A. Cohen.** 2003. Vpu exerts a positive effect on HIV-1 infectivity by down-modulating CD4 receptor molecules at the surface of HIV-1-producing cells. J Biol Chem **278:**28346-53.

180. **Levin, J. G., J. Guo, I. Rouzina, and K. Musier-Forsyth.** 2005. Nucleic acid chaperone activity of HIV-1 nucleocapsid protein: critical role in reverse transcription and molecular mechanism. Prog Nucleic Acid Res Mol Biol **80:**217-86.

181. **Levin, J. G., M. Mitra, A. Mascarenhas, and K. Musier-Forsyth.** 2010. Role of HIV-1 nucleocapsid protein in HIV-1 reverse transcription. RNA Biol **7:**754-74.

182. **Lewin, A. S., K. A. Drenser, W. W. Hauswirth, S. Nishikawa, D. Yasumura, J. G. Flannery, and M. M. LaVail.** 1998. Ribozyme rescue of photoreceptor cells in a transgenic rat model of autosomal dominant retinitis pigmentosa. Nat Med **4:**967-71.

183. **Li, L., H. S. Li, C. D. Pauza, M. Bukrinsky, and R. Y. Zhao.** 2005. Roles of HIV-1 auxiliary proteins in viral pathogenesis and host-pathogen interactions. Cell Res **15:**923-34.

184. **Li, L., D. Liang, J. Y. Li, and R. Y. Zhao.** 2008. APOBEC3G-UBA2 fusion as a potential strategy for stable expression of APOBEC3G and inhibition of HIV-1 replication. Retrovirology **5:**72.

185. **Li, X. Y., F. Guo, L. Zhang, L. Kleiman, and S. Cen.** 2007. APOBEC3G inhibits DNA strand transfer during HIV-1 reverse transcription. J Biol Chem **282:**32065-74.

186. **Li, Y., A. K. Kar, and J. Sodroski.** 2009. Target cell type-dependent modulation of human immunodeficiency virus type 1 capsid disassembly by cyclophilin A. J Virol **83:**10951-62.

187. **Li, Z., M. Zhang, C. Zhou, X. Zhao, N. Iijima, and F. R. Frankel.** 2008. Novel vaccination protocol with two live mucosal vectors elicits strong cell-mediated immunity in the vagina and protects against vaginal virus challenge. J Immunol **180:**2504-13.

188. **Liao, W., Z. Bao, C. Cheng, Y. K. Mok, and W. S. Wong.** 2008. Dendritic cell-derived interferon-gamma-induced protein mediates tumor necrosis factor-alpha stimulation of human lung fibroblasts. Proteomics **8:**2640-50.

189. **Lim, S. H., I. C. Liao, and K. W. Leong.** 2006. Nonviral gene delivery from nonwoven fibrous scaffolds fabricated by interfacial complexation of polyelectrolytes. Mol Ther **13:**1163-72.

190. **Lu, Y. L., P. Spearman, and L. Ratner.** 1993. Human immunodeficiency virus type 1 viral protein R localization in infected cells and virions. J Virol **67:**6542-50.

191. **Luo, K., B. Liu, Z. Xiao, Y. Yu, X. Yu, R. Gorelick, and X. F. Yu.** 2004. Amino-terminal region of the human immunodeficiency virus type 1 nucleocapsid is required for human APOBEC3G packaging. J Virol **78:**11841-52.

192. **Luo, K., T. Wang, B. Liu, C. Tian, Z. Xiao, J. Kappes, and X. F. Yu.** 2007. Cytidine deaminases APOBEC3G and APOBEC3F interact with human immunodeficiency virus type 1 integrase and inhibit proviral DNA formation. J Virol **81:**7238-48.

193. **Madani, N., and D. Kabat.** 1998. An endogenous inhibitor of human immunodeficiency virus in human lymphocytes is overcome by the viral Vif protein. J Virol **72:**10251-5.

194. **Maksakova, I. A., M. T. Romanish, L. Gagnier, C. A. Dunn, L. N. van de Lagemaat, and D. L. Mager.** 2006. Retroviral elements and their hosts: insertional mutagenesis in the mouse germ line. PLoS Genet **2:**e2.

195. **Malim, M. H.** 2009. APOBEC proteins and intrinsic resistance to HIV-1 infection. Philos

Trans R Soc Lond B Biol Sci **364:**675-87.
196. **Malim, M. H., and P. D. Bieniasz.** 2012. HIV Restriction Factors and Mechanisms of Evasion. Cold Spring Harb Perspect Med **2:**a006940.
197. **Malim, M. H., and M. Emerman.** 2008. HIV-1 accessory proteins--ensuring viral survival in a hostile environment. Cell Host Microbe **3:**388-98.
198. **Mangeat, B., P. Turelli, G. Caron, M. Friedli, L. Perrin, and D. Trono.** 2003. Broad antiretroviral defence by human APOBEC3G through lethal editing of nascent reverse transcripts. Nature **424:**99-103.
199. **Mangeat, B., P. Turelli, S. Liao, and D. Trono.** 2004. A single amino acid determinant governs the species-specific sensitivity of APOBEC3G to Vif action. J Biol Chem **279:**14481-3.
200. **Marcello, A., M. Zoppe, and M. Giacca.** 2001. Multiple modes of transcriptional regulation by the HIV-1 Tat transactivator. IUBMB Life **51:**175-81.
201. **Margolis, D. M.** 2010. Mechanisms of HIV latency: an emerging picture of complexity. Curr HIV/AIDS Rep **7:**37-43.
202. **Margottin, F., S. P. Bour, H. Durand, L. Selig, S. Benichou, V. Richard, D. Thomas, K. Strebel, and R. Benarous.** 1998. A novel human WD protein, h-beta TrCp, that interacts with HIV-1 Vpu connects CD4 to the ER degradation pathway through an F-box motif. Mol Cell **1:**565-74.
203. **Mariani, R., D. Chen, B. Schrofelbauer, F. Navarro, R. Konig, B. Bollman, C. Munk, H. Nymark-McMahon, and N. R. Landau.** 2003. Species-specific exclusion of APOBEC3G from HIV-1 virions by Vif. Cell **114:**21-31.
204. **Marin, M., K. M. Rose, S. L. Kozak, and D. Kabat.** 2003. HIV-1 Vif protein binds the editing enzyme APOBEC3G and induces its degradation. Nat Med **9:**1398-403.
205. **Marlink, R., P. Kanki, I. Thior, K. Travers, G. Eisen, T. Siby, I. Traore, C. C. Hsieh, M. C. Dia, E. H. Gueye, and et al.** 1994. Reduced rate of disease development after HIV-2 infection as compared to HIV-1. Science **265:**1587-90.
206. **Mbisa, J. L., R. Barr, J. A. Thomas, N. Vandegraaff, I. J. Dorweiler, E. S. Svarovskaia, W. L. Brown, L. M. Mansky, R. J. Gorelick, R. S. Harris, A. Engelman, and V. K. Pathak.** 2007. Human immunodeficiency virus type 1 cDNAs produced in the presence of APOBEC3G exhibit defects in plus-strand DNA transfer and integration. J Virol **81:**7099-110.
207. **Mehandru, S., M. A. Poles, K. Tenner-Racz, A. Horowitz, A. Hurley, C. Hogan, D. Boden, P. Racz, and M. Markowitz.** 2004. Primary HIV-1 infection is associated with preferential depletion of CD4+ T lymphocytes from effector sites in the gastrointestinal tract. J Exp Med **200:**761-70.
208. **Mehle, A., B. Strack, P. Ancuta, C. Zhang, M. McPike, and D. Gabuzda.** 2004. Vif overcomes the innate antiviral activity of APOBEC3G by promoting its degradation in the ubiquitin-proteasome pathway. J Biol Chem **279:**7792-8.
209. **Mehle, A., H. Wilson, C. Zhang, A. J. Brazier, M. McPike, E. Pery, and D. Gabuzda.** 2007. Identification of an APOBEC3G binding site in human immunodeficiency virus type 1 Vif and inhibitors of Vif-APOBEC3G binding. J Virol **81:**13235-41.
210. **Mehta, A., M. T. Kinter, N. E. Sherman, and D. M. Driscoll.** 2000. Molecular cloning of apobec-1 complementation factor, a novel RNA-binding protein involved in the editing of apolipoprotein B mRNA. Mol Cell Biol **20:**1846-54.
211. **Mercenne, G., S. Bernacchi, D. Richer, G. Bec, S. Henriet, J. C. Paillart, and R. Marquet.** 2010. HIV-1 Vif binds to APOBEC3G mRNA and inhibits its translation. Nucleic Acids Res **38:**633-46.
212. **Meyer-Ficca, M. L., R. G. Meyer, H. Kaiser, A. R. Brack, R. Kandolf, and J. H. Kupper.** 2004. Comparative analysis of inducible expression systems in transient transfection studies. Anal Biochem **334:**9-19.
213. **Michel, N., I. Allespach, S. Venzke, O. T. Fackler, and O. T. Keppler.** 2005. The Nef protein of human immunodeficiency virus establishes superinfection immunity by a dual strategy to downregulate cell-surface CCR5 and CD4. Curr Biol **15:**714-23.
214. **Mikhail, M., B. Wang, and N. K. Saksena.** 2003. Mechanisms involved in non-progressive HIV disease. AIDS Rev **5:**230-44.
215. **Misra, A., R. Thippeshappa, and J. T. Kimata.** 2013. Macaques as model hosts for studies of HIV-1 infection. Front Microbiol **4:**176.
216. **Mitchell, R. S., C. Katsura, M. A. Skasko, K. Fitzpatrick, D. Lau, A. Ruiz, E. B. Stephens, F. Margottin-Goguet, R. Benarous, and J. C. Guatelli.** 2009. Vpu antagonizes BST-2-mediated restriction of HIV-1 release via beta-TrCP and endo-lysosomal trafficking.

PLoS Pathog **5:**e1000450.
217. **Miyagi, E., S. Opi, H. Takeuchi, M. Khan, R. Goila-Gaur, S. Kao, and K. Strebel.** 2007. Enzymatically active APOBEC3G is required for efficient inhibition of human immunodeficiency virus type 1. J Virol **81:**13346-53.
218. **Moanna, A., R. Dunham, M. Paiardini, and G. Silvestri.** 2005. CD4+ T-cell depletion in HIV infection: killed by friendly fire? Curr HIV/AIDS Rep **2:**16-23.
219. **Monajemi, M., C. F. Woodworth, J. Benkaroun, M. Grant, and M. Larijani.** 2012. Emerging complexities of APOBEC3G action on immunity and viral fitness during HIV infection and treatment. Retrovirology **9:**35.
220. **Monie, D., R. P. Simmons, R. E. Nettles, T. L. Kieffer, Y. Zhou, H. Zhang, S. Karmon, R. Ingersoll, K. Chadwick, J. B. Margolick, T. C. Quinn, S. C. Ray, M. Wind-Rotolo, M. Miller, D. Persaud, and R. F. Siliciano.** 2005. A novel assay allows genotyping of the latent reservoir for human immunodeficiency virus type 1 in the resting CD4+ T cells of viremic patients. J Virol **79:**5185-202.
221. **Moore, J. P., and R. W. Doms.** 2003. The entry of entry inhibitors: a fusion of science and medicine. Proc Natl Acad Sci U S A **100:**10598-602.
222. **Muckenfuss, H., J. K. Kaiser, E. Krebil, M. Battenberg, C. Schwer, K. Cichutek, C. Munk, and E. Flory.** 2007. Sp1 and Sp3 regulate basal transcription of the human APOBEC3G gene. Nucleic Acids Res **35:**3784-96.
223. **Muller, B., U. Tessmer, U. Schubert, and H. G. Krausslich.** 2000. Human immunodeficiency virus type 1 Vpr protein is incorporated into the virion in significantly smaller amounts than gag and is phosphorylated in infected cells. J Virol **74:**9727-31.
224. **Muramatsu, M., K. Kinoshita, S. Fagarasan, S. Yamada, Y. Shinkai, and T. Honjo.** 2000. Class switch recombination and hypermutation require activation-induced cytidine deaminase (AID), a potential RNA editing enzyme. Cell **102:**553-63.
225. **Muranyi, W., S. Malkusch, B. Muller, M. Heilemann, and H. G. Krausslich.** 2013. Super-resolution microscopy reveals specific recruitment of HIV-1 envelope proteins to viral assembly sites dependent on the envelope C-terminal tail. PLoS Pathog **9:**e1003198.
226. **Muriaux, D., and J. L. Darlix.** 2010. Properties and functions of the nucleocapsid protein in virus assembly. RNA Biol **7:**744-53.
227. **Nakatani, Y., and V. Ogryzko.** 2003. Immunoaffinity purification of mammalian protein complexes. Methods Enzymol **370:**430-44.
228. **Narvaiza, I., S. Landry, and M. D. Weitzman.** 2012. APOBEC3 proteins and genomic stability: the high cost of a good defense. Cell Cycle **11:**33-8.
229. **Narvaiza, I., D. C. Linfesty, B. N. Greener, Y. Hakata, D. J. Pintel, E. Logue, N. R. Landau, and M. D. Weitzman.** 2009. Deaminase-independent inhibition of parvoviruses by the APOBEC3A cytidine deaminase. PLoS Pathog **5:**e1000439.
230. **Nathans, R., H. Cao, N. Sharova, A. Ali, M. Sharkey, R. Stranska, M. Stevenson, and T. M. Rana.** 2008. Small-molecule inhibition of HIV-1 Vif. Nat Biotechnol **26:**1187-92.
231. **Navarro, F., B. Bollman, H. Chen, R. Konig, Q. Yu, K. Chiles, and N. R. Landau.** 2005. Complementary function of the two catalytic domains of APOBEC3G. Virology **333:**374-86.
232. **Nazari, R., and S. Joshi.** 2009. HIV-1 gene therapy at pre-integration and provirus DNA levels. Curr Gene Ther **9:**20-5.
233. **Neagu, M. R., P. Ziegler, T. Pertel, C. Strambio-De-Castillia, C. Grutter, G. Martinetti, L. Mazzucchelli, M. Grutter, M. G. Manz, and J. Luban.** 2009. Potent inhibition of HIV-1 by TRIM5-cyclophilin fusion proteins engineered from human components. J Clin Invest **119:**3035-47.
234. **Neil, S., and P. Bieniasz.** 2009. Human immunodeficiency virus, restriction factors, and interferon. J Interferon Cytokine Res **29:**569-80.
235. **Neil, S. J., S. W. Eastman, N. Jouvenet, and P. D. Bieniasz.** 2006. HIV-1 Vpu promotes release and prevents endocytosis of nascent retrovirus particles from the plasma membrane. PLoS Pathog **2:**e39.
236. **Neil, S. J., T. Zang, and P. D. Bieniasz.** 2008. Tetherin inhibits retrovirus release and is antagonized by HIV-1 Vpu. Nature **451:**425-30.
237. **Newman, E. N., R. K. Holmes, H. M. Craig, K. C. Klein, J. R. Lingappa, M. H. Malim, and A. M. Sheehy.** 2005. Antiviral function of APOBEC3G can be dissociated from cytidine deaminase activity. Curr Biol **15:**166-70.
238. **Nguyen, D. H., S. Gummuluru, and J. Hu.** 2007. Deamination-independent inhibition of hepatitis B virus reverse transcription by APOBEC3G. J Virol **81:**4465-72.
239. **Nguyen, D. H., and J. Hu.** 2008. Reverse transcriptase- and RNA packaging signal-dependent

incorporation of APOBEC3G into hepatitis B virus nucleocapsids. J Virol **82:**6852-61.

240. **Nguyen, K. L., M. llano, H. Akari, E. Miyagi, E. M. Poeschla, K. Strebel, and S. Bour.** 2004. Codon optimization of the HIV-1 vpu and vif genes stabilizes their mRNA and allows for highly efficient Rev-independent expression. Virology **319:**163-75.
241. **Noe, A., J. Plum, and C. Verhofstede.** 2005. The latent HIV-1 reservoir in patients undergoing HAART: an archive of pre-HAART drug resistance. J Antimicrob Chemother **55:**410-2.
242. **Noguchi, C., N. Hiraga, N. Mori, M. Tsuge, M. Imamura, S. Takahashi, Y. Fujimoto, H. Ochi, H. Abe, T. Maekawa, H. Yatsuji, K. Shirakawa, A. Takaori-Kondo, and K. Chayama.** 2007. Dual effect of APOBEC3G on Hepatitis B virus. J Gen Virol **88:**432-40.
243. **Noguchi, C., H. Ishino, M. Tsuge, Y. Fujimoto, M. Imamura, S. Takahashi, and K. Chayama.** 2005. G to A hypermutation of hepatitis B virus. Hepatology **41:**626-33.
244. **Nolan, D., P. Reiss, and S. Mallal.** 2005. Adverse effects of antiretroviral therapy for HIV infection: a review of selected topics. Expert Opin Drug Saf **4:**201-18.
245. **Norman, J. M., M. Mashiba, L. A. McNamara, A. Onafuwa-Nuga, E. Chiari-Fort, W. Shen, and K. L. Collins.** 2011. The antiviral factor APOBEC3G enhances the recognition of HIV-infected primary T cells by natural killer cells. Nat Immunol **12:**975-83.
246. **Nowarski, R., E. Britan-Rosich, T. Shiloach, and M. Kotler.** 2008. Hypermutation by intersegmental transfer of APOBEC3G cytidine deaminase. Nat Struct Mol Biol **15:**1059-66.
247. **O'Donovan, D., K. Ariyoshi, P. Milligan, M. Ota, L. Yamuah, R. Sarge-Njie, and H. Whittle.** 2000. Maternal plasma viral RNA levels determine marked differences in mother-to-child transmission rates of HIV-1 and HIV-2 in The Gambia. MRC/Gambia Government/University College London Medical School working group on mother-child transmission of HIV. AIDS **14:**441-8.
248. **Onafuwa-Nuga, A. A., A. Telesnitsky, and S. R. King.** 2006. 7SL RNA, but not the 54-kd signal recognition particle protein, is an abundant component of both infectious HIV-1 and minimal virus-like particles. RNA **12:**542-6.
249. **Opi, S., S. Kao, R. Goila-Gaur, M. A. Khan, E. Miyagi, H. Takeuchi, and K. Strebel.** 2007. Human immunodeficiency virus type 1 Vif inhibits packaging and antiviral activity of a degradation-resistant APOBEC3G variant. J Virol **81:**8236-46.
250. **Opi, S., H. Takeuchi, S. Kao, M. A. Khan, E. Miyagi, R. Goila-Gaur, Y. Iwatani, J. G. Levin, and K. Strebel.** 2006. Monomeric APOBEC3G is catalytically active and has antiviral activity. J Virol **80:**4673-82.
251. **Ott, D. E., L. V. Coren, B. P. Kane, L. K. Busch, D. G. Johnson, R. C. Sowder, 2nd, E. N. Chertova, L. O. Arthur, and L. E. Henderson.** 1996. Cytoskeletal proteins inside human immunodeficiency virus type 1 virions. J Virol **70:**7734-43.
252. **Ott, M., M. Geyer, and Q. Zhou.** 2011. The control of HIV transcription: keeping RNA polymerase II on track. Cell Host Microbe **10:**426-35.
253. **Pace, M. J., E. H. Graf, L. M. Agosto, A. M. Mexas, F. Male, T. Brady, F. D. Bushman, and U. O'Doherty.** 2012. Directly infected resting CD4+T cells can produce HIV Gag without spreading infection in a model of HIV latency. PLoS Pathog **8:**e1002818.
254. **Paiardini, M., I. Frank, I. Pandrea, C. Apetrei, and G. Silvestri.** 2008. Mucosal immune dysfunction in AIDS pathogenesis. AIDS Rev **10:**36-46.
255. **Pandrea, I., G. Silvestri, R. Onanga, R. S. Veazey, P. A. Marx, V. Hirsch, and C. Apetrei.** 2006. Simian immunodeficiency viruses replication dynamics in African non-human primate hosts: common patterns and species-specific differences. J Med Primatol **35:**194-201.
256. **Panos, G., G. Samonis, V. G. Alexiou, G. A. Kavarnou, G. Charatsis, and M. E. Falagas.** 2008. Mortality and morbidity of HIV infected patients receiving HAART: a cohort study. Curr HIV Res **6:**257-60.
257. **Peeters, M., A. Gueye, S. Mboup, F. Bibollet-Ruche, E. Ekaza, C. Mulanga, R. Ouedrago, R. Gandji, P. Mpele, G. Dibanga, B. Koumare, M. Saidou, E. Esu-Williams, J. P. Lombart, W. Badombena, N. Luo, M. Vanden Haesevelde, and E. Delaporte.** 1997. Geographical distribution of HIV-1 group O viruses in Africa. AIDS **11:**493-8.
258. **Perez-Caballero, D., T. Zang, A. Ebrahimi, M. W. McNatt, D. A. Gregory, M. C. Johnson, and P. D. Bieniasz.** 2009. Tetherin inhibits HIV-1 release by directly tethering virions to cells. Cell **139:**499-511.
259. **Pertel, T., S. Hausmann, D. Morger, S. Zuger, J. Guerra, J. Lascano, C. Reinhard, F. A. Santoni, P. D. Uchil, L. Chatel, A. Bisiaux, M. L. Albert, C. Strambio-De-Castillia, W. Mothes, M. Pizzato, M. G. Grutter, and J. Luban.** 2011. TRIM5 is an innate immune sensor for the retrovirus capsid lattice. Nature **472:**361-5.

260. **Pery, E., K. S. Rajendran, A. J. Brazier, and D. Gabuzda.** 2009. Regulation of APOBEC3 proteins by a novel YXXL motif in human immunodeficiency virus type 1 Vif and simian immunodeficiency virus SIVagm Vif. J Virol **83:**2374-81.
261. **Petersen-Mahrt, S.** 2005. DNA deamination in immunity. Immunol Rev **203:**80-97.
262. **Peytavi, R., S. S. Hong, B. Gay, A. D. d'Angeac, L. Selig, S. Benichou, R. Benarous, and P. Boulanger.** 1999. HEED, the product of the human homolog of the murine eed gene, binds to the matrix protein of HIV-1. J Biol Chem **274:**1635-45.
263. **Phillips, A. N., D. Dunn, C. Sabin, A. Pozniak, R. Matthias, A. M. Geretti, J. Clarke, D. Churchill, I. Williams, T. Hill, H. Green, K. Porter, G. Scullard, M. Johnson, P. Easterbrook, R. Gilson, M. Fisher, C. Loveday, B. Gazzard, and D. Pillay.** 2005. Long term probability of detection of HIV-1 drug resistance after starting antiretroviral therapy in routine clinical practice. AIDS **19:**487-94.
264. **Pillai, S. K., M. Abdel-Mohsen, J. Guatelli, M. Skasko, A. Monto, K. Fujimoto, S. Yukl, W. C. Greene, H. Kovari, A. Rauch, J. Fellay, M. Battegay, B. Hirschel, A. Witteck, E. Bernasconi, B. Ledergerber, H. F. Gunthard, and J. K. Wong.** 2012. Role of retroviral restriction factors in the interferon-alpha-mediated suppression of HIV-1 in vivo. Proc Natl Acad Sci U S A **109:**3035-40.
265. **Plantier, J. C., M. Leoz, J. E. Dickerson, F. De Oliveira, F. Cordonnier, V. Lemee, F. Damond, D. L. Robertson, and F. Simon.** 2009. A new human immunodeficiency virus derived from gorillas. Nat Med **15:**871-2.
266. **Ponnazhagan, S., D. T. Curiel, D. R. Shaw, R. D. Alvarez, and G. P. Siegal.** 2001. Adeno-associated virus for cancer gene therapy. Cancer Res **61:**6313-21.
267. **Popovic, M., M. G. Sarngadharan, E. Read, and R. C. Gallo.** 1984. Detection, isolation, and continuous production of cytopathic retroviruses (HTLV-III) from patients with AIDS and pre-AIDS. Science **224:**497-500.
268. **Popper, S. J., A. D. Sarr, K. U. Travers, A. Gueye-Ndiaye, S. Mboup, M. E. Essex, and P. J. Kanki.** 1999. Lower human immunodeficiency virus (HIV) type 2 viral load reflects the difference in pathogenicity of HIV-1 and HIV-2. J Infect Dis **180:**1116-21.
269. **Prasad, V. R., and S. P. Goff.** 1990. Structure-function studies of HIV reverse transcriptase. Ann N Y Acad Sci **616:**11-21.
270. **Refsland, E. W., M. D. Stenglein, K. Shindo, J. S. Albin, W. L. Brown, and R. S. Harris.** 2010. Quantitative profiling of the full APOBEC3 mRNA repertoire in lymphocytes and tissues: implications for HIV-1 restriction. Nucleic Acids Res **38:**4274-84.
271. **Restle, T., B. Muller, and R. S. Goody.** 1990. Dimerization of human immunodeficiency virus type 1 reverse transcriptase. A target for chemotherapeutic intervention. J Biol Chem **265:**8986-8.
272. **Restle, T., B. Muller, and R. S. Goody.** 1992. RNase H activity of HIV reverse transcriptases is confined exclusively to the dimeric forms. FEBS Lett **300:**97-100.
273. **Reuman, E. C., S. Margeridon-Thermet, H. B. Caudill, T. Liu, K. Borroto-Esoda, E. S. Svarovskaia, S. P. Holmes, and R. W. Shafer.** 2010. A classification model for G-to-A hypermutation in hepatitis B virus ultra-deep pyrosequencing reads. Bioinformatics **26:**2929-32.
274. **Robertson, D. L., J. P. Anderson, J. A. Bradac, J. K. Carr, B. Foley, R. K. Funkhouser, F. Gao, B. H. Hahn, M. L. Kalish, C. Kuiken, G. H. Learn, T. Leitner, F. McCutchan, S. Osmanov, M. Peeters, D. Pieniazek, M. Salminen, P. M. Sharp, S. Wolinsky, and B. Korber.** 2000. HIV-1 nomenclature proposal. Science **288:**55-6.
275. **Rogozin, I. B., M. K. Basu, I. K. Jordan, Y. I. Pavlov, and E. V. Koonin.** 2005. APOBEC4, a new member of the AID/APOBEC family of polynucleotide (deoxy)cytidine deaminases predicted by computational analysis. Cell Cycle **4:**1281-5.
276. **Romani, B., S. Engelbrecht, and R. H. Glashoff.** 2009. Antiviral roles of APOBEC proteins against HIV-1 and suppression by Vif. Arch Virol **154:**1579-88.
277. **Ross, D. D., C. C. Joneckis, J. V. Ordonez, A. M. Sisk, R. K. Wu, A. W. N. R. E. Hamburger, and R. E. Nora.** 1989. Estimation of cell survival by flow cytometric quantification of fluorescein diacetate/propidium iodide viable cell number. Cancer Res **49:**3776-82.
278. **Rossi, J. J., C. H. June, and D. B. Kohn.** 2007. Genetic therapies against HIV. Nat Biotechnol **25:**1444-54.
279. **Rulli, S. J., Jr., C. S. Hibbert, J. Mirro, T. Pederson, S. Biswal, and A. Rein.** 2007. Selective and nonselective packaging of cellular RNAs in retrovirus particles. J Virol **81:**6623-31.

280. **Russell, R. A., and V. K. Pathak.** 2007. Identification of two distinct human immunodeficiency virus type 1 Vif determinants critical for interactions with human APOBEC3G and APOBEC3F. J Virol **81:**8201-10.
281. **Sabatier, J. M., E. Vives, K. Mabrouk, A. Benjouad, H. Rochat, A. Duval, B. Hue, and E. Bahraoui.** 1991. Evidence for neurotoxic activity of tat from human immunodeficiency virus type 1. J Virol **65:**961-7.
282. **Santa-Marta, M., F. A. da Silva, A. M. Fonseca, and J. Goncalves.** 2005. HIV-1 Vif can directly inhibit apolipoprotein B mRNA-editing enzyme catalytic polypeptide-like 3G-mediated cytidine deamination by using a single amino acid interaction and without protein degradation. J Biol Chem **280:**8765-75.
283. **Sarafianos, S. G., B. Marchand, K. Das, D. M. Himmel, M. A. Parniak, S. H. Hughes, and E. Arnold.** 2009. Structure and function of HIV-1 reverse transcriptase: molecular mechanisms of polymerization and inhibition. J Mol Biol **385:**693-713.
284. **Sarkis, P. T., S. Ying, R. Xu, and X. F. Yu.** 2006. STAT1-independent cell type-specific regulation of antiviral APOBEC3G by IFN-alpha. J Immunol **177:**4530-40.
285. **Sasada, A., A. Takaori-Kondo, K. Shirakawa, M. Kobayashi, A. Abudu, M. Hishizawa, K. Imada, Y. Tanaka, and T. Uchiyama.** 2005. APOBEC3G targets human T-cell leukemia virus type 1. Retrovirology **2:**32.
286. **Sastry, L., T. Johnson, M. J. Hobson, B. Smucker, and K. Cornetta.** 2002. Titering lentiviral vectors: comparison of DNA, RNA and marker expression methods. Gene Ther **9:**1155-62.
287. **Sayah, D. M., E. Sokolskaja, L. Berthoux, and J. Luban.** 2004. Cyclophilin A retrotransposition into TRIM5 explains owl monkey resistance to HIV-1. Nature **430:**569-73.
288. **Schafer, A., H. P. Bogerd, and B. R. Cullen.** 2004. Specific packaging of APOBEC3G into HIV-1 virions is mediated by the nucleocapsid domain of the gag polyprotein precursor. Virology **328:**163-8.
289. **Scherer, L. J., and J. J. Rossi.** 2011. Ex vivo gene therapy for HIV-1 treatment. Hum Mol Genet **20:**R100-7.
290. **Schrofelbauer, B., D. Chen, and N. R. Landau.** 2004. A single amino acid of APOBEC3G controls its species-specific interaction with virion infectivity factor (Vif). Proc Natl Acad Sci U S A **101:**3927-32.
291. **Schrofelbauer, B., T. Senger, G. Manning, and N. R. Landau.** 2006. Mutational alteration of human immunodeficiency virus type 1 Vif allows for functional interaction with nonhuman primate APOBEC3G. J Virol **80:**5984-91.
292. **Schumacher, A. J., G. Hache, D. A. Macduff, W. L. Brown, and R. S. Harris.** 2008. The DNA deaminase activity of human APOBEC3G is required for Ty1, MusD, and human immunodeficiency virus type 1 restriction. J Virol **82:**2652-60.
293. **Senavirathne, G., M. Jaszczur, P. A. Auerbach, T. G. Upton, L. Chelico, M. F. Goodman, and D. Rueda.** 2012. Single-stranded DNA scanning and deamination by APOBEC3G cytidine deaminase at single molecule resolution. J Biol Chem **287:**15826-35.
294. **Shandilya, S. M., M. N. Nalam, E. A. Nalivaika, P. J. Gross, J. C. Valesano, K. Shindo, M. Li, M. Munson, W. E. Royer, E. Harjes, T. Kono, H. Matsuo, R. S. Harris, M. Somasundaran, and C. A. Schiffer.** 2010. Crystal structure of the APOBEC3G catalytic domain reveals potential oligomerization interfaces. Structure **18:**28-38.
295. **Sharp, P. M., and B. H. Hahn.** 2008. AIDS: prehistory of HIV-1. Nature **455:**605-6.
296. **Sheehy, A. M., N. C. Gaddis, J. D. Choi, and M. H. Malim.** 2002. Isolation of a human gene that inhibits HIV-1 infection and is suppressed by the viral Vif protein. Nature **418:**646-50.
297. **Sheehy, A. M., N. C. Gaddis, and M. H. Malim.** 2003. The antiretroviral enzyme APOBEC3G is degraded by the proteasome in response to HIV-1 Vif. Nat Med **9:**1404-7.
298. **Shi, J., J. Zhou, V. B. Shah, C. Aiken, and K. Whitby.** 2011. Small-molecule inhibition of human immunodeficiency virus type 1 infection by virus capsid destabilization. J Virol **85:**542-9.
299. **Shindo, K., A. Takaori-Kondo, M. Kobayashi, A. Abudu, K. Fukunaga, and T. Uchiyama.** 2003. The enzymatic activity of CEM15/Apobec-3G is essential for the regulation of the infectivity of HIV-1 virion but not a sole determinant of its antiviral activity. J Biol Chem **278:**44412-6.
300. **Shirakawa, K., A. Takaori-Kondo, M. Yokoyama, T. Izumi, M. Matsui, K. Io, T. Sato, H. Sato, and T. Uchiyama.** 2008. Phosphorylation of APOBEC3G by protein kinase A regulates its interaction with HIV-1 Vif. Nat Struct Mol Biol **15:**1184-91.
301. **Shoeman, R. L., C. Huttermann, R. Hartig, and P. Traub.** 2001. Amino-terminal

polypeptides of vimentin are responsible for the changes in nuclear architecture associated with human immunodeficiency virus type 1 protease activity in tissue culture cells. Mol Biol Cell **12:**143-54.

302. **Siliciano, R. F., and W. C. Greene.** 2011. HIV latency. Cold Spring Harb Perspect Med **1:**a007096.
303. **Simon, F., P. Mauclere, P. Roques, I. Loussert-Ajaka, M. C. Muller-Trutwin, S. Saragosti, M. C. Georges-Courbot, F. Barre-Sinoussi, and F. Brun-Vezinet.** 1998. Identification of a new human immunodeficiency virus type 1 distinct from group M and group O. Nat Med **4:**1032-7.
304. **Simon, J. H. M., and M. H. Malim.** 1996. The human immunodeficiency virus type 1 Vif protein modulates the postpenetration stability of viral nucleoprotein complexes. J. Virol. **70:**5297-5305.
305. **Sloan, R. D., D. A. Donahue, B. D. Kuhl, T. Bar-Magen, and M. A. Wainberg.** 2010. Expression of Nef from unintegrated HIV-1 DNA downregulates cell surface CXCR4 and CCR5 on T-lymphocytes. Retrovirology **7:**44.
306. **Sloan, R. D., and M. A. Wainberg.** 2013. Harnessing the therapeutic potential of host antiviral restriction factors that target HIV. Expert Rev Anti Infect Ther **11:**1-4.
307. **Sodora, D. L., J. S. Allan, C. Apetrei, J. M. Brenchley, D. C. Douek, J. G. Else, J. D. Estes, B. H. Hahn, V. M. Hirsch, A. Kaur, F. Kirchhoff, M. Muller-Trutwin, I. Pandrea, J. E. Schmitz, and G. Silvestri.** 2009. Toward an AIDS vaccine: lessons from natural simian immunodeficiency virus infections of African nonhuman primate hosts. Nat Med **15:**861-5.
308. **Soros, V. B., W. Yonemoto, and W. C. Greene.** 2007. Newly synthesized APOBEC3G is incorporated into HIV virions, inhibited by HIV RNA, and subsequently activated by RNase H. PLoS Pathog **3:**e15.
309. **Stenglein, M. D., H. Matsuo, and R. S. Harris.** 2008. Two regions within the amino-terminal half of APOBEC3G cooperate to determine cytoplasmic localization. J Virol **82:**9591-9.
310. **Stopak, K., C. de Noronha, W. Yonemoto, and W. C. Greene.** 2003. HIV-1 Vif blocks the antiviral activity of APOBEC3G by impairing both its translation and intracellular stability. Mol Cell **12:**591-601.
311. **Strack, P. R., M. W. Frey, C. J. Rizzo, B. Cordova, H. J. George, R. Meade, S. P. Ho, J. Corman, R. Tritch, and B. D. Korant.** 1996. Apoptosis mediated by HIV protease is preceded by cleavage of Bcl-2. Proc Natl Acad Sci U S A **93:**9571-6.
312. **Strayer, D. S., R. Akkina, B. A. Bunnell, B. Dropulic, V. Planelles, R. J. Pomerantz, J. J. Rossi, and J. A. Zaia.** 2005. Current status of gene therapy strategies to treat HIV/AIDS. Mol Ther **11:**823-42.
313. **Strebel, K.** 2005. APOBEC3G & HTLV-1: inhibition without deamination. Retrovirology **2:**37.
314. **Strebel, K., and M. A. Khan.** 2008. APOBEC3G encapsidation into HIV-1 virions: which RNA is it? Retrovirology **5:**55.
315. **Stremlau, M., C. M. Owens, M. J. Perron, M. Kiessling, P. Autissier, and J. Sodroski.** 2004. The cytoplasmic body component TRIM5alpha restricts HIV-1 infection in Old World monkeys. Nature **427:**848-53.
316. **Sui, Y., Q. Zhu, S. Gagnon, A. Dzutsev, M. Terabe, M. Vaccari, D. Venzon, D. Klinman, W. Strober, B. Kelsall, G. Franchini, I. M. Belyakov, and J. A. Berzofsky.** 2010. Innate and adaptive immune correlates of vaccine and adjuvant-induced control of mucosal transmission of SIV in macaques. Proc Natl Acad Sci U S A **107:**9843-8.
317. **Sunseri, N., M. O'Brien, N. Bhardwaj, and N. R. Landau.** 2011. Human immunodeficiency virus type 1 modified to package Simian immunodeficiency virus Vpx efficiently infects macrophages and dendritic cells. J Virol **85:**6263-74.
318. **Suspene, R., C. Rusniok, J. P. Vartanian, and S. Wain-Hobson.** 2006. Twin gradients in APOBEC3 edited HIV-1 DNA reflect the dynamics of lentiviral replication. Nucleic Acids Res **34:**4677-84.
319. **Suzuki, Y., and R. Craigie.** 2007. The road to chromatin - nuclear entry of retroviruses. Nat Rev Microbiol **5:**187-96.
320. **Svarovskaia, E. S., H. Xu, J. L. Mbisa, R. Barr, R. J. Gorelick, A. Ono, E. O. Freed, W. S. Hu, and V. K. Pathak.** 2004. Human apolipoprotein B mRNA-editing enzyme-catalytic polypeptide-like 3G (APOBEC3G) is incorporated into HIV-1 virions through interactions with viral and nonviral RNAs. J Biol Chem **279:**35822-8.
321. **Swiggard, W. J., C. Baytop, J. J. Yu, J. Dai, C. Li, R. Schretzenmair, T. Theodosopoulos, and U. O'Doherty.** 2005. Human immunodeficiency virus type 1 can establish latent infection

in resting CD4+ T cells in the absence of activating stimuli. J Virol **79:**14179-88.
322. **Tanaka, M., T. Ueno, T. Nakahara, K. Sasaki, A. Ishimoto, and H. Sakai.** 2003. Downregulation of CD4 is required for maintenance of viral infectivity of HIV-1. Virology **311:**316-25.
323. **Taylor, B. S., and S. M. Hammer.** 2008. The challenge of HIV-1 subtype diversity. N Engl J Med **359:**1965-6.
324. **Tisdale, M., P. Ertl, B. A. Larder, D. J. Purifoy, G. Darby, and K. L. Powell.** 1988. Characterization of human immunodeficiency virus type 1 reverse transcriptase by using monoclonal antibodies: role of the C terminus in antibody reactivity and enzyme function. J Virol **62:**3662-7.
325. **Turelli, P., B. Mangeat, S. Jost, S. Vianin, and D. Trono.** 2004. Inhibition of hepatitis B virus replication by APOBEC3G. Science **303:**1829.
326. **Turner, B. G., and M. F. Summers.** 1999. Structural biology of HIV. J Mol Biol **285:**1-32.
327. **Usami, Y., S. Popov, E. Popova, M. Inoue, W. Weissenhorn, and G. G. H.** 2009. The ESCRT pathway and HIV-1 budding. Biochem Soc Trans **37:**181-4.
328. **Vallari, A., P. Bodelle, C. Ngansop, F. Makamche, N. Ndembi, D. Mbanya, L. Kaptue, L. G. Gurtler, C. P. McArthur, S. G. Devare, and C. A. Brennan.** 2010. Four new HIV-1 group N isolates from Cameroon: Prevalence continues to be low. AIDS Res Hum Retroviruses **26:**109-15.
329. **Vallari, A., V. Holzmayer, B. Harris, J. Yamaguchi, C. Ngansop, F. Makamche, D. Mbanya, L. Kaptue, N. Ndembi, L. Gurtler, S. Devare, and C. A. Brennan.** 2010. Confirmation of putative HIV-1 group P in Cameroon. J Virol **85:**1403-7.
330. **Van Maele, B., and Z. Debyser.** 2005. HIV-1 integration: an interplay between HIV-1 integrase, cellular and viral proteins. AIDS Rev **7:**26-43.
331. **Venzke, S., N. Michel, I. Allespach, O. T. Fackler, and O. T. Keppler.** 2006. Expression of Nef downregulates CXCR4, the major coreceptor of human immunodeficiency virus, from the surfaces of target cells and thereby enhances resistance to superinfection. J Virol **80:**11141-52.
332. **Virgen, C. A., and T. Hatziioannou.** 2007. Antiretroviral activity and Vif sensitivity of rhesus macaque APOBEC3 proteins. J Virol **81:**13932-7.
333. **von Schwedler, U., R. S. Kornbluth, and D. Trono.** 1994. The nuclear localization signal of the matrix protein of human immunodeficiency virus type 1 allows the establishment of infection in macrophages and quiescent T lymphocytes. Proc Natl Acad Sci U S A **91:**6992-6.
334. **Walker, B. D., and D. R. Burton.** 2008. Toward an AIDS vaccine. Science **320:**760-4.
335. **Wang, T., C. Tian, W. Zhang, K. Luo, P. T. Sarkis, L. Yu, B. Liu, Y. Yu, and X. F. Yu.** 2007. 7SL RNA mediates virion packaging of the antiviral cytidine deaminase APOBEC3G. J Virol **81:**13112-24.
336. **Wang, X., Z. Ao, L. Chen, G. Kobinger, J. Peng, and X. Yao.** 2012. The cellular antiviral protein APOBEC3G interacts with HIV-1 reverse transcriptase and inhibits its function during viral replication. J Virol **86:**3777-86.
337. **Wang, X., Y. Han, Y. Dang, W. Fu, T. Zhou, R. G. Ptak, and Y. H. Zheng.** 2010. Moloney leukemia virus 10 (MOV10) protein inhibits retrovirus replication. J Biol Chem **285:**14346-55.
338. **Wang, Y., L. A. Bergmeier, R. Stebbings, T. Seidl, T. Whittall, M. Singh, N. Berry, N. Almond, and T. Lehner.** 2009. Mucosal immunization in macaques upregulates the innate APOBEC 3G anti-viral factor in CD4(+) memory T cells. Vaccine **27:**870-81.
339. **Wang, Y., T. Whittall, D. Rahman, E. M. Bunnik, R. Vaughan, J. Scholler, L. A. Bergmeier, D. Montefiori, M. Singh, H. Schuitemaker, and T. Lehner.** 2012. The role of innate APOBEC3G and adaptive AID immune responses in HLA-HIV/SIV immunized SHIV infected macaques. PLoS One **7:**e34433.
340. **Watts, J. M., K. K. Dang, R. J. Gorelick, C. W. Leonard, J. W. Bess, Jr., R. Swanstrom, C. L. Burch, and K. M. Weeks.** 2009. Architecture and secondary structure of an entire HIV-1 RNA genome. Nature **460:**711-6.
341. **Wayengera, M.** 2011. Proviral HIV-genome-wide and pol-gene specific zinc finger nucleases: usability for targeted HIV gene therapy. Theor Biol Med Model **8:**26.
342. **White, T. E., A. Brandariz-Nunez, J. C. Valle-Casuso, S. Amie, L. Nguyen, B. Kim, J. Brojatsch, and F. Diaz-Griffero.** 2013. Contribution of SAM and HD domains to retroviral restriction mediated by human SAMHD1. Virology **436:**81-90.
343. **Wilen, C. B., J. C. Tilton, and R. W. Doms.** 2012. HIV: cell binding and entry. Cold Spring Harb Perspect Med **2**.
344. **Wilkinson, K. A., R. J. Gorelick, S. M. Vasa, N. Guex, A. Rein, D. H. Mathews, M. C.**

**Giddings, and K. M. Weeks.** 2008. High-throughput SHAPE analysis reveals structures in HIV-1 genomic RNA strongly conserved across distinct biological states. PLoS Biol **6:**e96.

345. **Worobey, M., P. Telfer, S. Souquiere, M. Hunter, C. A. Coleman, M. J. Metzger, P. Reed, M. Makuwa, G. Hearn, S. Honarvar, P. Roques, C. Apetrei, M. Kazanji, and P. A. Marx.** 2010. Island biogeography reveals the deep history of SIV. Science **329:**1487.
346. **Wu, X., H. Liu, H. Xiao, J. A. Conway, E. Hehl, G. V. Kalpana, V. Prasad, and J. C. Kappes.** 1999. Human immunodeficiency virus type 1 integrase protein promotes reverse transcription through specific interactions with the nucleoprotein reverse transcription complex. J Virol **73:**2126-35.
347. **Wyatt, R., and J. Sodroski.** 1998. The HIV-1 envelope glycoproteins: fusogens, antigens, and immunogens. Science **280:**1884-8.
348. **Xiao, W., S. C. Berta, M. M. Lu, A. D. Moscioni, J. Tazelaar, and J. M. Wilson.** 1998. Adeno-associated virus as a vector for liver-directed gene therapy. J Virol **72:**10222-6.
349. **Xin, K. Q., H. Mizukami, M. Urabe, Y. Toda, K. Shinoda, A. Yoshida, K. Oomura, Y. Kojima, M. Ichino, D. Klinman, K. Ozawa, and K. Okuda.** 2006. Induction of robust immune responses against human immunodeficiency virus is supported by the inherent tropism of adeno-associated virus type 5 for dendritic cells. J Virol **80:**11899-910.
350. **Xin, K. Q., T. Ooki, H. Mizukami, K. Hamajima, K. Okudela, K. Hashimoto, Y. Kojima, N. Jounai, Y. Kumamoto, S. Sasaki, D. Klinman, K. Ozawa, and K. Okuda.** 2002. Oral administration of recombinant adeno-associated virus elicits human immunodeficiency virus-specific immune responses. Hum Gene Ther **13:**1571-81.
351. **Xu, H., E. Chertova, J. Chen, D. E. Ott, J. D. Roser, W. S. Hu, and V. K. Pathak.** 2007. Stoichiometry of the antiviral protein APOBEC3G in HIV-1 virions. Virology **360:**247-56.
352. **Xu, H., E. S. Svarovskaia, R. Barr, Y. Zhang, M. A. Khan, K. Strebel, and V. K. Pathak.** 2004. A single amino acid substitution in human APOBEC3G antiretroviral enzyme confers resistance to HIV-1 virion infectivity factor-induced depletion. Proc Natl Acad Sci U S A **101:**5652-7.
353. **Yang, O. O., P. T. Nguyen, S. A. Kalams, T. Dorfman, H. G. Gottlinger, S. Stewart, I. S. Chen, S. Threlkeld, and B. D. Walker.** 2002. Nef-mediated resistance of human immunodeficiency virus type 1 to antiviral cytotoxic T lymphocytes. J Virol **76:**1626-31.
354. **Yang, Y., F. Guo, S. Cen, and L. Kleiman.** 2007. Inhibition of initiation of reverse transcription in HIV-1 by human APOBEC3F. Virology **365:**92-100.
355. **Yao, X. J., J. Friborg, F. Checroune, S. Gratton, F. Boisvert, R. P. Sekaly, and E. A. Cohen.** 1995. Degradation of CD4 induced by human immunodeficiency virus type 1 Vpu protein: a predicted alpha-helix structure in the proximal cytoplasmic region of CD4 contributes to Vpu sensitivity. Virology **209:**615-23.
356. **Yao, X. J., G. Kobinger, S. Dandache, N. Rougeau, and E. Cohen.** 1999. HIV-1 Vpr-chloramphenicol acetyltransferase fusion proteins: sequence requirement for virion incorporation and analysis of antiviral effect. Gene Ther **6:**1590-9.
357. **Yao, X. J., A. J. Mouland, R. A. Subbramanian, J. Forget, N. Rougeau, D. Bergeron, and E. A. Cohen.** 1998. Vpr stimulates viral expression and induces cell killing in human immunodeficiency virus type 1-infected dividing Jurkat T cells. J Virol **72:**4686-93.
358. **Yao, X. J., R. A. Subbramanian, N. Rougeau, F. Boisvert, D. Bergeron, and E. A. Cohen.** 1995. Mutagenic analysis of human immunodeficiency virus type 1 Vpr: role of a predicted N-terminal alpha-helical structure in Vpr nuclear localization and virion incorporation. J Virol **69:**7032-44.
359. **Yap, M. W., S. Nisole, and J. P. Stoye.** 2005. A single amino acid change in the SPRY domain of human Trim5alpha leads to HIV-1 restriction. Curr Biol **15:**73-8.
360. **Yu, Q., R. Konig, S. Pillai, K. Chiles, M. Kearney, S. Palmer, D. Richman, J. M. Coffin, and N. R. Landau.** 2004. Single-strand specificity of APOBEC3G accounts for minus-strand deamination of the HIV genome. Nat Struct Mol Biol **11:**435-42.
361. **Yu, X., Y. Yu, B. Liu, K. Luo, W. Kong, P. Mao, and X. F. Yu.** 2003. Induction of APOBEC3G ubiquitination and degradation by an HIV-1 Vif-Cul5-SCF complex. Science **302:**1056-60.
362. **Yu, Y., Z. Xiao, E. S. Ehrlich, X. Yu, and X. F. Yu.** 2004. Selective assembly of HIV-1 Vif-Cul5-ElonginB-ElonginC E3 ubiquitin ligase complex through a novel SOCS box and upstream cysteines. Genes Dev **18:**2867-72.
363. **Zennou, V., D. Perez-Caballero, H. Gottlinger, and P. D. Bieniasz.** 2004. APOBEC3G incorporation into human immunodeficiency virus type 1 particles. J Virol **78:**12058-61.
364. **Zhang, F., W. N. Landford, M. Ng, M. W. McNatt, P. D. Bieniasz, and T. Hatziioannou.**

2011. SIV Nef proteins recruit the AP-2 complex to antagonize Tetherin and facilitate virion release. PLoS Pathog **7:**e1002039.

365. **Zhang, H., B. Yang, R. J. Pomerantz, C. Zhang, S. C. Arunachalam, and L. Gao.** 2003. The cytidine deaminase CEM15 induces hypermutation in newly synthesized HIV-1 DNA. Nature **424:**94-8.

366. **Zhang, K. L., B. Mangeat, M. Ortiz, V. Zoete, D. Trono, A. Telenti, and O. Michielin.** 2007. Model structure of human APOBEC3G. PLoS One **2:**e378.

367. **Zhang, Q., Z. Liu, Z. Mi, X. Li, P. Jia, J. Zhou, X. Yin, X. You, L. Yu, F. Guo, J. Ma, C. Liang, and S. Cen.** 2011. High-throughput assay to identify inhibitors of Vpu-mediated down-regulation of cell surface BST-2. Antiviral Res **91:**321-9.

368. **Zhang, W., J. Du, K. Yu, T. Wang, X. Yong, and X. F. Yu.** 2010. Association of potent human antiviral cytidine deaminases with 7SL RNA and viral RNP in HIV-1 virions. J Virol **84:**12903-13.

369. **Zheng, Y., Z. Ao, B. Wang, K. D. Jayappa, and X. Yao.** 2011. Host protein Ku70 binds and protects HIV-1 integrase from proteasomal degradation and is required for HIV replication. J Biol Chem **286:**17722-35.

370. **Zheng, Y. H., K. T. Jeang, and K. Tokunaga.** 2012. Host restriction factors in retroviral infection: promises in virus-host interaction. Retrovirology **9:**112.